LAPPEENRANTA UNIVERSITY OF TECHNOLOGY

Department of Mechanical Engineering

LASER CUTTING OF AUSTENITIC STAINLESS STEEL WITH A HIGH QUALITY LASER BEAM

The topic of the thesis has been approved by the Department Council of Mechanical Engineering on 18th January 2006

Examiner 1: Professor Veli Kujanpää
Examiner 2: Professor Flemming O. Olsen
Supervisor: Docent Antti Salminen

Lappeenranta, 16th May 2006

Catherine Wandera

Skinnarilankatu 28 A 5

53850 Lappeenranta

Finland

Phone: +358 41 702 1174

ACKNOWLEDGEMENT

I acknowledge the grace of God for the successful completion of this masters thesis work, which was done in Lappeenranta University of Technology Laser Processing Laboratory from October 2005 to May 2006.

I am grateful to Prof. Veli Kujanpää, Prof. Flemming Olsen from Technical University of Denmark and Dr. Antti Salminen for guiding and examining my research work. With their efforts, I have gained much knowledge in laser materials processing. I am also thankful to other people at the Laser Processing Laboratory for their help and colleagues in the masters program with whom I have always shared ideas.

Last but not least, many thanks go to my parents and fiancé Milton for their continuous encouragement and support.

Glory be to God Almighty.

Thank you

Lappeenranta, 16ᵗʰ May 2006

Catherine Wandera

ABSTRACT

Lappeenranta University of Technology

Department of Mechanical Engineering

Author: Catherine Wandera

Title: **Laser Cutting of Austenitic Stainless Steel with a High Quality Laser Beam**

Thesis for the Degree of Master of Science in Technology, 2006

108 pages, 69 figures, 4 tables and 3 appendices

Examiner 1: Professor Veli Kujanpää

Examiner 2: Professor Flemming O. Olsen

Supervisor: Docent Antti Salminen

Keywords: disk laser, fiber laser, high quality laser beam, laser cutting, austenitic stainless steel

The thin disk and fiber lasers are new solid-state laser technologies that offer a combination of high beam quality and a wavelength that is easily absorbed by metal surfaces and are expected to challenge the CO_2 and Nd:YAG lasers in cutting of metals of thick sections (thickness greater than 2mm). This thesis studied the potential of the disk and fiber lasers for cutting applications and the benefits of their better beam quality.

The literature review covered the principles of the disk laser, high power fiber laser, CO_2 laser and Nd:YAG laser as well as the principle of laser cutting. The cutting experiments were made with the disk, fiber and CO_2 lasers using nitrogen as an assist gas. The test material was austenitic stainless steel of sheet thickness 1.3mm, 2.3mm, 4.3mm and 6.2mm for the disk and fiber laser cutting experiments and sheet thickness of 1.3mm, 1.85mm, 4.4mm and 6.4mm for the CO_2 laser cutting experiments. The experiments focused on the maximum cutting speeds with appropriate cut quality. Kerf width, cut edge perpendicularity and surface roughness were the cut characteristics used to analyze the cut

quality. Attempts were made to draw conclusions on the influence of high beam quality on the cutting speed and cut quality.

The cutting speeds were enormous for the disk and fiber laser cutting experiments with the 1.3mm and 2.3mm sheet thickness and the cut quality was good. The disk and fiber laser cutting speeds were lower at 4.3mm and 6.2mm sheet thickness but there was still a considerable percentage increase in cutting speeds compared to the CO_2 laser cutting speeds at similar sheet thickness. However, the cut quality for 6.2mm thickness was not very good for the disk and fiber laser cutting experiments but could probably be improved by proper selection of cutting parameters.

TABLE OF CONTENTS

LIST OF SYMBOLS AND ABBREVIATIONS

λ	wavelength
K	beam quality factor
M^2	times diffraction limit factor (beam quality factor, $M^2 = 1/K$)
D	beam diameter at the optic
d_f	focused beam diameter
z	depth of focus
f	focal length
F	focal length divided by the beam diameter at the optic
Θ	full divergence angle of the beam
d_0	beam waist diameter
ψ	angle between the plane of polarization and cutting direction
p	plane of polarization
c	cutting direction
U	perpendicularity tolerance
R_z	mean height of the profile
R_a	an integral of the absolute value of the roughness profile
cw	continuous wave laser power
NA	Numerical Aperture
BPP	Beam Parameter Product (beam quality factor, $BPP = \lambda M^2/\pi$)
CO_2	Carbon dioxide
DPSSLs	diode pumped solid state lasers
Er: Glass	Erbium: Glass
HAZ	heat affected zone
LPSSLs	Lamp Pumped Solid State Lasers
Nd: YAG	Neodymium –Yttrium Aluminium Garnet
TEM_{00}	lowest order beam mode/ diffraction limit
Yb: YAG	Ytterbium: Yttrium Aluminium Garnet

1. INTRODUCTION

Stainless steel is used extensively in a number of everyday applications in the home, industry, hospitals, food processing, farming, aerospace, construction, chemical, electronics, and energy industries; the austenitic grade of stainless steel is the most used by far. Cutting of stainless steel sheets is one of the primary requirements in the fabrication of most of the components. Laser cutting offers several advantages over conventional cutting methods such as plasma cutting. The advantages of laser cutting include high productivity thanks to the high cutting speeds, narrow kerf width (minimum material lost), straight cut edges, low roughness of cut surfaces, minimum metallurgical distortions, easy integration with computer numerically controlled (CNC) machines for cutting complex profiles and it is a non contact process suitable for cutting in areas with limited access. /1,2,3,4,5/

In the early 1980's, laser cutting had a limited application, being mostly used in high technology industries such as aerospace and the available commercial equipment could only cut light sheet (1-2 mm) because of their limited power output. /6/ Laser technology has continued to develop over the years and now many types of lasers are commercially available. With the development of high power lasers, laser materials processing is now being used as part of the production route for many items such that the laser is finding increasing commercial use as a cutting tool. /7/ The laser development trends indicate that there are more tendencies towards smaller and more efficient semiconductor lasers. The beam quality and available power output of a particular laser cutting system affects the cut quality obtained, the quality of the cutting process and the range of thickness that can be satisfactorily cut. /8/

The CO_2 laser and Nd:YAG laser (solid state laser) are the main lasers used for industrial cutting applications. The CO_2 laser is the most commonly used, especially for cutting of thick sections, because of its better beam quality compared with the Nd:YAG laser of a similar power level and the CO_2 lasers are also available in higher output powers than the Nd:YAG lasers. The Nd:YAG laser beam quality becomes poorer with increase in output power. Nevertheless, the solid-state lasers have recently gained increasing importance in

1

high power applications mainly due to several consequences of their wavelength such as a higher absorptivity, lower sensitivity against laser-induced plasma and the use of optical fibres for beam delivery. /7,9,10,11/

The new solid-state laser technologies of the thin disk and high power fiber lasers - which offer a combination of high beam quality and a wavelength that is easily absorbed by metal surfaces - are now challenging the CO_2 and Nd:YAG lasers in cutting applications. The output powers of the thin disk and fiber lasers are scalable to the kilowatt range without much detrimental effect on the beam quality. These systems are promising for cutting applications because their high beam quality enables focusing of the laser beam to a small spot producing high power density that is essential for cutting of metals and enhances higher cutting speeds. /12,13,14/

This study consists of two parts - the literature review and experimental part. The disk laser, fiber laser and CO_2 laser technologies, the laser cutting process and the characteristic properties of the laser cut are discussed in the literature review. Most work reviewed in the literature covered only cutting with the CO_2 laser and Nd:YAG laser and the few that covered cutting with either the disk laser or fiber laser considered mostly the cutting speeds without a detailed analysis of the cut quality obtained.

In the experimental part of this study, the potential of the disk laser and the fiber laser for cutting applications and the possible consequences of their high beam quality was investigation with comparison to the CO_2 laser. The cutting experiments covered cutting of austenitic stainless steel (grades AISI 304 and AISI 316) of sheet thickness of 1.3mm, 2.3mm, 4.3mm and 6.2mm using the disk and fiber lasers and sheet thickness of 1.3mm, 1.85mm, 4.4mm and 6.4mm using the CO_2 laser. The cut qualities were analyzed by measuring the kerf width, perpendicularity of the cut edges and the roughness of the cut surfaces. The cut quality was classified according to the EN ISO 9013: 2002 standard for thermal cuts. /15/

LITERATURE REVIEW

2. DISK LASER TECHNOLOGY

The thin disk laser concept is a laser design for diode-pumped solid-state lasers, which allows the realization of lasers with high output power, having very good efficiency and also excellent beam quality. The optical distortion of the laser beam is low due to the surface cooling of the disk and therefore operation of the thin disk laser is possible in fundamental mode at extremely high output power. /12,13/

2.1 Thin Disk design

The principle of the thin disk laser design is shown in figure 1. The laser crystal is shaped as a disk with a diameter of several mm - depending on the output power/energy - and a thickness of 100 μm to 200 μm, depending on the laser active material, the doping concentration and the pump design. The thin disk material is Yttrium-Aluminium-Garnet (YAG) and the central active portion of the disk may be doped with Ytterbium (Yb) ions. /13/
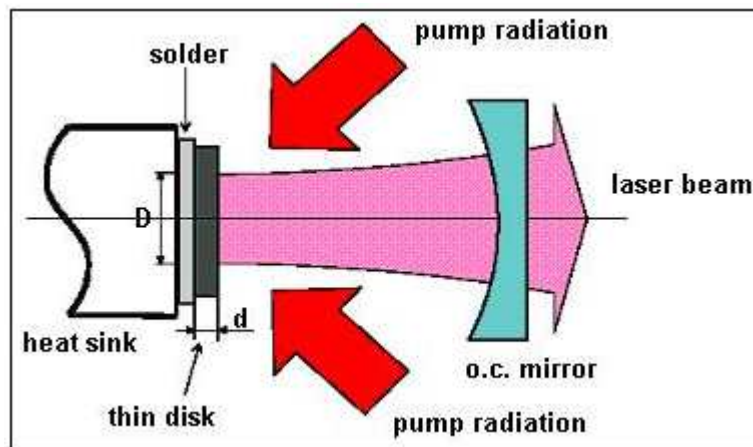

Figure 1. Thin disk laser design: The laser crystal is shaped as a disk with a diameter of several mm (depending on the output power) and a thickness of 100 μm to 200 μm /13/

Increase in the heat dissipation capacity of a disk varies inversely with the disk thickness, therefore, the thinnest possible disk that is consistent with the pump geometry must be used to maximize the output intensity. However, a disk with a small thickness has very short absorption distance; therefore, its absorption of single pass pump radiation is low. The use of a highly absorbing gain medium in combination with a pumping geometry that allows multi-passing of the pump light ensures efficient absorption of pump power by the thin gain sample. For that reason, Ytterbium-doped YAG (Yb:YAG), which emits a laser beam with a wavelength of 1070-nm, is currently the preferred disk material because of its high absorption of the 940-nm pump light. The Yb:YAG disks can be made much thinner than the Nd:YAG disks. /16/

The back side of the disk is highly reflectively coated for both the laser and the pump wavelengths and acts as the mirror in the resonator; the front side is antireflectively coated for both wavelengths. The disk is mounted with its back side on a water-cooled heat sink using indium based or gold-tin solder allowing a very stiff fixation of the disk on the heat sink without any deformation of the disk. /13,16/

2.2 Thin disk laser operation principle

In principle, the thin disk is optically excited from the front surface by high power, diode laser modules assembled in stacks. The parabolic mirror reflects the pump light (wavelength 940 nm) emitted by the laser diodes onto the thin disk laser active Yb:YAG crystal. The pump light is reflected from the coated backside of the disk and strikes the parabolic mirror a second time, deflects onto a retro reflector and returns to the parabolic mirror from which it is recoupled into the disk. The process continues until after 16 passes when the pump light is completely absorbed and a high quality laser beam with a wavelength of 1070nm is emitted as shown in figure 2. The reflective layer on the backside of the disk and an outcoupling mirror, situated in front of the parabolic reflector, set up the resonator. The high quality laser beam emitted is coupled into the optic fiber of 150 μm or 300 μm in core diameter and long fibers, 100 m, are allowed. /16,17/
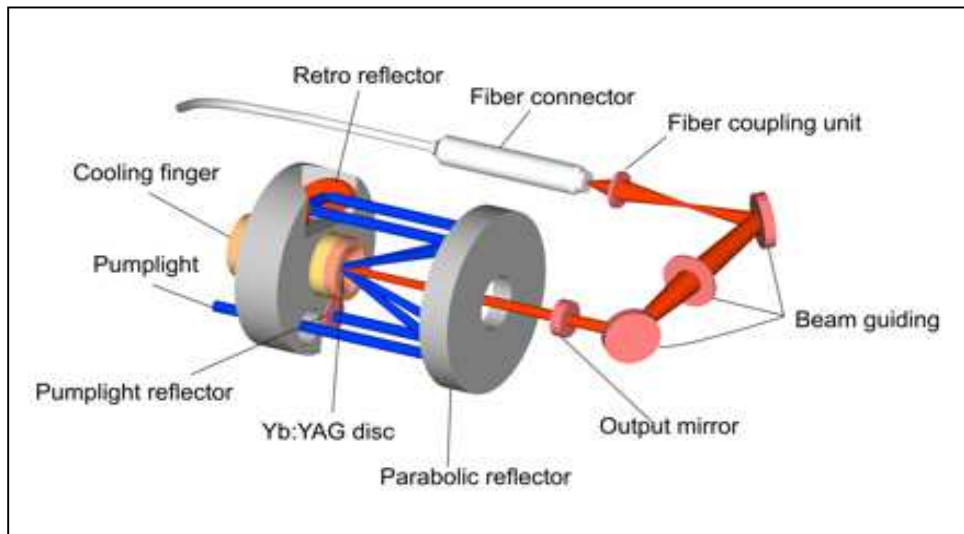
Figure 2. Thin Disk laser principle /17/

The disk laser is based on a "multi-pass-excitation–concept" and high values for regenerative amplification in order to compensate for the small crystal volume. The multi pass pump geometries developed by scientists at the University of Stuttgart accommodate the use of thin disks. With this approach, the pump beam is re-imaged through the sample more than 16 times to increase the net absorption path. /13,16,18/

Other pumping principle – Edge pumped disk

John Vetrovec et al. explored an alternative pump configuration, by edge pumping a composite thin disk laser, as a way of addressing the very complicated pump geometry and the limitations it imposes on power scaling. The composite thin disk consists of a doped central active portion and an undoped perimetral edge. Figure 3 shows the edge pumped disk. /19/ However, edge pumping is not the usual pumping method used for the thin disk laser.
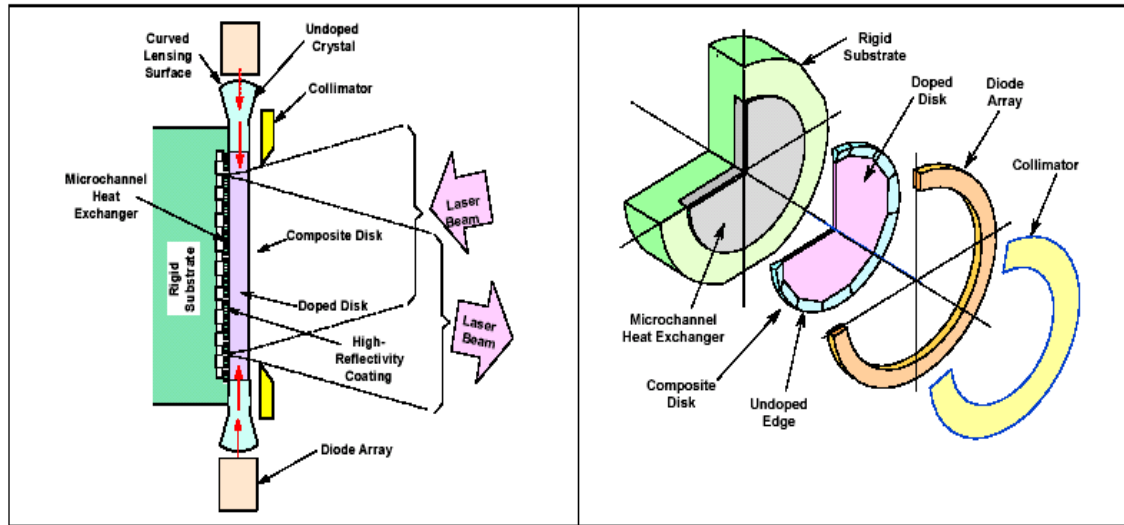
Figure 3. (a) Edge pumped disk   (b) Exploded view of edge pumped disk /19/

2.3 Power scaling and beam quality

Thin disk laser configurations have a capacity for continuous wave (cw) output powers exceeding 1 kW and enable the generation of high average power by minimizing the distance over which waste heat is transported. With each disk producing kilowatts of power, power scaling by the thin disc laser concept can be achieved by increasing the pump diameter on the disc or use of several discs arranged along a folded resonator axis, the approach shown on the right-hand side of figure 4. Alternatively, power scaling can be achieved by polarization coupling of two different resonators. /12/
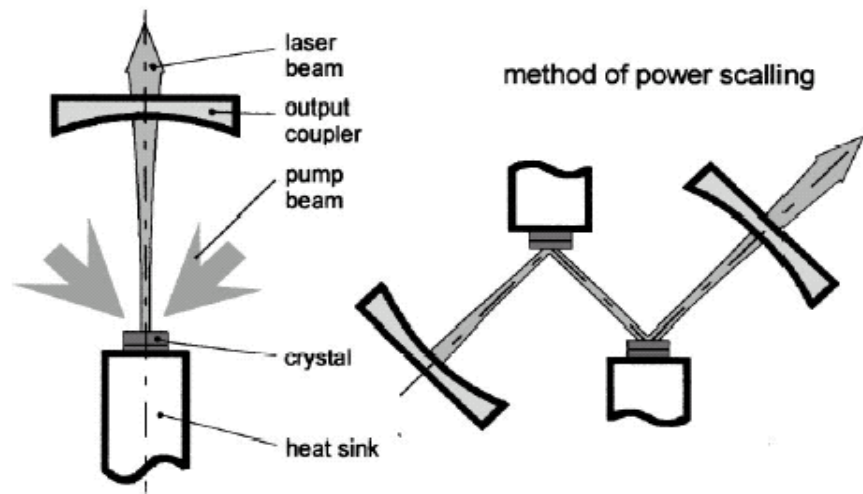
Figure 4. The thin disc laser: Scheme (left) and principle of power scaling by the number of discs. /12/

The Beam Parameter Product (BPP) describes the beam quality of the laser beam in relation to the ideal TEM_{00} mode. The implications of the BPP for laser materials processing will be discussed in detail in chapter 5. Tables 1 and 2 illustrate the laser powers and the corresponding beam quality of the thin disk laser systems and the diode-pumped solid-state laser rod systems in continuous wave mode. The thin disk laser has a better beam quality, characterized by a low Beam Parameter Product (BPP), than the conventional solid-state lasers with rod systems. The high-powered disk laser, with an output power of 4000 W, has a beam quality of 8 mm.mrad and the output can be coupled into a 200-μm-diameter optical fiber. It is also worth noting that the disk laser enables scaling up of output power without loss in beam quality while for the rod systems, scaling up of output power causes loss in beam quality. /16,18,20,21/

Table 1: High-Powered Disk Laser /16/

Laser device		HLD 251	HLD 501	HLD 1001.5	HLD 2002	HLD 4002
Max. Output power	[W]	300	600	1500	2650	5300
Laser power[*]	[W]	250	500	1000	2000	4000
Beam quality	[mm.mrad]	4	4	6	8	8
Laser light cable	[μm]	100	100	150	200	200

[*] at the workpiece, controlled over entire life of diodes

Table 2: Diode-pumped cw solid state lasers (Rod systems) /16/

Laser device		HLD 1003	HLD 2304	HLD 3006	HLD 3504	HLD 4506
Max. output power	[W]	1300	3000	4000	4500	6000
Laser power[*]	[W]	1000	2300	3000	3500	4500
Beam quality	[mm.mrad]	12	16	25	16	25
Laser light cable	[μm]	300	400	600	400	600

[*] at the workpiece, controlled over entire life of diodes

The superior beam quality of the disk laser brings many advantages such as the reduction of the focal diameter. The other benefits include higher cutting and welding speeds, shorter cycle times and lower heat input into the workpiece. /16,17,22/

2.4 Temperature profile comparison of rod systems and thin disk laser

For the rod systems, the heat load on the lasing medium creates an optical distortion of the laser light. Cooling of the rod occurs radially such that only the outer surfaces of the rod are cooled while the center of the rod is at a higher temperature forming a parabolic temperature profile. This thermal gradient from center to edges of the rod creates a

mechanical stress that results in the optical distortion termed thermal lensing, whereby the laser crystal acts as a lens with shorter focal length at higher powers thus resulting in poorer beam quality at higher powers. Rod diameters vary from 2 to 10 mm and lengths from 50 to over 200 mm; the larger and longer rods produce more laser power but at poorer beam qualities. Rods longer than 250 mm have optical design limitations as the thermal lensing of the rod increases with increase in the rod length and pump power. /7,10,13,23/

The thermal lensing that occurs in rod systems is virtually eliminated by the disk laser's geometric relationship between the excitation source, cooling and resonator resulting into significant increase in beam quality at a given power level. The disk laser utilizes a thin disk, which increases the cooled surface area with respect to the laser volume. Cooling of the thin disk takes place by axial heat flow resulting in a radially homogeneous temperature profile and negligible residual thermal lensing. Increasing the disk surface area or reducing the disk thickness improves the continuous or average power while maintaining a constant beam quality. /13,16,23/ Figure 5 shows the cooling patterns for the thin disk and the rod lasers.
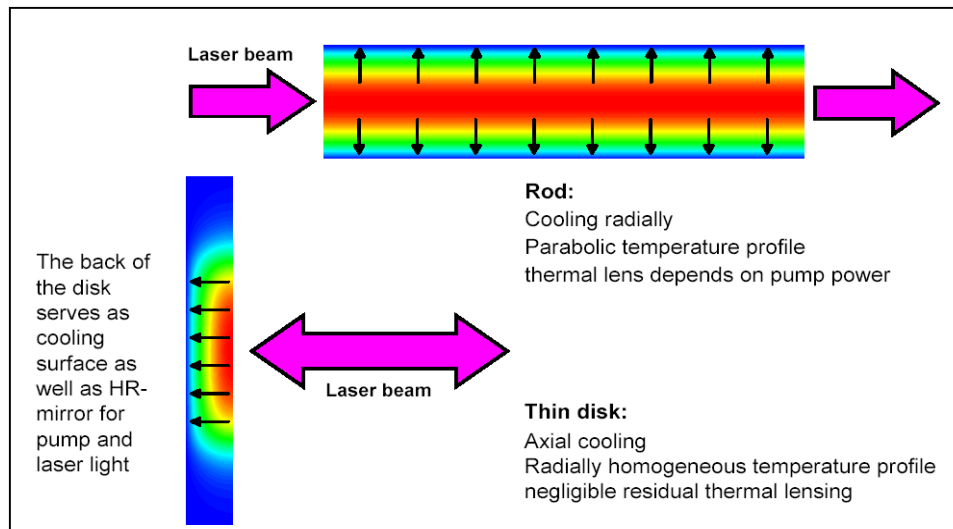
Figure 5. Temperature profiles of the Thin disk and Rod lasers /23/

Fine cutting and drilling lasers require much better beam quality because the cut width is directly related to beam quality and wide cut kerfs greatly increase heat input into the part.

Welding lasers on the other hand can employ poorer beam quality because larger focus spots increase joint area such as in lap joints thus improving weld strength and tolerance to joint position. /10/

2.5 Applications and prospects

The high beam quality of the disk laser offers benefits in macro applications such as scanner welding, keyhole welding and cutting. /23/ It also provides higher rates of feed and shorter cycle times with minimal heat input, which is advantageous when welding aluminium or cutting thin sheet metal. /16/

The disk laser, having a shorter infrared wavelength than the CO_2 laser, might find favorable application in processing of highly reflective and conductive metals such as silver and copper because its wavelength is highly absorbed by these metal surfaces. The high beam quality will also enable new applications such as Laser Selective Melting, whereby complex 3-D parts can be produced out of metal powder layer by layer. The use of smaller fibers (200 μm) for beam delivery will permit higher power densities that could have an impact on laser cutting systems and remote welding. The reduced fiber diameter also allows a larger working area and a larger working distance. In general, the disk laser might find wide application in areas of the present Nd:YAG laser and much more. /16,24,25,26,27/

3. HIGH POWER FIBER LASER

The fibre laser is one of the new developments of diode pumped solid-state lasers (DPSSLs). /12/ The fiber lasers have been primarily used in communications. However, the new development of the double-clad high power fiber lasers for materials processing promise to disrupt existing technology bases such as the Nd:YAG laser, opening an opportunity for fiber lasers in significant non-telecommunications markets such laser welding, cutting and marking. /28/ The primary material processing fiber lasers are at the Ytterbium (Yb) 1070nm wavelength, consistent with where the YAG laser operates. /29/ The ytterbium fibre (Yb:glass) lasers with output powers upto 50kW far exceed the laser

powers that are available using Nd:YAG laser technology, while also offering a better beam quality. The fiber laser offers great potential in terms of welding and cutting operations. The single mode Erbium fiber (Er:glass) lasers with wavelengths from 1530nm to 1600nm are available at output powers of $1 - 100$ W and beam quality M^2 less than 1.1mm.mrad. /30,31,32/

3.1 Design and operation principle

A fiber laser is made from several meters of multi-clad single mode active fiber, side pumped by single stripe multimode diodes. The wall plug efficiency of the Yb fiber laser is greater than 20%, which allows the device to be air-cooled. Figure 6 illustrates the scheme of the clad-pumped fiber laser. /12,29/
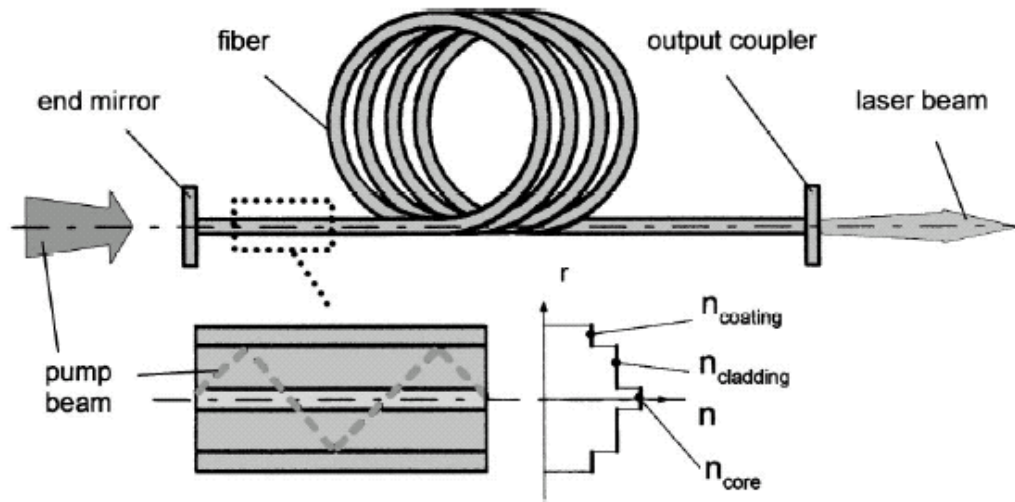
Figure 6. Scheme of the clad-pumped fibre laser /12/

The radiation of the diode lasers is focused into the relatively large nonactive cladding part of the pump core (diameter of 100μm, Numerical Aperture, $NA \approx 0.4$) from where the diode pump light is then coupled to the active medium in the fiber core (see figure 6). The pump light, confined in the pump core by a coating with a lower index of refraction,

propagates along the optical axis crossing the monomode laser core and exciting there the laser active medium over a length of several meters. The laser light exits the cavity through a single mode passive fiber that could be up to 50 meters long. The beam quality corresponding to diffraction-limited values ($M^2 < 1.1$) is a function of the fiber's optical properties only and is independent of temperature or power. /12,29/

3.2 Power scaling and beam quality

Fibre lasers offer the advantage of being easily scalable such that output power in the kW-range can be achieved by incoherent coupling of several fibre lasers.   Kilowatt and multi-kilowatt laser output is obtained by combining single mode fiber modules and the combined output delivered through a single multimode fiber. Although the output is no longer single mode, the systems have excellent beam properties equal to or lower than conventional CO_2 or Nd:YAG lasers. The beam delivery fiber for a 1-kilowatt system is 100 microns and for a 10-kilowatt system is 300 microns, which allows for longer working distances and more consistent processing than conventional Nd:YAG lasers with fiber delivery. The reliability remains high, due to the module construction, with no additional component stress as power is increased. /12,29/

3.3 Applications

Fiber lasers have a wide range of applications and hence have the potential to dominate the material processing market in the future. These lasers are demonstrating process and cost advantages across the entire spectrum of material processing applications including: metal cutting, welding, silicon cutting, ceramic scribing, spot welding, bending, powder deposition, surface modification and marking. The applications by industry include:

- Automotive: welding transmission components, welding a sheet metal, cutting hydro-formed parts, marking, remote welding
- Computer: spot welding, annealing, silicon cutting

- Aerospace: welding Aluminum and Titanium, surface build up on blades, cutting aerospace components
- Medical device: marking, cutting, spot welding /29/

4. OTHER CUTTING LASERS

Lasers that are capable of producing high power laser beams of high beam quality are suitable for cutting applications. The CO_2 and Nd: YAG lasers are the two laser technologies have for long been the workhorses for high power applications such as cutting. The CO_2 laser has gained considerable acceptance as a cutting tool because a very high power density can be achieved with such a laser and CO_2 lasers are available in high power levels. /33,34/ The CO_2 laser and Nd:YAG laser with output power capabilities of upto 8,000 W and 4,500 W respectively are now available for cutting applications. The CO_2 lasers with even higher output powers (upto 20,000 W) are powerhorses for welding and surface treatment applications. /35,36,37,38/

4.1 CO_2 laser

CO_2 lasers emit the infrared laser radiation with a wavelength of 10.6 μm and posses overall efficiencies of approximately 10 to 13%. The laser-active medium in a CO_2 laser is a mixture of CO_2, N_2 and He gases, where CO_2 is the laser-active molecule. The stimulation of the laser-active medium is accomplished by electrical discharge in the gas. During the stimulation process, the nitrogen molecules transfer energy from electron impact to the CO_2 molecules. The transition from energetically excited CO_2 molecules (upper vibrational level) to a lower energy level (lower vibrational level) is accompanied by photon release leading to emission of a laser beam. The CO_2 molecules return to the ground state by colliding with the helium atoms, which comprise the major share of the gas mixture, and the CO_2 molecules in the ground state are then available for another cycle. The stimulation of the electrical gas discharge in the gas mixture is accomplished by either direct current or radio frequency stimulation. In direct current stimulated lasers, gas discharge between

electrodes allows the electrical energy to be directly coupled into the laser gas while the radio frequency stimulated lasers are characterized by capacitive incoupling of the electrical energy needed for gas discharge. /33,39/

There are different designs of the CO_2 laser that use different modes of gas flow and cooling enabling effective beam delivery over a wide range of output power. The CO_2 laser technology includes the following designs: Transverse flow (cross-flow) laser, Fast-axial flow laser, Diffusion-cooled slab laser and Sealed-Off laser. They can be operated in either the CW mode or pulsed mode. The beam power and beam quality of the transverse flow (cross-flow) CO_2 laser (multi-mode, $K \geq 0.18$) are favorable for laser welding applications. The CO_2 laser designs that are used for cutting applications are discussed in the following sections. /35,39/

4.1.1 Fast-axial flow CO₂ laser

The fast-axial flow lasers have different designs based on different beam paths. The different beam paths of the fast-axial flow laser designs include triangular beam path, rectangular beam path and beam trajectory planes oriented at a 45˚ angle to each other. Due to their physical principle, the fast-axial flow lasers provide a better beam quality than cross-flow lasers. /39/

Figure 7 shows a fast-axial flow laser design with an optical resonator that consists of a rear mirror and a diamond outcoupling mirror. The beam trajectory of this fast-axial flow laser is mirror-folded in four paths and forms two planes oriented at a 45˚ angle to each other. Three of the four paths, all consisting of quartz glass tubes, contain a total of 12 electrode pairs for radio frequency excitation of the laser gas mixture passing through the tubes. Turbines generate the laser gas flow and the laser gas flows through a heat exchanger before and after passing through the turbine. The cooling water, which passes through the heat exchanger in a separate closed loop, cools down the laser gas. The performance stability of the fast-axial flow laser is directly related to the thermal stability of the supplied laser gas therefore the temperature regulation for the water loop must be highly constant. A

linearly polarized laser radiation is emitted through the resonator construction eliminating the need for additional polarization optics outside the resonator. /35,39/

1. Rear mirror
2. Laser beam
3. Diamond-output mirror
4. Excited discharge (12 x)
5. Fold mirror (4x)
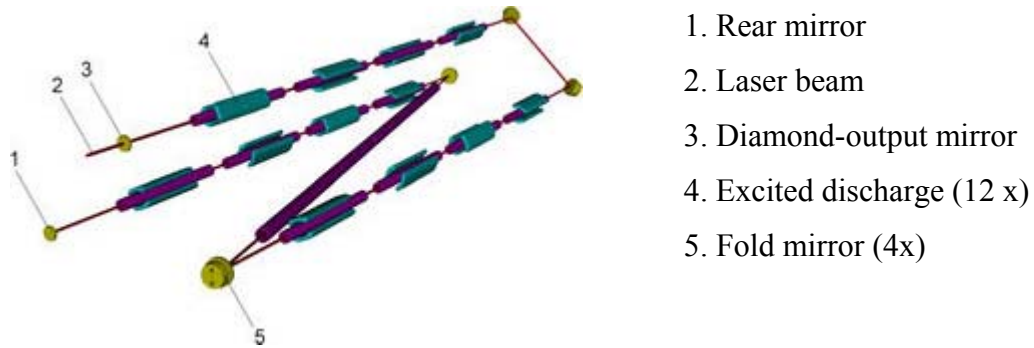
Figure 7. Fast Axial flow (FAF) laser with beam trajectory planes oriented at $45°$ angle /35/

4.1.2 Diffusion-cooled (slab) CO₂ laser

The diffusion cooled (slab) CO_2 lasers, available in a power range between 1 and 5 kW, have a highly compact design. These lasers are equipped with large-area copper electrodes and radio frequency gas discharge takes place between the electrodes as illustrated in figure 8. The narrow inter-electrode spacing allows effective heat removal from the discharge chamber via the directly water-cooled electrodes giving rise to comparatively high power density. Heat transport is exclusively by diffusion hence the name "diffusion-cooled laser". The unstable resonator consists of rotation-parabolic mirrors, allowing outcoupling of a laser beam with extremely good focusing properties. External, water-cooled, reflective beam shaping components are used to convert the originally rectangular beam to a rotation symmetrical beam with a beam quality of $K \geq 0.9$. The major advantages of this type of laser include the compact and almost entirely wear-resistant design, and the practically negligible gas consumption. /35,39/
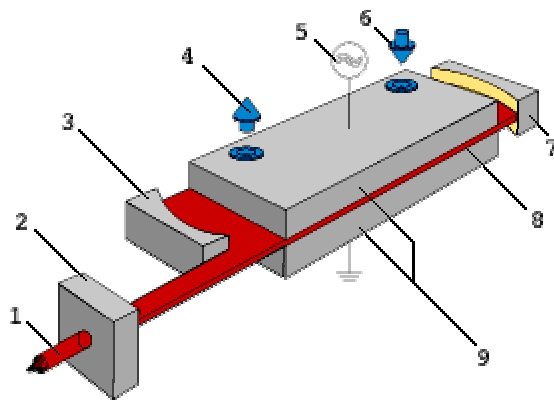
1. Laser beam
2. Beam shaping unit
3. Output mirror
4. Cooling water
5. RF excitation
6. Cooling water
7. Rear mirror
8. RF excited discharge
9. Wave-guiding electrodes

Figure 8. Diffusion-cooled (slab) CO_2 laser /35/

4.1.3 Sealed-Off CO_2 laser

The Sealed-Off CO_2 laser is based on sealed gas laser expertise of the diffusion-cooled Slab laser technology. The Sealed-Off CO_2 lasers are maintenance-free, completely sealed and require no external gas, making them robust and highly reliable. These lasers are available with output powers of upto 600 W and are typically used for cutting of non-metals (paper, glass, plastics) and metals, rapid prototyping and marking applications. /35,40,41/

4.2 Nd:YAG laser

The Nd:YAG laser is a solid-state laser consisting of a crystal that absorbs light energy in the 810 nm region to produce the 1064 nm laser output. The laser active medium is a synthetic single crystal of yttrium-aluminum- garnet (YAG) that is doped with a low percentage of the rare earth neodymium (Nd^{3+} ion) and emits infrared laser radiation with a wavelength of 1.064 μm. The YAG is the host for the Nd^{3+} ion and the lasing action is developed in the Nd^{3+} ion. The crystal is fabricated into a rod and the volume of a given rod determines its average power capability. The excitation of the active medium is accomplished by broadband optical radiation - from flash lamps (pulsed), an intense arc

lamp (continuous wave mode, CW) or laser diodes - which is coupled into the crystal. /10,33/

Unlike gas lasers, the Nd:YAG laser crystal is optically active in the resonator therefore its optical characteristics vary with the laser parameters, affecting the output beam quality. The YAG crystal acts as a positive lens when it is pumped because of the high temperature at the center as cooling water is in contact only with the outer surface and this thermal lensing of the rod increases with increasing pump power. /10/ The lamp pumped and diode pumped Nd:YAG lasers are discussed in the sections that follow.

4.2.1 Lamp pumped Nd:YAG lasers

For pulsed Nd:YAG lasers, the flash lamps are specifically designed for the typical repetitive high-peak-current electrical pulses that create the laser pulses. The flash lamps have special design features to improve their reliability and life because of the high peak currents in the lamp during a pulse. The wall thickness is optimized for high-pressure spikes, the electrodes shaped for repeatable arc production, and the mass and placement of the electrodes is optimized for minimal thermal stresses where the metal electrode is sealed to the glass enveloped. /10/

Lamps for cw lasers have slightly different designs because of their continuous mode of operation. A laser operating in the cw mode requires much higher pumping energy because of lower photon flux in the laser and the lamps must be able to withstand the higher average power delivered to them. Cooling must be optimized for the high-power operation but the high-pressure spikes of pulsing lamps are not a concern for cw lamps therefore the lamp jacket walls can be thinner but the electrode size must be increased for better cooling. /10/ Figure 9 shows the structure of a lamp pumped Nd:YAG rod laser.
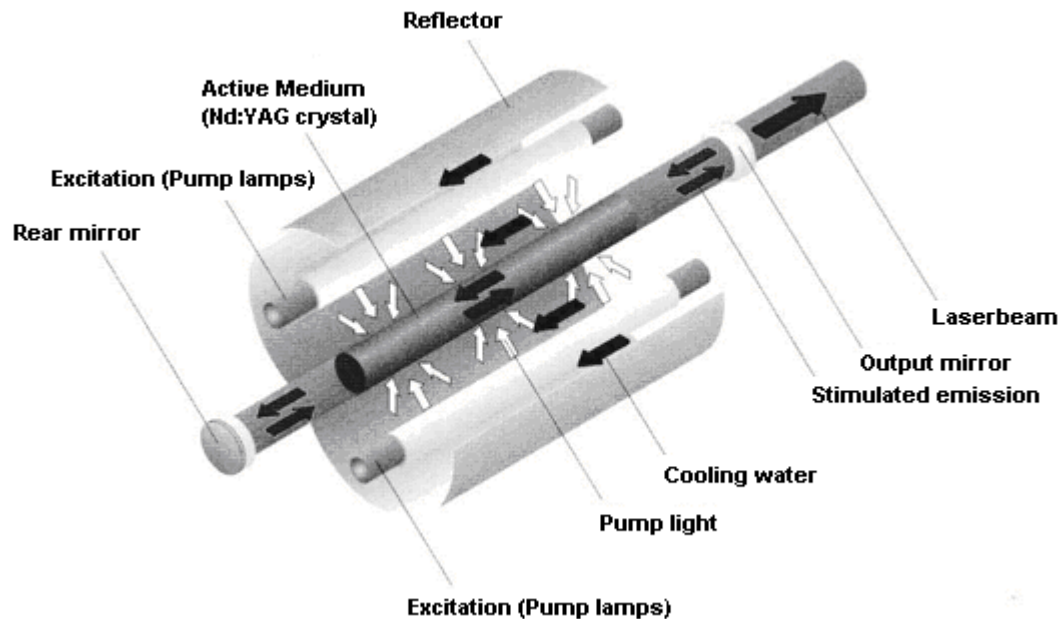
Figure 9. Scheme showing the structure of a lamp-pumped rod laser /39/

4.2.2 Diode pumped Nd:YAG lasers

The replacement of lamps by diodes to pump the laser crystals offers substantial advantages in terms of increased efficiency, reduced cooling, and smaller size and weight as compared to lamp pumping. The longer lifetime of diodes (10,000 h appears realistic) is beneficial with respect to running costs. As a result of the lower heat release in the crystal, the temperature-dependent thermal lens effect is less pronounced in the diode pumped solid-state lasers (DPSSLs) but it is not completely eliminated. However, the concepts of the new generation of high-power DPSSLs – thin disc and fiber lasers - overcome the thermal lens effect yielding a higher beam quality. /10,12/

The diode pump light can be injected into the end of the rod, termed end-pumped lasers (figure 10), however, the use of side-pumped resonators (figure 11) is most common for high power lasers and more efficient coupling of diode pump light into the laser medium. /10/
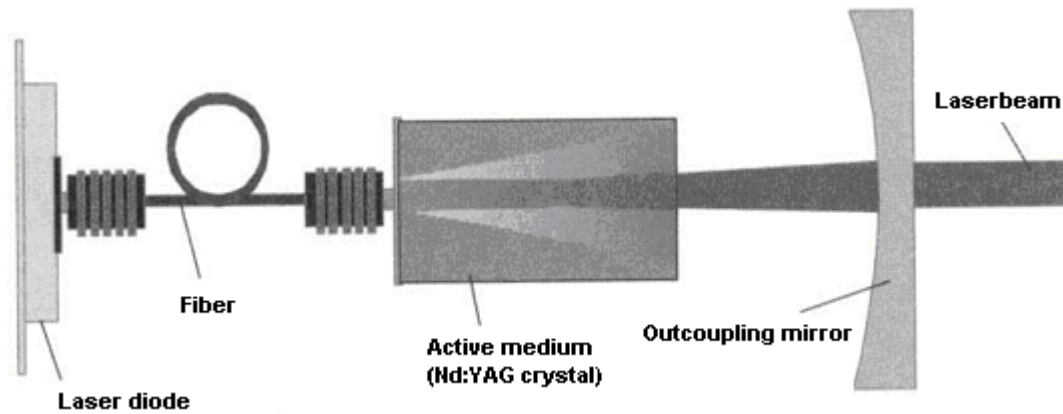
Figure 10. Principle of a diode pumped rod laser. (End-pumped: Longitudinal pumping) /39/
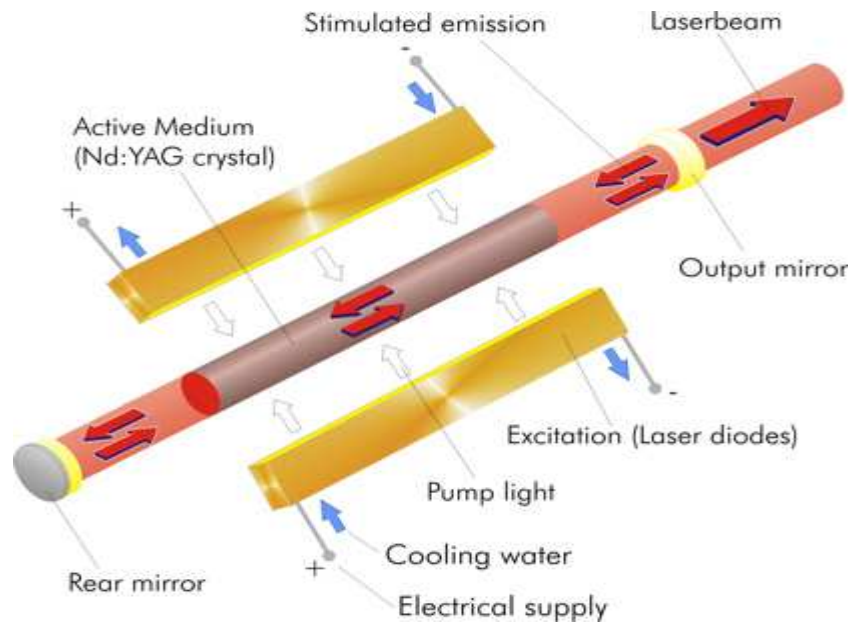
Figure 11. Principle of a diode pumped rod laser. (Side pumped: Transverse pumping) /39/

Although, the traditional Nd:YAG lasers are limited in output power level, the wavelength of the Nd:YAG laser is more easily absorbed by metal surfaces as compared to the CO_2 laser wavelength making the Nd:YAG laser more suitable for processing of metals that have a high reflectivity such as aluminium and copper. Additionally, the use of optical fibers for beam handling is an advantage for YAG lasers in terms of flexibility and

integration in the industry. The Nd:YAG laser has much been used for high precision or microprocessing applications /9,42,43/

The disadvantages of the traditional Nd:YAG lasers like poor beam quality and low efficiency are being effectively reduced by the new concepts of diode pumped systems of the thin disk and fiber lasers. These new developments of high power solid-state lasers in the kW power range coupled with a higher beam quality will enable new applications, which were originally only achievable with CO_2 lasers. /12/

5. IMPLICATIONS OF BEAM QUALITY (BPP)

The Beam Parameter Product (BPP) is widely used to characterize the quality of the beam. The BPP is described by the Times diffraction limit factor (M^2) which tells how much larger is the BPP of the laser under consideration compared to the physically lowest for a beam in the TEM_{00} mode (Diffraction limit). Therefore, a low BPP characterizes a high beam quality. Figure 12, which is a status of 1999 shows the M^2 data for commercially available and laboratory –state lasers. /12/

In recent years, the thin disk and fiber laser systems are now commercially available at higher power levels and better beam quality than that shown in figure 12. The trumpf disk lasers deliver up to 4000 W laser power with beam quality of 8 mm.mrad and IPG photonics high power cw fiber lasers deliver up to 20000 W with excellent beam parameter product. The thin disk and fiber lasers can be used for welding and cutting applications. /16,44/
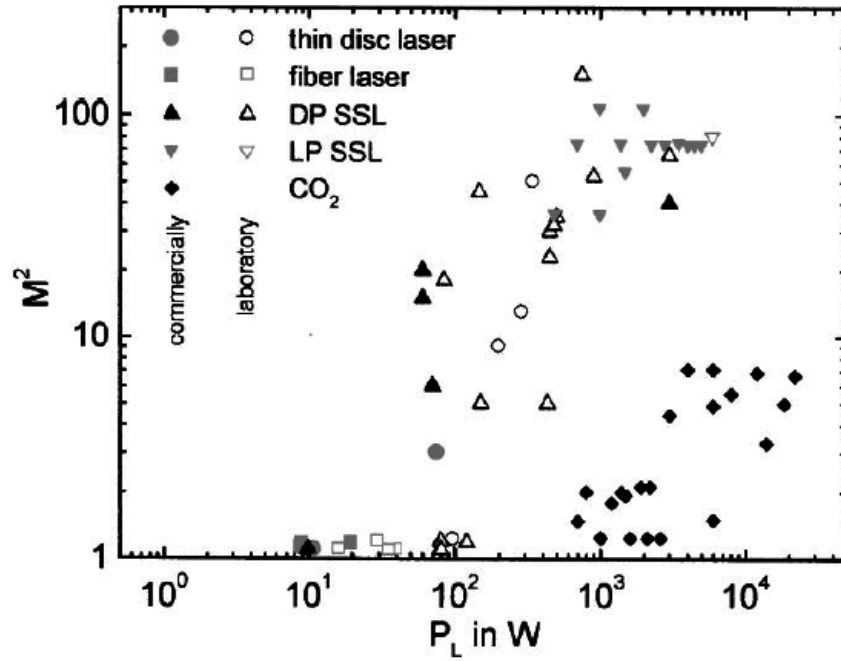
Figure 12. Times diffraction limit factor M^2 depending on laser power of devices for materials processing. /12/

Besides the wavelength, which affects the physical mechanisms involved in energy coupling and hence process efficiency, stability and quality, another inherent and equally important property of the laser beam is its BPP. A low BPP is beneficial for both the process and system. /12/

5.1 Process benefits of low BPP

For the deep penetration welding and cutting processes, a characteristic temperature has to be reached in the material for melting and evaporation to occur while some energy is lost by heat conduction away from the interaction zone. Consequently, these processes are characterized by energy thresholds such that a power intensity exceeding the threshold value is required in order to yield a safe process and this is more easily reached the smaller the focused diameter (d_f) for a given power. The maximum achievable speed for welding or cutting also roughly scales with the power intensity. At a given value of traverse speed, v, the welding depth or cut thickness can be raised proportionally to the power intensity. The

beneficial effect of high beam quality (low value of BPP or M^2) is in achieving a smaller focused diameter, which reduces the necessary power for doing a particular job. /12/

5.2 System benefits of low BPP

To obtain a particular focused diameter (d_f), the F-number (focal length divided by beam diameter on the optic) can be made larger if M^2 is smaller which is beneficial in designing of focusing heads basing on two aspects that are explained below. /12/

Firstly, increasing the F-number by applying optics with larger focal lengths enlarges the working distance and the depth of focus thereby making the process less sensitive to variations in the working distance due to handling or workpiece inaccuracies. The optics would also be less exposed to fume and spatters. /12/

Secondly, the beam diameter (D) at the optic can be made smaller if a smaller focal length (f) can be tolerated. Consequently, the optic and the focusing head can be made smaller in size and mass making it favorable with respect to better accessibility and higher dynamics of the robot handling the focusing head. This aspect is also important for multi-focus techniques, as it is easier to build focusing optics for the combination or splitting of beams into a desired focus matrix when the diameters of the individual beams can be kept smaller. /12/

Furthermore, the beam quality is essential if a beam combination at the entrance side of the fiber is intended to increase the power at the workpiece above the level available by a single device or module. The attainable focused diameter after fiber transmission is closely related to the fiber diameter (d) and a small fiber diameter, which is favored by a high beam quality, is desirable. /12/

6. LASER CUTTING

Laser cutting is a thermal cutting process in which a cut kerf (slot) is formed by the heating action of a focused traversing laser beam of power density on the order of 10^4 W mm^{-2} in combination with the melt shearing action of a stream of inert or active assist gas. /45/ The focused laser beam melts the material throughout the material thickness and a pressurized gas jet, acting coaxially with the laser beam, blows away the molten material from the cut kerf. The basic principle of laser cutting is shown in figure 13 and the terms related to the cutting process are illustrated in figure 14. /9,11,25/
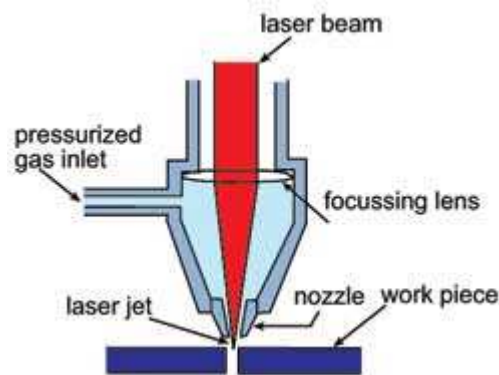
Figure 13. Basic principle of laser cutting /46/
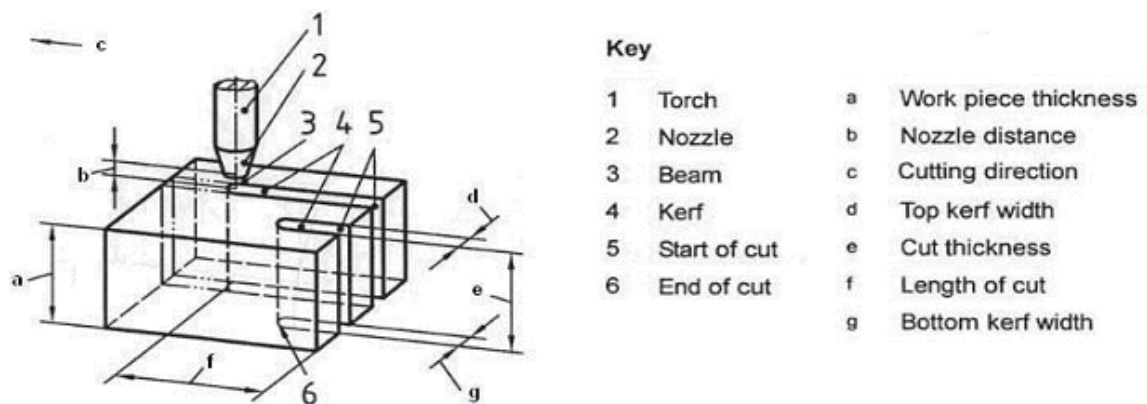
Figure 14. Terms related to the cutting process of the workpiece /15/

The laser cutting process types, defined according to their dominant transformation process, include: laser fusion cutting (inert gas cutting), laser oxygen cutting and laser vaporization

cutting. These cutting methods - discussed in detail in the following sections - are applicable for the cutting of metals commonly used in industry. /9,11/

6.1 Laser fusion cutting

The laser fusion cutting process, also called inert gas melt shearing, is based on transformation of the material along the kerf into the molten state by heating with laser energy and the molten material blown out of the kerf by a high-pressure inert gas jet. The laser beam is the only heat source during this cutting process and the high-pressure inert gas jet is responsible for melt ejection. The inert gas jet (mainly nitrogen or argon) is also responsible for shielding the heated material from the surrounding air as well as protecting the laser optics. Figure 15 is a schematic of laser fusion cutting. /9,11,25,45/
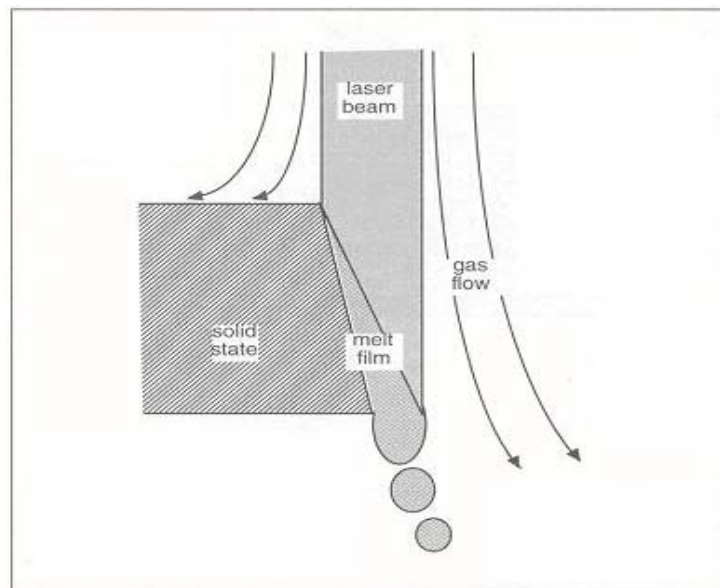
Figure 15. A sketch of laser fusion cutting /9/

Laser fusion cutting is applicable to all metals especially stainless steels and other highly alloyed steels, aluminium and titanium alloys. A high quality cut edge is formed but the cutting speeds are relatively low in comparison with active gas cutting mechanisms. The advantage of this process is that the resulting cut edges are free of oxides and have the same corrosion resistance as the substrate. The cut edges may be welded without any post-cutting

preparation. The main technical demand is to avoid adherent melt (dross attachment) at the bottom edges of the kerf. A high pressure (above 10 bar) is recommended to remove liquid that can adhere to the underside and solidify as dross. /9,11, 25,45/

6.2 Laser oxygen cutting

The principle of laser oxygen cutting is that the focused laser beam heats the material in an oxidizing atmosphere and ignites an exothermic oxidation reaction of the oxygen with the material. The exothermic reaction supports the laser cutting process by providing additional heat input in the cutting zone resulting into higher cutting speeds compared to laser cutting with inert gases. The laser beam is responsible for igniting and stabilizing a burning process within the kerf, and the assist gas blows out the molten material from the cut zone and protects the laser optics. Figure 16 is a schematic of laser oxygen cutting. /9,11, 25,45/
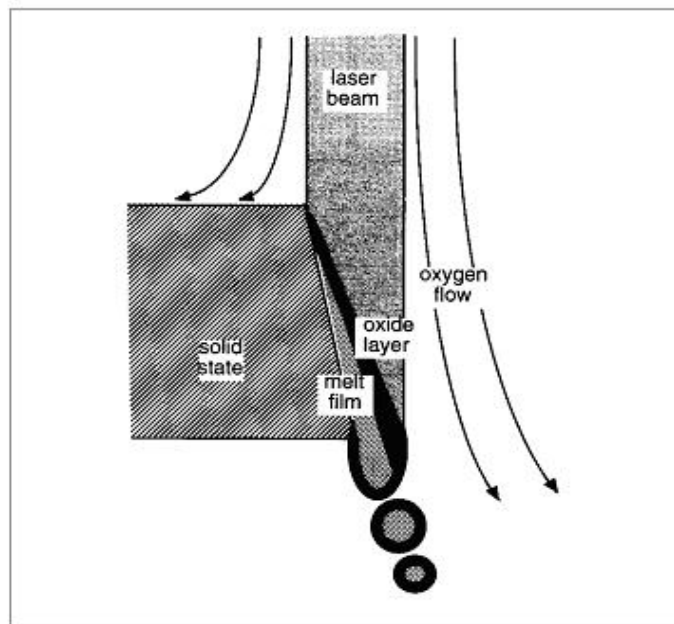
Figure 16. A sketch of laser oxygen cutting /9/

Laser oxygen cutting is applicable to mild steel and low-alloyed steel. The formation of the oxide layer on the cutting front increases the absorption of the laser radiation compared to absorption of a pure metallic melt. The oxides reduce the viscosity and surface tension of

the melt and thereby simplify melt ejection. However, the resulting cut edges are oxidized. /9/

6.3 Laser vaporization cutting

During laser vaporization cutting, the material is heated beyond its melting temperature and eventually vaporized. A process gas jet is used to blow the material vapor out of the kerf to avoid precipitation of the hot gaseous emissions on the workpiece and to prevent them from condensation within the developing kerf. Figure 17 is a schematic of laser vaporization cutting. /9,11/
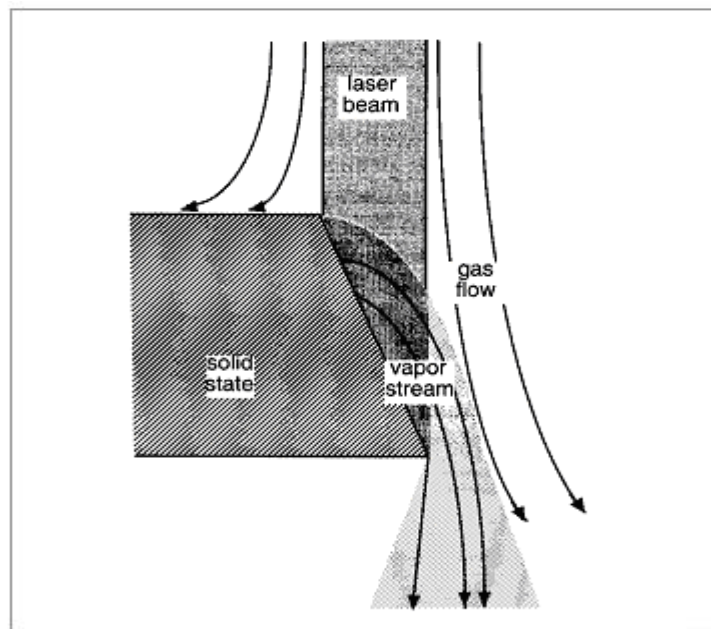
Figure 17. A sketch of laser vaporization cutting /9/

Typical materials that are cut by the vaporization method are acrylic, polymers, wood, paper, leather and some ceramics. This method has a high power requirement that depends on the thermal properties of the material. High power densities are obtained by appropriate adjustment of the laser radiation and focusing. For cutting of metals, laser vaporization cutting is the method with the lowest speed among other methods; however, it is suitable for very precise, complex cut geometries in thin workpieces. /9,45/

7. LASER CUTTING PARAMETERS

The laser cutting parameters are dependent on the beam characteristics, the cutting rate required, the composition and thickness of the material to be cut, and the desired cut edge quality. The laser cutting process and cut quality depend upon the proper selection of laser and workpiece parameters. /45,47/ Deficiencies in cutting quality may be related to the slow process drifts and disturbances that are caused by velocity fluctuations, variation in power and spatial intensity distribution as well as optical integrity perturbations. /34/ The effects of the beam parameters, process parameters and material parameters are described in the following sections.

7.1 Beam parameters

These are parameters that characterize the properties of the laser beam and include the wavelength, power and intensity, beam quality and polarization. Prior to significant heating of the workpiece, the incident laser beam is reflected, scattered and absorbed in proportions determined by the wavelength of the irradiation, the state of polarization of the laser beam, the angle of incidence and the optical properties of the surface. /47/

7.1.1 Wavelength

Reflectivity of metallic materials to laser light is a function of laser wavelength whereby metals are highly reflective to long infrared wavelengths (CO_2 laser wavelength) than the shorter infrared wavelengths (Nd:YAG laser wavelength). /48,49/ An Nd:YAG beam can be focused to a smaller diameter than a CO_2 laser beam, providing more accuracy, a narrower kerf width and low surface roughness. /45/ Figure 18 shows the absorption phenomena of some frequently used metals over a range of different laser wavelengths.
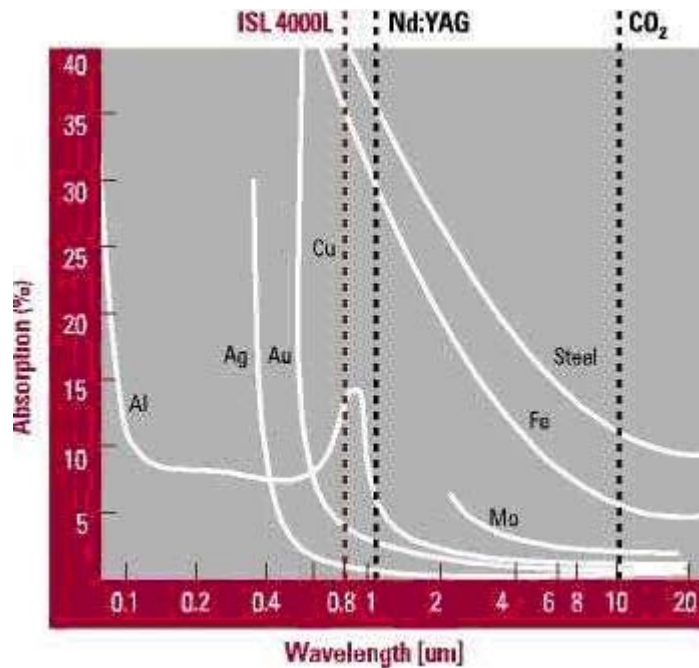
Figure 18. Absorption phenomena of typical metals over a range of different laser wavelengths. /50/

Absorption of the longer infrared wavelength of a CO_2 laser (10.6μm) is governed by the electrical conductivity of the material. At room temperature, highly conducting metals such as gold, silver, aluminium and copper absorb only a very small amount of CO_2 laser radiation and reflect the large majority of it, medium conductors such as steel show an absorption of around 10% and insulators such as plastics and wood-based materials show a perfect absorption. On the other hand, the absorption of the shorter infrared wavelength of the Nd:YAG laser (1.06μm) is governed by the lattice atoms. For metals, this mechanism leads to good absorption that is higher than in the case of CO_2 laser wavelength. However, insulators show only negligible absorption and nearly perfect transmission of radiation at the Nd:YAG wavelength because insulators require large energy to be ionized in order for absorption of radiation to take place. Nevertheless, the suitability of a particular laser for an application than others is more often attributed to other laser parameters such as peak power, pulse length and focusability other than wavelength characteristics. Both Nd:YAG and CO_2 lasers can overcome the high initial reflectivity of many metals provided the intensity of the focused beam is sufficiently high. /48,49/

28

Metals that are highly reflective to the CO_2 laser light at room temperature become better absorbers when they are heated. After a cut has been started, the cut acts as a black body and the incident laser light is strongly absorbed by the thin molten layer. The reflectivity of the laser light impinging on the melt surface is dependent on the angle of incidence of the laser beam, plane of polarization of the laser light and the optical properties of the molten material. The heating - increased absorption - heating cycle is difficult to set up in the very highly reflective non-ferrous metals such as copper and aluminium. This is because these metals combine a high reflectivity with a high thermal conductivity, which reduces the efficiency of the cutting process. /9,11,25/

7.1.2 Power and intensity

Laser power is the total energy emitted in the form of laser light per second while the intensity of the laser beam is the power divided by the area over which the power is concentrated. High beam intensity, obtained by focusing the laser beam to a small spot, is desirable for cutting applications because it causes rapid heating of the kerf leaving little time for the heat to dissipate to the surrounding which results into high cutting speeds and excellent cut quality. Additionally, reflectivity of most metals is high at low beam intensities but much lower at high intensities and cutting of thicker materials requires higher intensities. The optimum incident power is established during procedure development because excessive power results in a wide kerf width, a thicker recast later and an increase in dross while insufficient power cannot initiate cutting. /45,49/

High power beams can be achieved both in pulsed and continuous modes; however, high power lasers do not automatically deliver high intensity beams. Therefore, the focusability of the laser beam is an important factor to be considered. /49/

7.1.3 Beam quality

The laser beam quality is characterized by the mode of a laser beam, which is the energy distribution through its cross section. A good beam mode having uniform energy distribution is essential for laser cutting because it can be focused to a very small spot giving high power density, which leads to high cutting speeds and low roughness. Higher order modes with zones of elevated energy density outside the major spot may result in a poor cut quality due to heating of the material outside the kerf. /49/

Theoretically, the lowest order mode, TEM_{00}, refers to a gaussian intensity distribution about a central peak. The TEM_{00} mode gives the smallest focused spot size with very high intensity in comparison with higher order beam modes. The TEM_{00} mode also has the largest depth of focus and therefore gives the best performance when cutting thicker materials. The highest edge quality can be obtained if the Rayleigh length (depth of focus) is equal to the sheet thickness. However, in practice, high power lasers usually deliver higher order modes that give a larger focused spot size than the TEM_{00} mode. The laser beam quality is measured by factors K or M^2 ($M^2 = 1/K$) and the TEM_{00} mode has a beam quality factor, K, close to 1 while higher order modes have lower K-values. An M^2 value of 1 corresponds to a 'perfect' gaussian beam profile but all real beams have M^2 values greater than 1. /45,49,51/

The K or M^2 value is sufficient for the comparison of laser beams from similar laser systems having the same wavelength. The Beam Parameter Product (BPP) is the standard measure of beam quality that is used for the comparison of laser beams from different laser systems because it includes the wavelength effects. The BPP is defined by the relationship in equation 1 below.

$$BPP = \Theta d_0/4 = \lambda M^2/\pi$$ ....(1)

In this relation, Θ denotes the full divergence angle, d_0 the waist diameter, λ the wavelength and M^2 the times diffraction limit factor which tells how much larger is the BPP of the laser under consideration compared to the physically lowest value of λ/π for a

beam in the TEM$_{00}$ mode (diffraction limit). The focus diameter (d_f) achievable with a given focusing number (F - focal length divided by the beam diameter on the optic) is directly proportional to the BPP as illustrated in equation 2 below.

$$d_f = (\Theta d_0)F = (4\lambda/\pi)M^2F = 4F \cdot BPP \text{...(2)}$$

The depth of focus (z) describing the distance within which the beam's cross-section and hence its power density varies up to a factor of 2, also directly depends on the BPP as equation 3 illustrates.

$$z = d_f F = (\Theta d_0)F^2 = (4\lambda/\pi)M^2F^2 = 4F^2 \cdot BPP \text{................................(3)} \ /12/$$

The CO$_2$ lasers for high speed cutting have K-values around 0.8 while Nd:YAG lasers in the kW-range tend to have lower beam qualities than CO$_2$ lasers of the corresponding power. /49/ However, the new developments of the solid-state laser namely: the thin disk laser and fiber laser have noticeably better beam qualities than Nd:YAG lasers. /16,31/

7.1.4 Beam polarization

In laser cutting, the laser light is coupled into the material on the cut front where light absorption takes place in a thin surface molten layer. The reflectivity of the laser light impinging on the melt surface is dependent on the angle of incidence of the laser light, plane of polarization of the laser light and optical properties of the molten material. /52/

Laser beam polarization can be linear (also called plane polarization), circular, elliptic or random. Linear polarization exists in two possibilities, either parallel or perpendicular to the plane of incidence, and the two options are absorbed differently in different directions during the cutting process. The material is a good absorber of parallel-polarized light at an irradiation angle known as Brewster's angle, which is about 80°. On the other hand, the perpendicularly polarized light is reflected more strongly. /48,49,53/

The influence of beam polarization during cutting is basically related to the inclination of the cut kerf resulting from the relationship between the polarization surface and the cutting direction. The polarization influence becomes larger as the plate thickness increases and is

most significant on cutting of materials with a high reflectivity for normal incident radiation i.e. metallic materials than when cutting materials with a low reflectivity for normal incident radiation i.e. nonmetals. When cutting of materials with a high reflectivity for normal incident radiation is performed with a linear polarized laser, the absorption of energy in the cutting kerf depends upon the angle, ψ, between the plane of polarization, p, and the cutting direction, c, as shown in figure 19. /45,49,54,55/
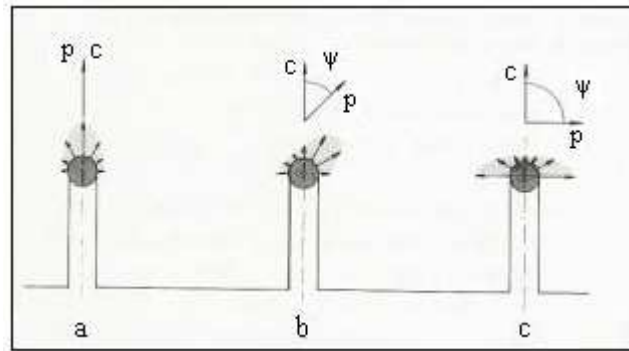
Figure 19. The relative absorption of energy for different orientations of the cutting direction and direction of polarization, whereby ψ is the angle between the plane of polarization, p, and the cutting direction, c. /55/

When the angle ψ, is 0°, the front of the cutting kerf absorbs more energy than the sides but when the angle, ψ, is 90°, the front of the cutting kerf absorbs less energy than the sides. Therefore, the cutting speed can be higher when cutting in the same direction as the plane of polarization than when cutting in a direction perpendicular to the plane of polarization. The energy absorption is asymmetric when ψ is between 0° and 90° causing an asymmetric cutting profile. A smaller cut kerf width is obtained when cutting in the direction of polarization than when cutting in the perpendicular direction. /55/

The perfectly circularly polarized light achieves nearly uniform cut kerfs in every direction but the linearly or elliptically polarized light produces a variation on the inclination of the cut kerf. /54/ Metal cutting with a linear polarized beam is an advantage if cutting can be done in direction of the polarization but curve cutting with a linear polarized beam causes variation in the cutting profile as shown in figure 20 in which the cut edges are not square

in some positions. /55/ When cutting is to be performed in more than one direction, circular or random beam polarization is favorable in order to get a uniform cut of a high quality. /49/
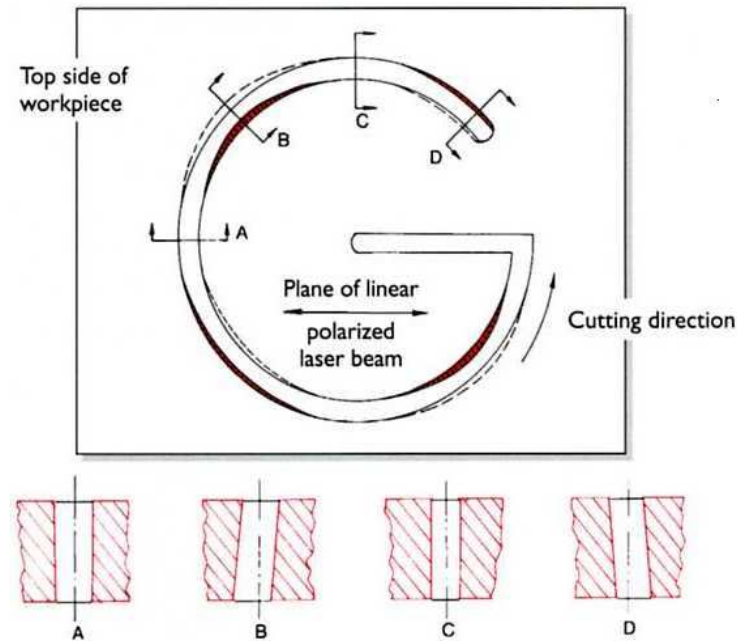
Figure 20. Effects of polarization in cutting /49/

Beam polarization is of concern for CO_2 laser cutting since the light from a CO_2 laser is linearly polarized but light from Nd:YAG lasers is randomly polarized and so cutting performance is not affected by direction. A phase-shift mirror is used in cutting machines with CO_2 lasers to change light with linear polarization into circular polarization. /45,49/

7.2 Process parameters

The process parameters include those characteristics of the laser cutting process that can be altered in order to improve the quality of the cutting process and achieve the required cutting results. However, some process parameters are normally not altered by the operator.

7.2.1 Continuous wave (cw) or pulsed (p) laser power

High intensity can be achieved in both pulsed and continuous beams. The peak pulse power in pulsed cutting or the average power in continuous cutting determines the penetration. A high power CW laser beam is preferred for smooth, high cutting rate applications particularly with thicker sections because the highest cutting speeds can be obtained with high average power levels. However, the removal of molten or vaporized material is not efficient enough to prevent some of the heat in the molten/vaporized material from being transferred to the kerf walls causing heating of the workpiece and deterioration of the cut quality. A lower energy pulsed beam is preferred for precision cutting of fine components producing better cuts than a high power CW laser because the high peak power in the short pulses ensures efficient heating while the low average power results in a slow process with an effective removal of hot material from the kerf reducing dross formation. A pulsed beam of high peak power is also advantageous when processing materials with a high thermal conductivity and when cutting narrow geometries in complex sections where overheating is a problem. /45,49/

The striations formed during pulsed cutting are finer than those formed during continuous wave cutting (see figure 21). Additionally, cutting at sharp corners is better achieved with pulsed cutting than continuous wave cutting as illustrated in figure 22. /25,49/
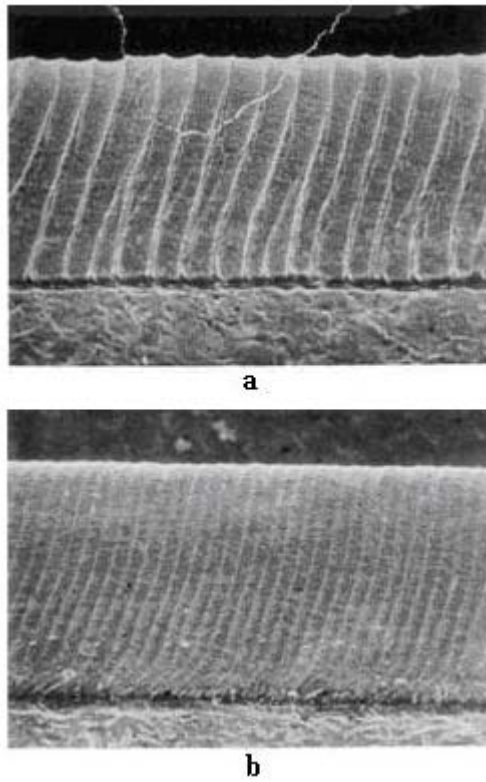
Figure 21. A comparison of (**a**) continuous wave laser cutting and (**b**) pulsed laser cutting /25/
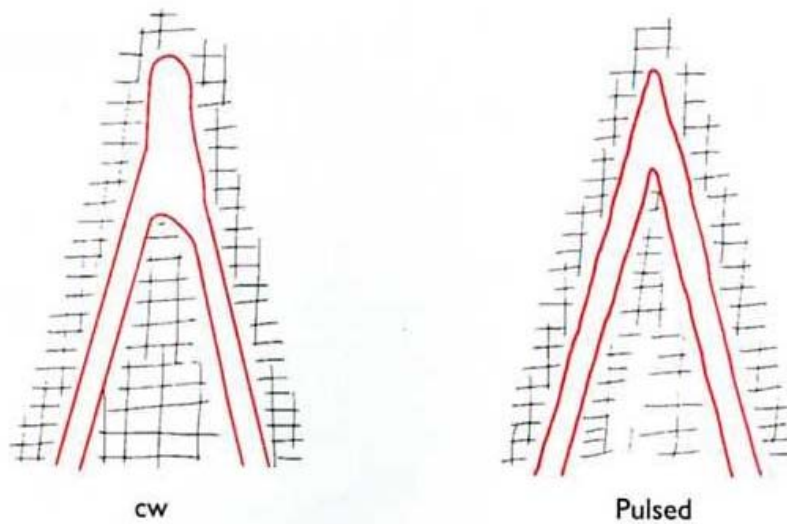
Figure 22. Effect of pulsing at a sharp corner /49/

7.2.2 Focal length of the lens

Solid-state lasers usually utilize fiber optics for beam delivery and a collimator is used to form the divergent laser beam emitting from the light cable into a parallel laser beam. After the laser beam has passed the laser light cable and the collimator, the focusing lens then focuses the parallel laser beam onto the workpiece. CO_2 lasers do not utilize fiber optics for beam delivery; therefore, the beam emitted by the laser is directly focused onto the workpiece using a focusing lens. The laser cutting process requires focusing a high-power laser beam to a small spot that has sufficient power density to produce a cut through the material. The focal length of the focusing lens determines the focused spot size and also the depth of focus which is the effective distance over which satisfactory cutting can be achieved. /45,49/

The focusability of laser beams is illustrated in figure 23 in which $2 \cdot z$ is the depth of focus (Rayleigh length) and equation 4 shows the parameters that determine the focused spot size (d_f). It indicates that a small spot diameter is favored by a short focal length (f), good beam quality having K-value close to 1 ($M^2 = \frac{1}{K}$), large raw beam diameter at the lens (D) and short wavelength of the laser beam (λ). The depth of focus is also dependent on the same parameters as the focused spot diameter; generally a small spot size is associated with a short depth of focus. /49/

$$d_f = \frac{4\lambda}{\pi} \cdot \frac{f}{D} \cdot \frac{1}{K} = \frac{4\lambda}{\pi} \cdot \frac{f}{D} \cdot M^2 \dots\dots\dots\dots\dots\dots\dots\dots\dots\dots\dots\dots\dots\dots(4)$$
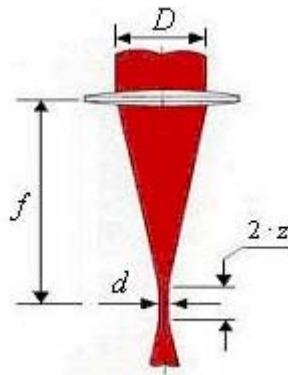
Figure 23. Focusability of laser beams /49/

For cutting of thin materials (less than 4mm in thickness), a short focal length - typically 63mm - gives a narrow kerf and smooth edge because of the small spot size. A longer focal length is preferred for thick section cutting where the depth of focus should be around half the plate thickness. /45/ The use of long focal length lenses enlarges the working distance, minimizes the contamination of the lens and increases the depth of focus. A high quality laser beam would enable the use of longer focusing optics without compromising on the focused spot size. The critical factors that determine the selection of the lens for a cutting application are the focused spot diameter and the depth of focus so the focal length has to be optimized with respect to the material thickness to be cut. /27,49/

7.2.3 Focal position relative to the material surface

The focal position has to be controlled in order to ensure optimum cutting performance. Differences in material thickness may also require focus alterations and variations in laser beam shape. /49/

When cutting with oxygen, the maximum cutting speed is achieved when the focal plane of the beam is positioned at the plate surface for thin sheets or about one third of the plate thickness below the surface for thick plates. However, the optimum position is closer to the lower surface of the plate when using an inert gas because a wider kerf is produced that allows a larger part of the gas flow to penetrate the kerf and eject molten material. Larger nozzle diameters are used in inert gas cutting. If the focal plane is positioned too high relative to the workpiece surface or too far below the surface, the kerf width and recast layer thickness increase to a point at which the power density falls below that required for cutting. /45/

7.2.4 Cutting speed

The energy balance for the laser cutting process is such that the energy supplied to the cutting zone is divided into two parts namely; energy used in generating a cut and the energy losses from the cut zone. It is shown that the energy used in cutting is independent of the time taken to carry out the cut but the energy losses from the cut zone are proportion to the time taken. Therefore, the energy lost from the cut zone decreases with increasing cutting speed resulting into an increase in the efficiency of the cutting process. A reduction in cutting speed when cutting thicker materials leads to an increase in the wasted energy and the process becomes less efficient. The levels of conductive loss, which is the most substantial thermal loss from the cut zone for most metals, rise rapidly with increasing material thickness coupled with the reduction in cutting speed. /56/

The cutting speed must be balanced with the gas flow rate and the power. As cutting speed increases, striations on the cut edge become more prominent, dross is more likely to remain on the underside and penetration is lost. When oxygen is applied in mild steel cutting, too low cutting speed results in excessive burning of the cut edge, which degrades the edge quality and increases the width of the heat affected zone (HAZ). In general, the cutting speed for a material is inversely proportional to its thickness. The speed must be reduced when cutting sharp corners with a corresponding reduction in beam power to avoid burning. /45/

7.2.5 Process gas and gas pressure

The process gas has five principle functions during laser cutting. An inert gas such as nitrogen expels molten material without allowing drops to solidify on the underside (dross) while an active gas such as oxygen participates in an exothermic reaction with the material. The gas also acts to suppress the formation of plasma when cutting thick sections with high beam intensities and focusing optics are protected from spatter by the gas flow. The cut edge is cooled by the gas flow thus restricting the width of the HAZ. /45/

The choice of process gas has a significant effect on the productivity and quality of the laser cutting process. The commonly used gases are oxygen (active gas) and nitrogen (inert gas) with each having its own advantages and potential disadvantages. Although nitrogen is not purely inert, it is the most commonly used gas for inert gas cutting because it is relatively cheap. Purely inert gases, argon and helium, are common choices when cutting titanium since they prevent the formation of oxides or brittle titanium nitrides. /1,11,45/

Nitrogen gas is the preferred gas for the cutting of stainless steel, high-alloyed steels, aluminium and nickel alloys and it requires higher gas pressures to remove the molten material from the cut kerf. The high gas pressure provides an extra mechanical force to blow out the molten material from the cut kerf. When high-pressure nitrogen cutting is used to cut stainless steel, it produces a bright, oxide free cut edge but the processing speeds are lower than in oxygen assisted cutting. The main problem associated with the inert gas cutting is the formation of burrs of resolidified material on the underside of the kerf. Burr-free cutting conditions are achieved by optimization of the principle processing parameters; nozzle diameter, focal position and gas pressure. The nitrogen pressure lies in the range of 10-20 bar and the pressure requirement increases with increasing material thickness. Nitrogen gas purity should be above 99.8%. /1,9,11,45,49/

Oxygen is normally used for cutting of mild steel and low-alloyed steels. Use of oxygen causes an exothermic reaction, which contributes to the cutting energy resulting into high cutting speeds and the ability to cut thick sections up to 12mm. However, oxygen cutting leads to oxidized cut edges and requires careful control of process parameters to minimize dross adherence and edge roughness. The oxygen gas nozzle pressure usually lies in the range of 0.5-5 bar. The oxygen pressure is reduced as plate thickness is increased to avoid burning effects and the nozzle diameter is increased. High gas purity is important – mild steel of 1mm thickness can be cut up to 30% more quickly using 99.9% or 99.99% purity oxygen in comparison with the standard oxygen purity of 99.7%. /1,9,11,45,49/

Figure 24 shows the typical cutting speeds for high pressure nitrogen cutting of stainless steel and oxygen assisted cutting of mild steel with 2 kW CO_2 laser. The cutting speeds and

maximum material thickness cut are relatively higher for the oxygen assisted cutting than for high pressure nitrogen cutting. /49/
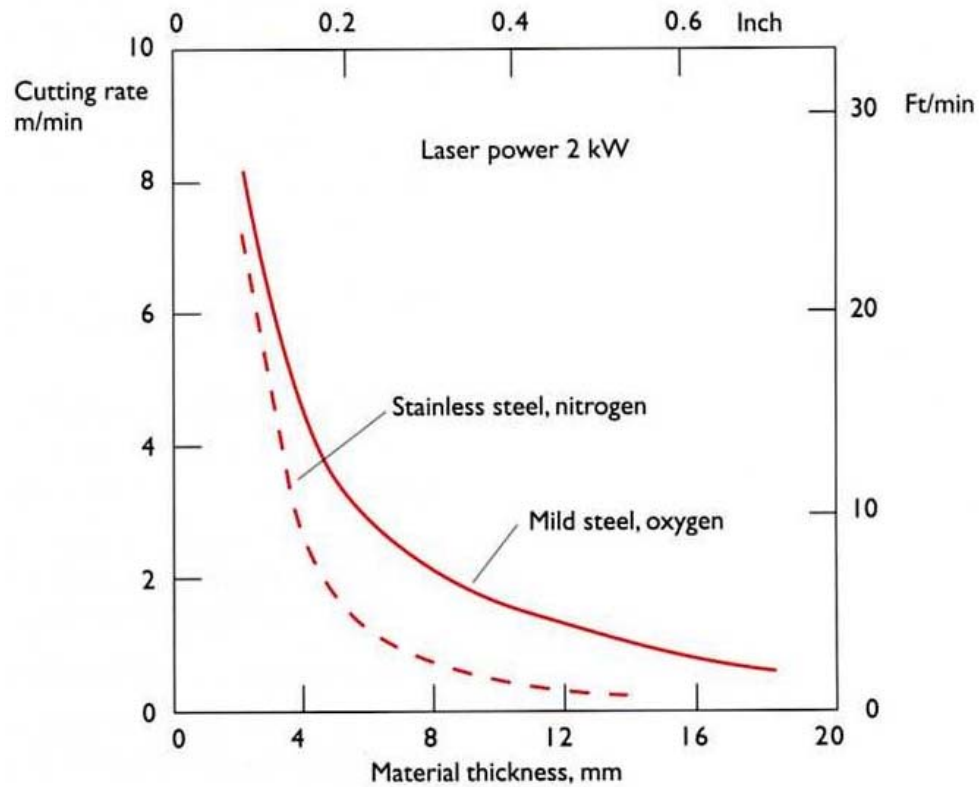
Figure 24. Cutting speed for a 2kW CO_2 laser. Oxygen is used as cutting gas for mild steel. High pressure nitrogen (20 bar) is used for stainless steel /49/

7.2.6 Nozzle diameter and standoff distance

The nozzle delivers the cutting gas to the cutting front ensuring that the gas is coaxial with the laser beam and stabilizes the pressure on the workpiece surface to minimize turbulence in the melt pool. The nozzle design, particularly the design of the orifice, determines the shape of the cutting gas jet and hence the quality of the cut. The diameter of the nozzle, which ranges from 0.8 mm and 3 mm, is selected according to the material and plate thickness. /45/ Due to the small size of the focused laser beam, the cut kerf created during laser cutting is often smaller than the diameter of the nozzle. Consequently, only a portion of the gas jet formed by the nozzle penetrates the kerf, which necessitates the use of a high

gas pressure. /49/ Off-axis nozzles have also been used in mirror focusing applications but the cutting pressure is limited to 200Kpa. /57/

The stand-off distance is the distance between the nozzle and the workpiece. This distance influences the flow patterns in the gas, which have a direct bearing on the cutting performance and cut quality. Large variations in pressure can occur if the stand-off distance is greater than about 1mm. A stand-off distance smaller than the nozzle diameter is recommended because larger standoff distances result in turbulence and large pressure changes in the gap between the nozzle and workpiece. With a short standoff distance, the kerf acts as a nozzle and the nozzle geometry is not so critical. Figure 25 shows the nozzle geometry definitions. /45,49/
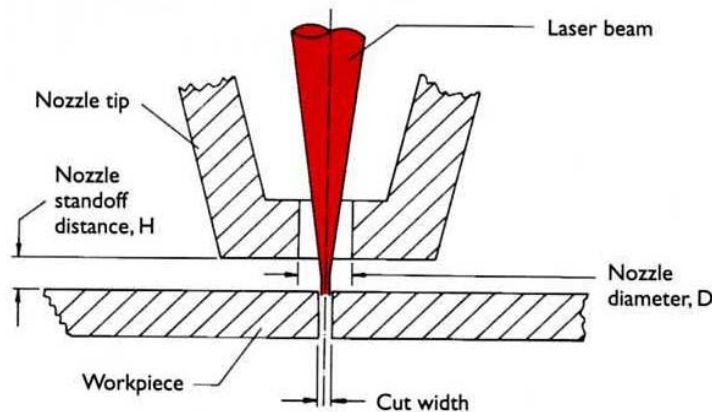
Figure 25. Nozzle geometry – definitions /49/

Kai Chen et al examined the effects of processing parameters such as gas pressure and nozzle standoff distance on cut quality. Their numerical simulations and laser cutting experiments revealed that the fluctuation of pressure gradient and shear force at the machining front has detrimental effects on the removal capability of the gas jet, which often results in poorer cut quality. /58/

The structure of shocks present in supersonic flow from laser cutting nozzles results in a reduction of the stagnation pressure accross the shock. The interaction of the shocks with a workpiece result in a cutting pressure that shows large variations as a function of nozzle

standoff distance. For higher nozzle pressures, the cutting perfomance is impaired by the formation of a strong normal shock (the Mach Shock disk, MSD). The flow downstream of the MSD is subsonic having suffered a large drop in stagnation pressure and results in a low laser cutting pressure. Besides causing a significant reduction in the cutting pressure, the MSD also encourages the formation of a stable stagnation bubble on the surface of the workpiece. The stagnation bubble could result in ineffective debris removal and plasma formation due to absorbtion of laser radiation by trapped debris. /57/

7.2.7 Nozzle Alignment

Nozzle misalignment may cause poor cutting quality, as the process is extremely susceptible to any discrepancy in the alignment of the cutting gas jet with the laser beam. The gas flow from the nozzle generates a pressure gradient on the material surface, which is coaxial with the nozzle itself. If the nozzle and the focused laser beam are coaxial, the cutting zone established by the beam will lie directly under the central core of the gas jet and there will be uniform lateral gas flow. Figure 26 (a) illustrates the equilibrium set up if the gas jet and laser beam are coaxial. However, nozzle-laser beam misalignment (see figure 26 (b)) leads to an overall directional gas flow across the top of the cut zone which can lead to unwanted cut edge burning and dross adhesion. /25,45/
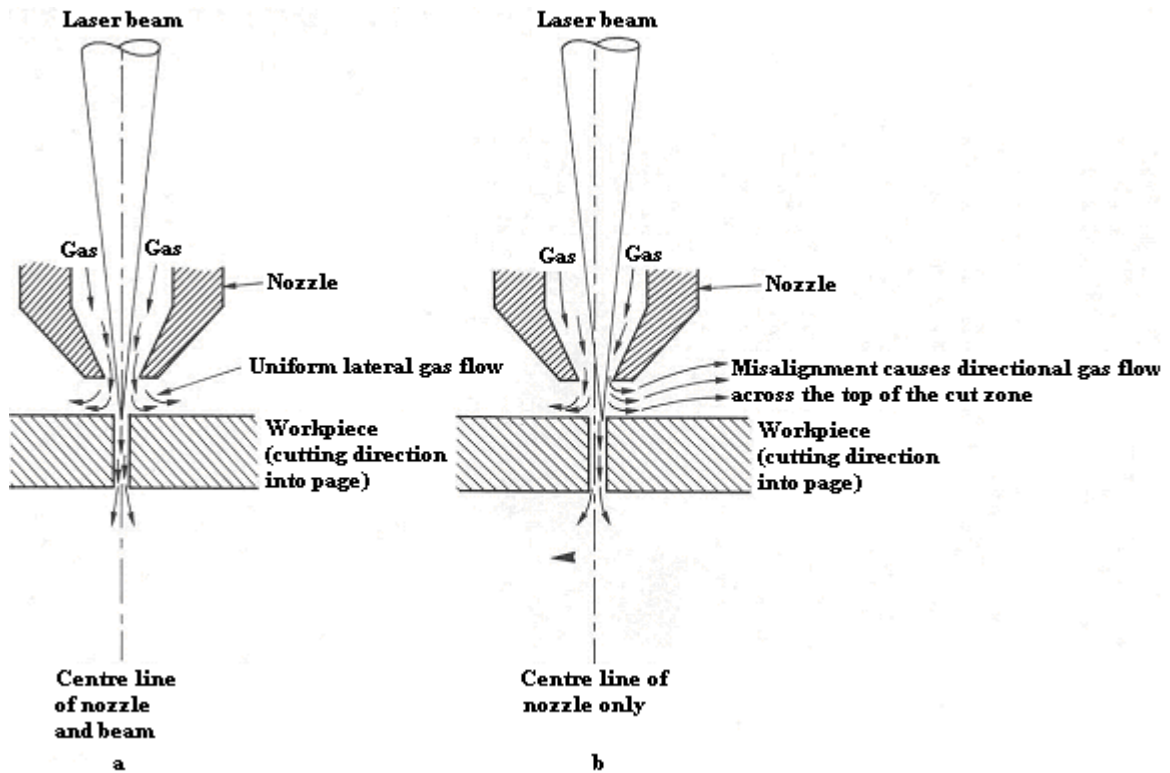
Figure 26. (a) The equilibrium set up when the gas jet and laser beam are coaxial
(b) Nozzle-laser beam misalignment. /25/

However, previous studies have shown that an off-axis nozzle arrangement has some considerable advantages over the coaxial nozzle-laser beam arrangement. When coaxial gas nozzles are applied, the nozzle diameter is considerably larger than the cut kerf therefore the pressure losses in the kerf are larger than those in the nozzle. Since the preferable nozzle standoff distance should be in the range of 0.3mm or more, most of the gas flows out in between the nozzle and the workpiece and expands uniformly in all directions. The radial velocity of the gas is zero in the centerline of symmetry and then increases as the gas is expanding. The radial flow affects the gas flow down into the kerf so that the flow down into the kerf is largest if the laser beam is in front of the centerline of the nozzle and smallest if the laser beam is behind the centerline. Therefore, a nozzle arrangement where the laser beam is in front of the centerline of a coaxial nozzle is more efficient than a normal coaxial nozzle-laser beam alignment. It has been shown that the cutting range wherein good cut qualities can be obtained is expanded by utilizing off-axis beam

43

arrangement compared to co-axial laser beam and gas jet. Additionally, the gas consumption is lower for off-axis cutting than for on-axis cutting. /59/

7.3 Material properties

The laser is used to cut a wide range of engineering materials, which include metals such as mild steel, titanium and stainless steel, as well as nonmetallic materials like ceramics, glass, wood, paper and plastics. Cutting of metals requires higher power densities to melt the material but lower power densities are required for cutting of non-metals. /9/ The focused laser radiation that strikes the metal surface is partly absorbed and partly reflected by the metal surface. The fraction of the incident laser power absorbed, determined by the reflectivity of the metal surface, varies as the material heats up partly due to the temperature dependence of the optical properties of the material and partly due to the changes in the surface appearance, metallurgical phase and interaction of the incident light with ejected particulate and gaseous material near the surface. The thermal and physical properties of the material are important in choosing the right laser-material combination as well as the process parameters. /47,49/

7.3.1 Thermal properties

The efficiency of laser cutting depends on efficient energy coupling into the material; therefore, the thermal characteristics of the material play a vital role in determining both the ability of the laser to cut and the quality of the cutting process. /11/

The high reflectivity of some metals to infrared laser light can lead to difficulties with initiation and maintenance of the cutting process. During cutting of metals with high thermal conductivity, the heat is transported rapidly from the cutting front therefore high power levels or low cutting speeds are required to maintain a cutting front. However, reducing cutting speed causes instabilities that can result in abnormal molten regions, blowouts and poor edge quality. Greater amount of energy is required for cutting of

materials with high values of specific heat capacity and those materials with high latent heats of melting and vaporization. /45/

7.3.2 Physical properties

The surface conditions such as presence of grease or paint may interfere with the cutting process resulting in unpredictable performance. Changes in scale thickness or the presence of rolled-in defects and grooves are detrimental to edge quality. However, the presence of a thin, uniform oxide layer can facilitate absorption of the laser beam and improve cutting performance. /45/

Molten materials with high values of surface tension and low viscosity are more difficult to remove from the cutting front by the assist gas resulting into adherent dross on the underside of the cut. The plate thickness determines the relationship between the rate at which cutting can be performed and the incident beam power for a given set of processing parameters. /45/

8. LASER CUTTING OF STAINLESS STEEL

Laser inert gas cutting is the most applicable process type used for cutting of stainless steel. Laser oxygen cutting is also applied in cases where the cut face oxidation is not a critical matter. Laser cutting of stainless steel with inert gas (nitrogen) and active gas (oxygen) as assisting gases are discussed. The workplace safety concerns for both processes are also discussed.

8.1 Laser inert gas cutting of stainless steel

During the laser inert gas cutting process (also called laser fusion cutting), the laser beam is the only heat source and the high-pressure inert gas jet provides the mechanical force for

melt ejection. Stainless steels have relatively low thermal conductivity, which enables them to be cut at relatively high rates since energy remains at the cutting front rather than being dissipated into the material ahead of the cutting front. The nickel present in austenitic grades of stainless steel affects energy coupling and heat transfer limiting the thickness that can be cut with a given laser beam power. /45/

Nitrogen is the most commonly used assist gas for this cutting technique because of its low chemical activity and its cheapness compared with truly inert gases such as argon. Cutting with nitrogen produces cut edges of a high quality but the cutting speed is usually lower than when cutting with oxygen. Dross adhesion to the bottom edge of the material due to the high viscosity of the molten material may be a problem in nitrogen cutting but it is generally addressed by using very high assist gas pressures. A high pressure nitrogen gas jet is used when cut edge quality is of greater importance than cutting speed. Figure 27 is a schematic of the cut zone when laser cutting stainless steel, there is adherent dross on the bottom edge of the sheet. /25,45,56,60/
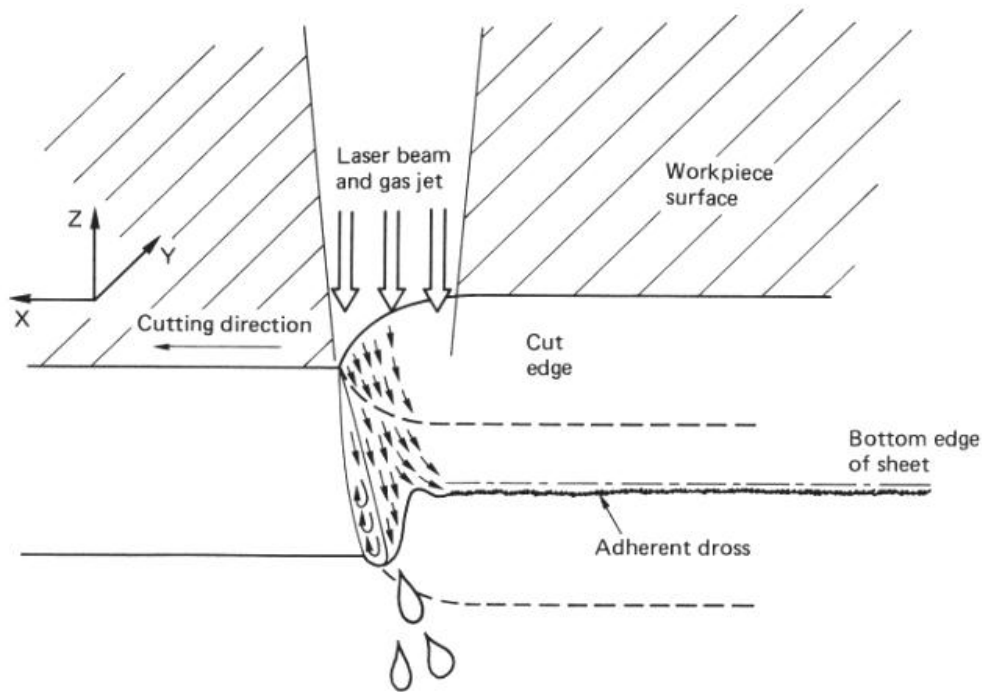
Figure 27. A schematic of the cut zone when laser cutting stainless steel. /25/

Figure 28 shows a typical good quality cut edge produced by high pressure inert gas cutting of 5mm thick stainless steel using a CO_2 laser with the employed gas pressure of 14 bar, cutting speed of 1.1 m/min and a laser power of 1.4 kW. /25/
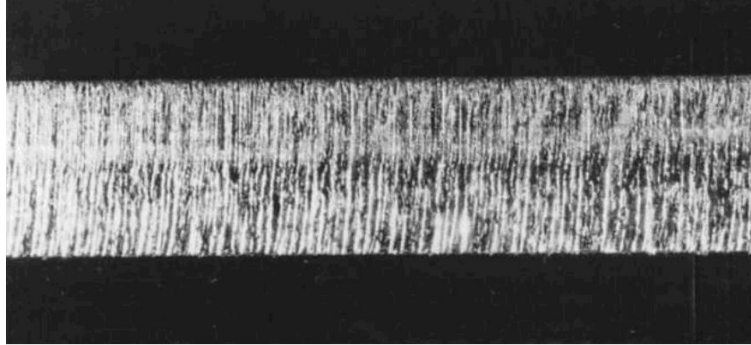
Figure 28. The stainless steel cut edge produced by high-pressure nitrogen cutting. /25/

A comparison of maximum cutting speeds for nitrogen assisted laser cutting of stainless steel (AISI 304) with the CO_2 laser and fiber laser are shown in figure 29. Higher cutting speeds are achieved with the fiber laser. /61/
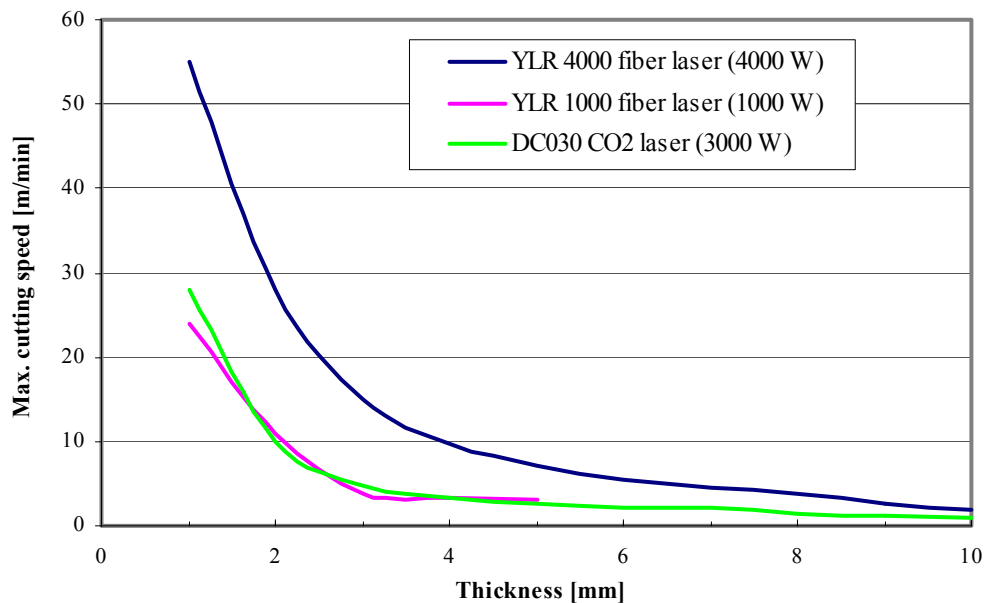
Figure 29. Comparison of maximum cutting speeds with different lasers (The material is stainless steel AISI 304, Nitrogen assisted laser cutting) /61/

8.2 Laser oxygen cutting of stainless steel

During oxygen assisted cutting of stainless steel, chromium that has the greatest affinity for oxygen of all the alloying elements present is oxidized preferentially readily forming oxides with a high melting temperature. These oxides do not dissolve in the molten material but form a seal that limits the exothermic reaction in the upper part of the cutting front. The high surface tension of the oxide leads to dross formation and a rough cut surface. The residual oxide layers left on the cut edge have a higher chromium content than the base material and the solidified melt underlying the oxidized edge has a depleted chromium level. Other alloying elements can also create problems when they react with active gases. /25,45/ Figure 30 shows a schematic of the changes in chemistry across the cross section of the stainless steel cut edge and the typical cut quality obtained is shown in figure 31.
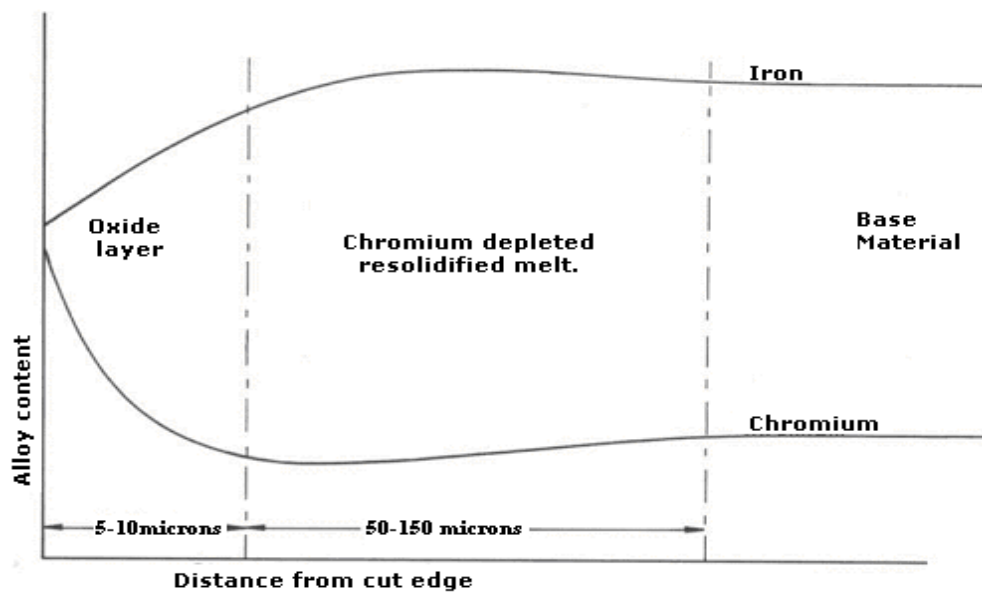
Figure 30. A schematic of the changes in chemistry across the cross section of stainless steel cut edge. /25/
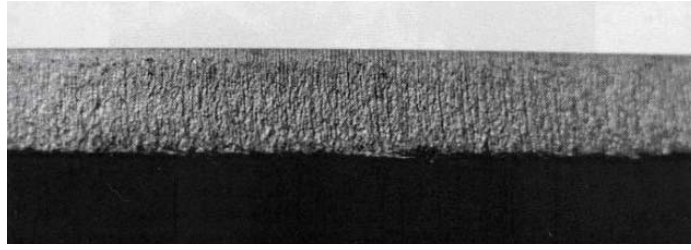
Figure 31. A typical example of a stainless steel cut edge (4 mm thick) produced by oxygen cutting. /25/

The oxidation of stainless steel during cutting is more complex than the mild steel case because the reaction involves the formation of three oxides (Fe_2O_3, Cr_2O_3 and NiO) rather than two (FeO and Fe_2O_3) in mild steel cutting. The formation of the three oxides generates more heat than the simple oxidation of iron to FeO. Therefore, this cutting process is characterized by higher cutting speeds than in fusion cutting. The cutting speed decreases greatly with increase in material thickness and higher laser powers are required to cut thicker materials (see figure 32). /25,56/
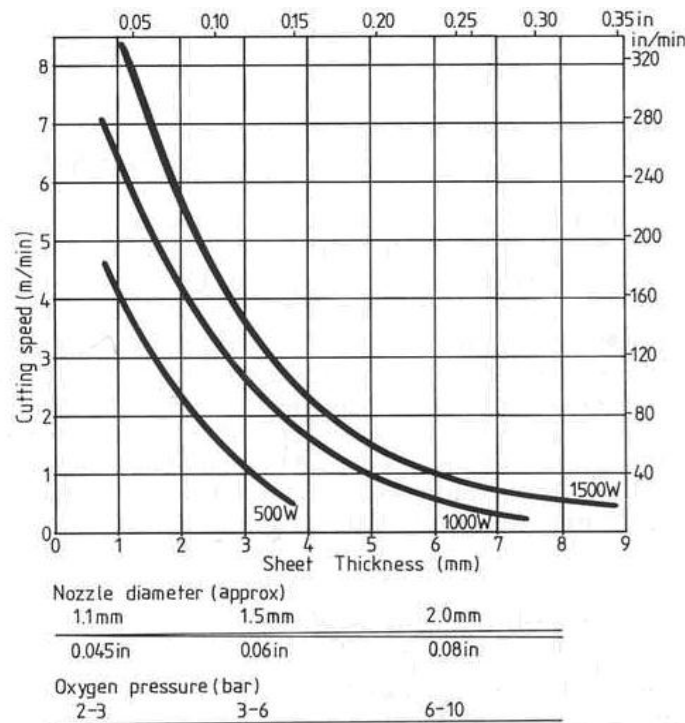
Figure 32. Typical cutting speeds for oxygen-assisted cutting of stainless steels with CO_2 laser. /25/

49

While chromium oxide in small concentrations protects the base material, the chromium oxides formed under laser cutting with even small concentrations of oxygen usually cause corrosion. Therefore, any oxidation of the cut surface must be avoided in order to preserve the corrosion resistance. /62/ Cutting of stainless steel with inert gas is often favored because it avoids the dross problem caused by the formation of high melting point oxides of chromium when stainless steel is cut with oxygen gas. /63/

8.3 Workplace safety during laser cutting of stainless steel

Although, the gases used for laser cutting stainless steel are not toxic, they can be potentially hazardous and the hazards associated with these gases include fume, gas properties and pressure. Precautions must be taken to avoid inhalation of chromium vapour that is generated when cutting stainless steels. /1,45/

The increasing focus on workplace safety has led to assessment of the hazards associated with fume generation from the laser cutting process. Fume extraction is a requirement of laser cutting and most systems are equipped with integral fume extraction systems. The cutting of stainless steel provides an example of how the choice of assist gas can affect the levels of fume generation. An analysis of cutting fume was carried out by Gabzdyl to determine fume formation rates, chemical composition of the fume and the particle size distribution. The results showed that the amount of fume generated by oxygen cutting was 100 times greater than that produced by nitrogen cutting. The particle size and distribution of the oxygen generated fume was smaller, predominantly in the less than 6μm range, a size that is considered to be the most problematical hygienically while the particle size of the fume generated by nitrogen assisted cutting was found to be significantly larger. The chemical analysis of the fume generated by both processes showed that the percentage of chromium (VI), a known carcinogen, in the fume was lower when cutting with nitrogen. /1/

There is a danger to human life if ambient oxygen concentrations fall below 18% while conditions of oxygen enrichment make many materials susceptible to combustion. Operation of the high pressure nitrogen cutting in a confined area causes a risk of oxygen

depletion therefore good ventilation around the laser cutting area is essential as even oxygen and nitrogen can be potentially hazardous. Nitrogen cutting that usually utilizes high pressure requires pipelines and equipment that are suitable for the pressure. /1/

9. CHARACTERISTIC PROPERTIES OF THE LASER CUT

The cut quality is determined by the amount of material removed and the material affected by the cutting process. The characteristic properties of the laser cut that are used to describe the cut quality include the kerf width, perpendicularity of the cut edges, surface roughness, dross attachment and size of heat-affected zone (HAZ). The process parameters influence the efficiency of the laser cutting process and the quality of the cut edge obtained. /2,11,34,64/

The cutting standard EN ISO 9013: 2002 gives tolerances for the perpendicularity of the cut edges and surface roughness. The evaluation and consequences of the imperfections depends on the specific job requirements. /15/ Figure 33 is an illustration of the characteristic properties of the laser cut surface in which dross, cut roughness and heat affected zone (HAZ) are shown.

1. Process gas
2. Cutting nozzle
3. Nozzle offset
4. Cutting speed
5. Molten material
6. Dross
7. Cut roughness
8. Heat affected zone
9. Kerf width
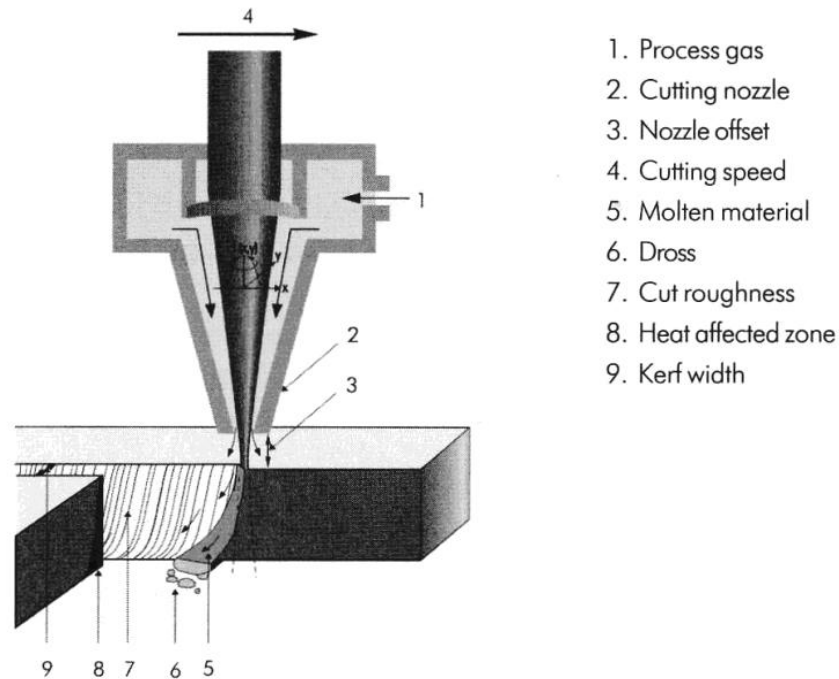
Figure 33. Laser cut surface characteristics /39/

9.1 Kerf width

The kerf width refers to the width of the slot that is formed during through-thickness cutting and is normally narrower at the bottom surface of the workpiece than at the top surface. The kerf width represents the amount of material removed during the cutting process, which is essentially wasted material; therefore, a smaller kerf width is always desirable especially when small details are to be cut. The width of the cut kerf corresponds to the circular beam waist size which is determined mainly by the laser beam quality and focusing optics. The power at the focused spot, cutting speed and the assist gas jet also have influence on the size of the cut kerf. /2,11,34,45,56/

Yilbas examined the effects of laser output power, cutting speed and energy coupling factor at the workpiece surface on the resulting kerf size. Figure 34 shows the variation of kerf width with cutting speed, laser output power and energy coupling factor. Increases in laser power, energy coupling factor and reduction in cutting speed were found to result in increased kerf width. /65,66/
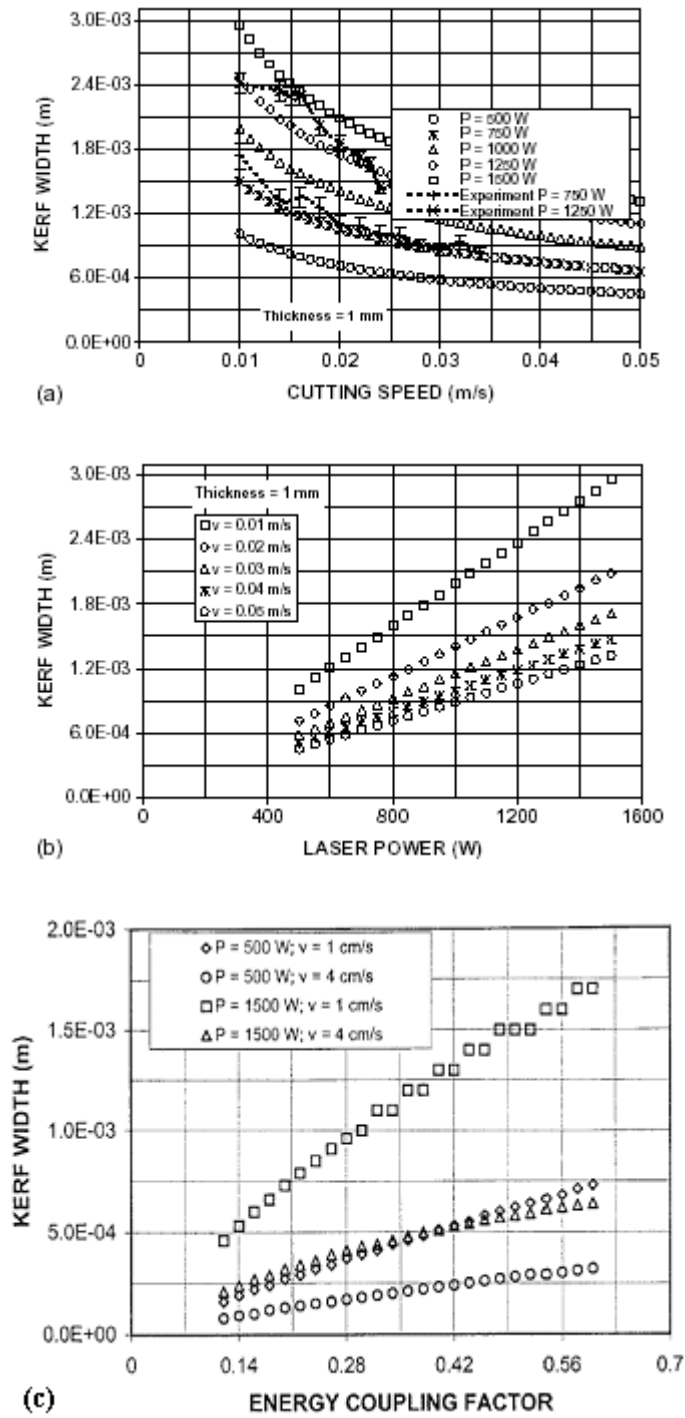
Figure 34. (a) Variation of the kerf width with cutting speed

(b) Variation of the kerf width with laser output power

(c) Variation of kerf width with energy coupling factor /65,66/

9.2 Perpendicularity or angularity of the cut edges

The perpendicularity or squareness and inclination tolerance, u, is the greatest perpendicular distance between the actual surface and the intended surface as illustrated in figure 35. It is the sum of the angular deviation and the concavity or convexity of the surface. Quality classes are defined for thermal cutting techniques in which the perpendicularity and angularity are expressed in terms of the material thickness, a. /15,45/

u - **Perpendicularity tolerance**

Δa - **Thickness reduction for determination of** u
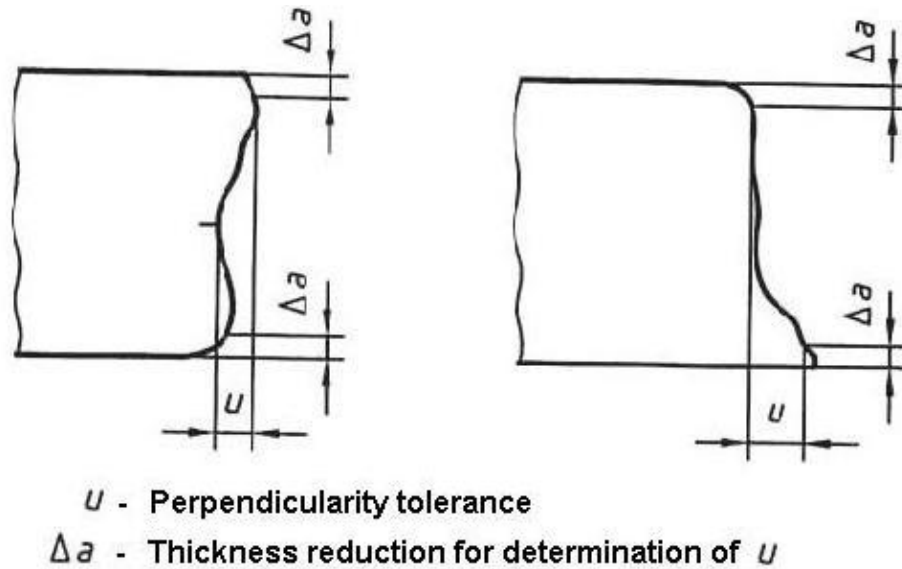
Figure 35. Perpendicularity tolerance of a straight laser cut /15/

9.3 Surface roughness

Surface roughness is the unevenness or irregularity of the surface profile and is measured as the mean height of the profile, R_z, or as an integral of the absolute value of the roughness profile, R_a. The mean height of the profile, R_z, is used in quality classification. The length of measurement is 15mm, which is divided into five partial measuring lengths. The distance between the highest peak and the lowest trough is determined for each partial measuring length and R_z, measured in micrometers, is the average of the five distances. Figure 36 is an illustration of single profile elements of five bordering single measured distances from which the average roughness of the profile can be obtained. /15,45/
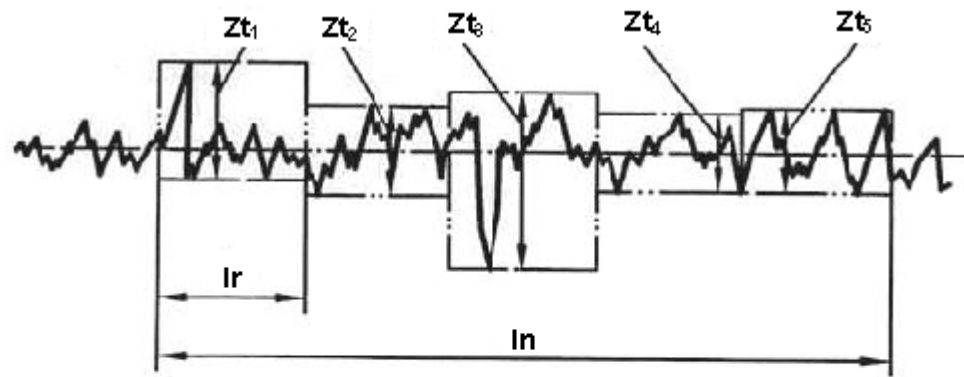
Where

Zt₁ to Zt₅   represent single profile elements;

In   is the evaluation length;

Ir   is the single sampling length (1/5 of In).

Figure 36. Mean height of the profile /15/

The cut surface is roughened by natural striations that result from the non-steady nature of laser cutting. Yilbas /34/ investigated the mechanism that initiates the striation and concluded that sideways burning, liquid layer oscillation at the surface and variation in the absorbed power due to surface plasma are the main reasons for the striations. /47/

Fluctuations in the melt thickness and temperature gradients cause oscillations in the melt front propagation, which can result in formation of striations. These melt oscillations can cause course striations in the lower region of the kerf but are not the reason for striation formation in the top of the kerf because this type of striations require a relative large melt thickness compared to the melt thickness in the upper region of the kerf. /67/

In laser oxygen cutting, the interaction between the material and the incident energy behaves in a cyclic manner, shown in figure 37, generating a pulsed-type cut edge covered in regular striations even though the energy input to the cutting zone is constant. /25,56/

PLAN VIEW

STEEL SHEET

A	B	C	D	E
Heating	Burning	Extinction	Reinitiation	Striation Generation

(a) A schematic showing how striations can be generated

Ignition isotherm

Cut face

kerf

Cut edge

Extinction isotherm

(b) Striation formation due to sideways burning
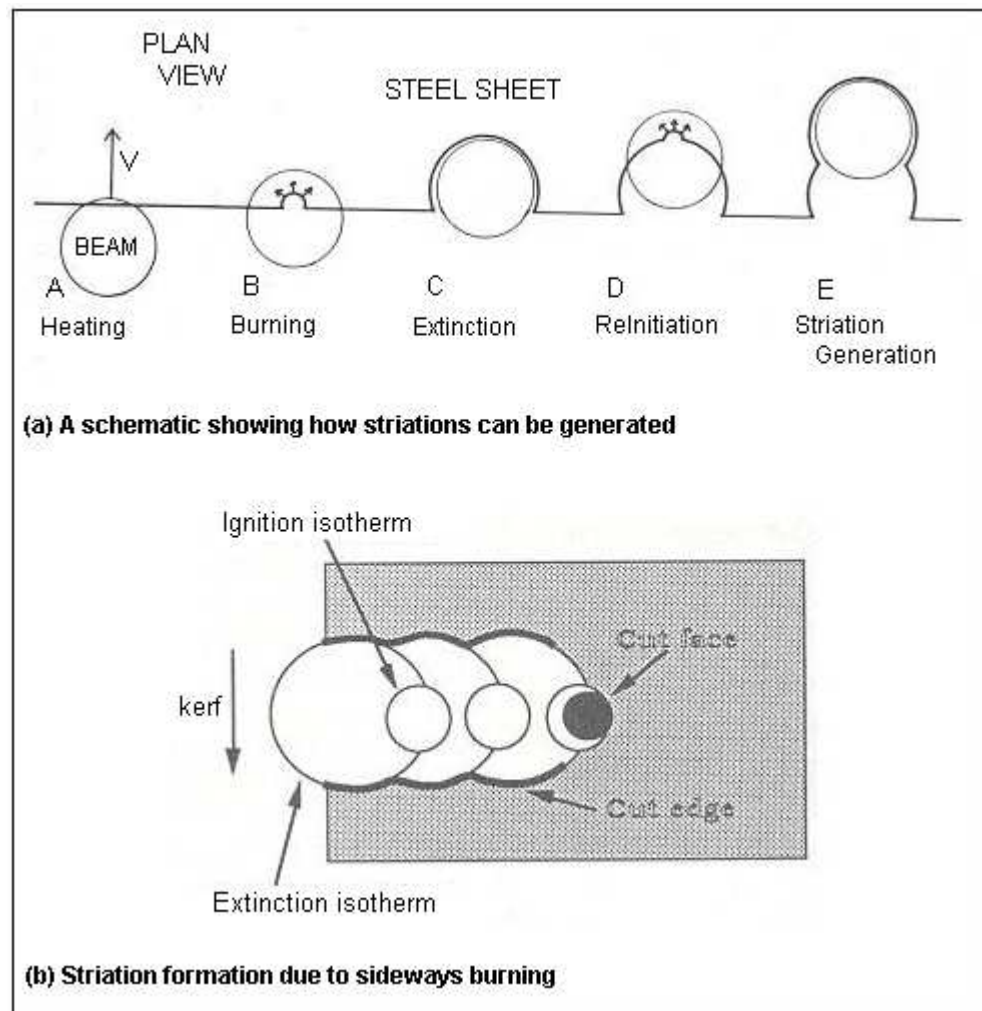
Figure 37. Striation formation /25,68/

During laser oxygen cutting of mild steel, the ignition phase occurs when a focused high power laser beam in conjunction with the co-axial oxygen jet cause the mild steel sheet to exothermically oxidize when high power laser beam touches the cutting front. The highly energetic burning front moves rapidly away from the center of the laser beam and once the laser beam has been left behind, the burning front cools and extinguishes. The moving laser then initiates the re-ignition of the next area and the process continues thus generating a pattern of striations along the cut edge. One cycle of the reaction was found to be just the same as a space of the striation. At cutting speeds faster than oxidation rate, the front face cannot move ahead of the laser beam so that the front face and the laser beam move at the same speed. /25,56,69/ In slow cutting, the ignition temperature is reached and then burning occurs proceeding outwards in all directions from the ignition point causing course

striations on the cut edge. The distance between striations increases with increasing cutting speed. The general rule is that the faster the cut, the less heat penetration and the better the cut quality. /68/ The laser cut surfaces show two different striation patterns, one with a finer structure adjacent to the upper surface and one with a coarser pattern adjacent to the lower surface of the workpiece. /70/

In inert gas cutting where no exothermic oxidation reaction occurs, the striations are associated with the inefficient removal of the molten material. The cut surface quality in nitrogen cutting is improved by use of higher gas pressures compared to the gas pressures used in oxygen cutting. /71/

9.4 Dross attachment and burrs

A burr is the highly adherent dross (solidified material) or slag (solidified oxides) that forms on the underside of the cut. Molten materials with high values of surface tension and low viscosity are more difficult to remove from the cutting front by the assist gas and can result into adherent dross on the underside. The oxide generated during cutting of stainless steel is made up of high melting point components such as Cr_2O_3 (melting point approximately 2180^oC) and hence this freezes quicker causing a dross problem. Dross can be removed during processing by use of a gas jet directed from the underside of the workpiece. Alternatively, it can be removed mechanically after cutting. /45,68/

9.5 Heat Affected zone (HAZ) width

The thermal heat of laser cutting produces a heat affected zone (HAZ) next to the cut edge. The heat affected zone is the part of the material whose metallurgical structure is affected by heat but is not melted. Microstructural variation in the heat-affected-zone is one of the characteristics that determine the quality of the laser cut. /34,72/ The HAZ width increases as the energy input per unit length and cut thickness increase. HAZ width is important when cuts are to be made near heat-sensitive components. /45/ Figure 38 shows the several

physical mechanisms including conduction, phase change, plasma formation, surface absorption and molten-layer flow, which affect the efficiency of laser cutting. /73/
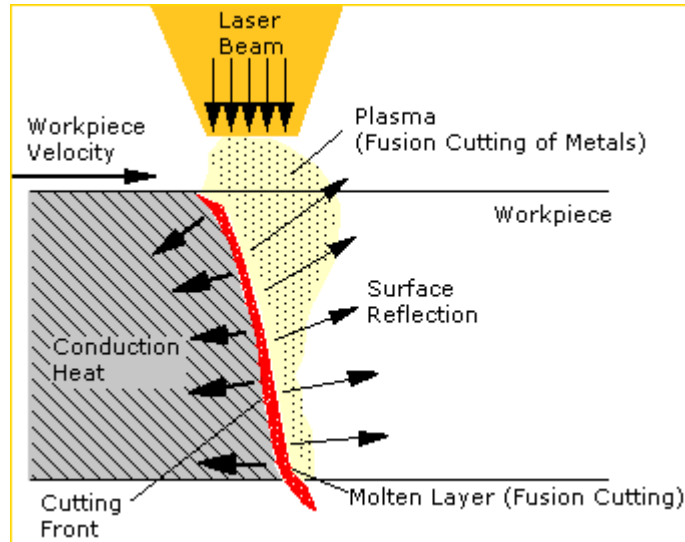
Figure 38. The main effects during laser cutting /73/

The formation of the heat-affected zone (HAZ) during cutting of austenitic stainless steel is considered to be negligible because the material is not hardenable by heat treatment. However, the heat conduction into the workpiece influences bulk phenomena such as grain refinement, carbide formation and other sulfide and phosphide impurities that might exist due to the alloying elements resulting into the formation of a detectable HAZ. /73/

EXPERIMENTAL PART

10. PURPOSE OF THE EXPERIMENTAL STUDY

The purpose of the experiment was to analyze the cutting performance and cut quality of the disk laser, fiber laser and CO_2 laser by investigating the effects of a given set of parameters of the laser cutting process. The parameters investigated included: material thickness, cutting speed and focus position.

The high beam quality of the disk laser and fiber laser is expected to enhance cutting speeds and produce a better quality cut kerf that is characterized by a smaller kerf width and perpendicular cut edges with low surface roughness.

11. EXPERIMENTAL EQUIPMENT AND TEST PROCEDURES

Three sets of experiments were done with three different laser types, namely disk laser, fiber laser and CO_2 laser. Because of the numerous parameters that affect the laser cutting process, a procedure of trial and error was used to choose a range of parameters that could produce a reasonable cut at the highest cutting speeds possible for each laser type and the different material thickness considered.

11.1 Test material

The test material used in the cutting experiments was austenitic stainless steel (AISI 304 and AISI 316), which was available in the form of sheets. Austenitic grades are the most commonly used stainless steels accounting for more than 70% of production with type 304 being the most commonly specified grade by far. The test material thickness used for the cutting experiments using the disk, fiber and CO_2 cutting lasers are given in table 3.

Table 3. The test material thickness used

Test material	Measured test material thickness (mm)			Thickness rounded to nearest mm
	Disk laser	Fiber laser	CO_2 laser	Disk/Fiber/CO_2 lasers
AISI 304	1.30	1.30	1.30	1
AISI 316 for Disk and fiber AISI 304 for CO_2	2.30	2.30	1.85	2
AISI 304	4.30	4.30	4.40	4
AISI 304	6.20	6.20	6.40	6

11.2 Disk laser experiments

A Trumpf disk laser, model HLD 4002, shown in figure 39, was used for the disk laser cutting experiments. This system has a beam quality of 8 mm.mrad with a maximum laser power output of 4 kW at the workpiece and utilizes an optic fiber with core diameter of 200 μm for beam delivery.

Figure 39. The Trumpf disk laser HLD 4002

The variables in the cutting experiments included material thickness, cutting speed and the focus position. The pressure of the nitrogen gas, employed as the assist gas, was varied

from 6 bar to 30 bar depending on the material thickness so as to ensure effective ejection of the molten material during the cutting process.

An optimum cutting speed was specified for each material thickness with a 4 kW power level after some preliminary experiments with power levels, which included 1 kW, 2 kW, 3 kW and 4 kW. The 4 kW power level was chosen for all the subsequent tests with a specific cutting procedure in which linear cut slots, 100mm long, were made. The cutting speed was varied by 5% and 10% above and below the normal operating level as recommended by the machine manufacturer as illustrated in figure 40. The cuts were kept at sufficient distance apart from each other and from the workpiece edges in order to avoid interference. In another cutting condition, the focus position was varied with steps of -6mm, -3mm, 0, +3mm and +6mm from the workpiece surface for material thickness of 1.3mm and 2.3mm. The details of the cutting parameters are contained in appendix 1.
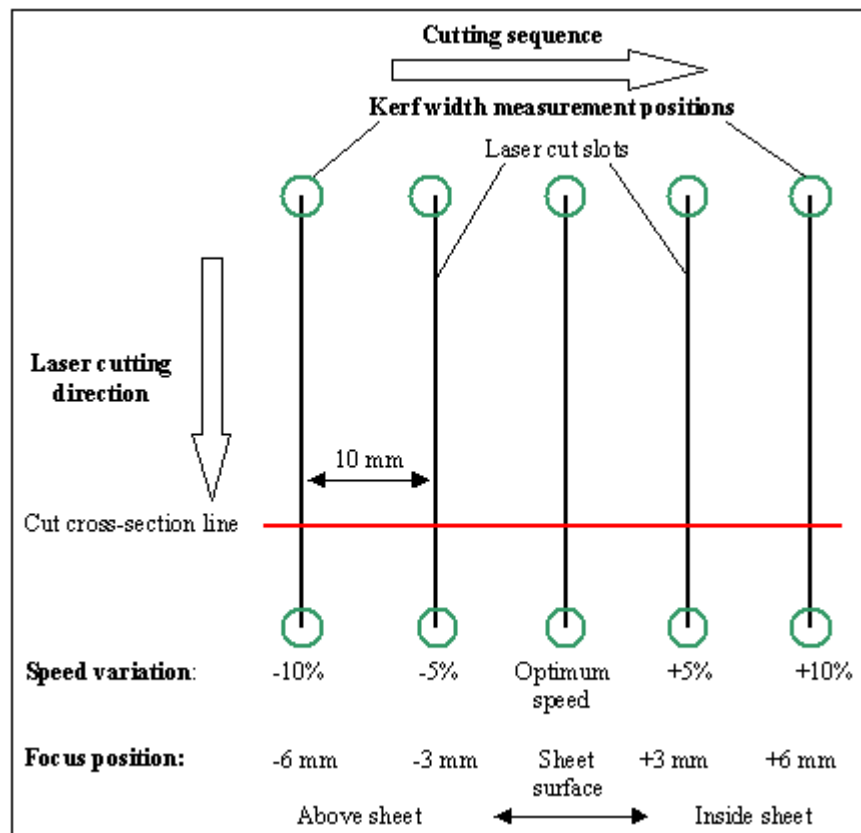
Figure 40. Schematic diagram of the test procedures

11.3 Fiber laser experiments

A 2D-laser cutting machine with linear drives (Arnold GmbH & Co. KG) with a 4 kW-fiber laser IPG 4000W (IPG Laser GmbH, Burbach) available at FhG-IWS Dresden for R&D work was used for the fiber laser cutting experiments in this thesis. This machine is of the gantry type and the z-axis is equipped with the cutting head with an integrated capacitive distance control by Precitec. The control is activated as soon as the distance between the cutting head and work gets lower than 5 or 10 mm (optionally). The whole machine including laser is CNC-controlled by the Sinumerik 840D software by Siemens, version 5.3. The mechanical part of the laser-cutting machine together with the beam delivery system is shown in figure 41. The maximum acceleration of this machine is $42 m/s^2$ for the x- and y-axes and the maximum velocity along the axes is 280m/min. The high acceleration is essential for accurate contour cuts with a high cutting rate.
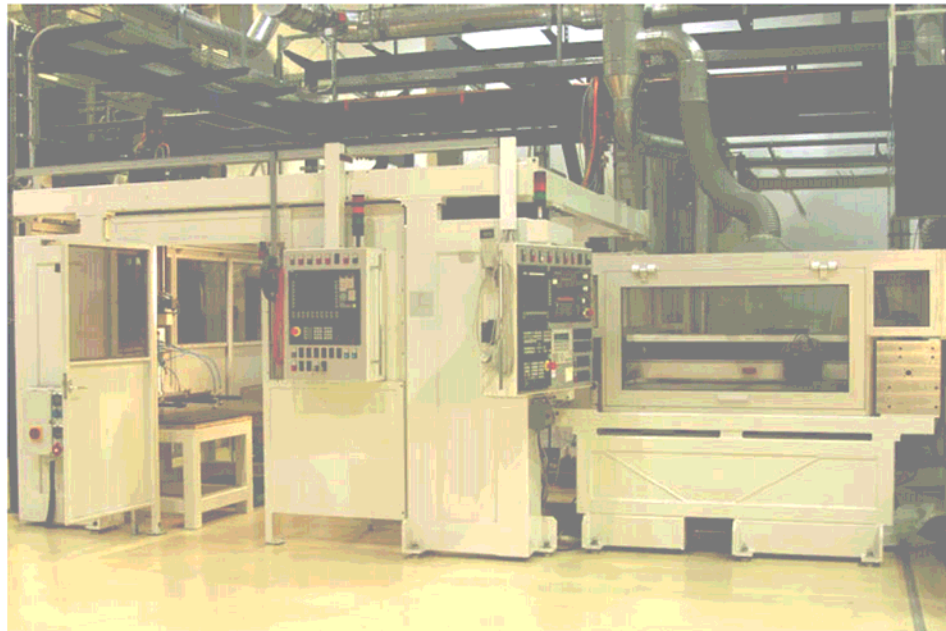
Figure 41. Cutting machine with linear drives Type 1FN3 by Arnold

The laser source was a fiber laser, YLR 4000W (IPG Laser GmbH, Burbach) shown in figure 42 (a), with a maximum laser power output of 4000 W and a beam quality of

2.5mm.mrad. A light conducting cable with a fiber diameter of 50 μm carries out the transfer of the laser beam to the cutting optics.

A HP 1,5" cutting head (figure 42(b)) with a collimation of focal length 50mm and a focusing lens of focal lengths 5" (127mm) and 7,5" (190.5mm) was used for the cutting tests. Thus, for a fiber diameter of 50 μm, the imaging ratio was 1:2,54 for 5" focal length and a theoretical focus diameter of 127 μm. For the 7,5" focal length, the imaging ratio was 1:3,8 and consequently a theoretical focus diameter of 190,5 μm.

(a)   (b)

Figure 42. (a) Fiber laser YLR 4000W (IPG Laser GmbH, Burbach)

  (b) Cutting head HP 1,5"

Five identical linear cuts of 150mm length were made for each cutting condition. The cuts were kept at sufficient distance from each other and from the workpiece edges in order to avoid interference.

Focal lengths of 5" (127mm) and 7,5" (190.5mm) were used with nitrogen as cutting gas. The cutting parameters were optimized in order to achieve the best cut quality at the highest cutting speeds. The influence of process parameters such as laser power, cutting velocity, focus position, nozzle distance, and cutting gas pressure and nozzle diameter was investigated (see appendix 2).

The procedure of optimization was demonstrated with the cutting of 1.3mm sheet thickness. The validation was started at a feed rate of 10 m/min for the focal length of 5" (127mm) and the parameters were varied in such a way that the feed rate could be increased step-by-step with the result that the cutting could be done in a process safe way. This was successful for a sheet thickness of 1.3mm at a laser power of 4000 W and with a cutting velocity of up to 55 m/min (12 bar cutting gas pressure and a nozzle of 2.0 mm).

11.4 CO_2 laser experiments

A CO_2 laser machining center with a maximum output power of 6000 W, shown in figure 43, was used to conduct the CO_2 laser cutting experiments.

Figure 43. The CO_2 laser-machining center (Trumatic L6050)

The cutting experiments were performed with the laser power of 4000 W and sheet thickness of 1.3mm, 1.85mm, 4.4mm and 6.4mm with nitrogen as the assist gas. Some

preliminary tests were conducted while adjusting the process parameters namely gas pressure, nozzle diameter, nozzle standoff distance and focal length so as to determine the maximum cutting speeds for each sheet thickness.

The cutting tests were then performed with the maximum cutting speeds for each sheet thickness and linear cuts of 100mm length were made. Five cut slots were made as the cutting speed was varied by 5% and 10% above and below the already specified maximum cutting speed, as provided by the machine manufacturer (see figure 40). The CO_2 laser cutting parameters are given in appendix 3.

12. MEASUREMENTS

In this thesis, the laser cut quality was monitored by measuring the kerf width, perpendicularity of the cut edges and the surface roughness. The width of the heat-affected zone (HAZ) was not measured because the test material was austenitic stainless steel, which does not show a considerable microstructural phase transformation during heat treatment and is therefore considered non hardenable by heat treatment.

12.1 Kerf width measurement

Digital imaging of the cut kerfs was done using a Leica M25 microscope and a Canon S40 digital camera. The Canon S40 digital camera was used to take these photographs through the Leica M25 microscope whose eyepiece was connected to the lens of the digital camera. The illumination and magnification were varied for each material thickness so as to get clear photographs of the top and bottom cut kerfs at the start and end points of each cut slot.

The kerf width measurements were then made from the cut kerf photographs using the UTHSCSA ImageTool Version 3.0 program. The UTHSCSA ImageTool program is a free image processing and analysis program developed at the University of Texas Health Science Center at San Antonio, Texas and is available from the Internet from the address

. The kerf width measurements were taken at four positions A, B, C and D, as shown in figure 44 below and the average value of these measurements was recorded as the kerf width of this cut. The kerf width varied over the length of the cut and measurements were taken at the leading (end of cut) and trailing (start of cut) positions on the cut. Both the top and bottom surfaces kerf width were measured.
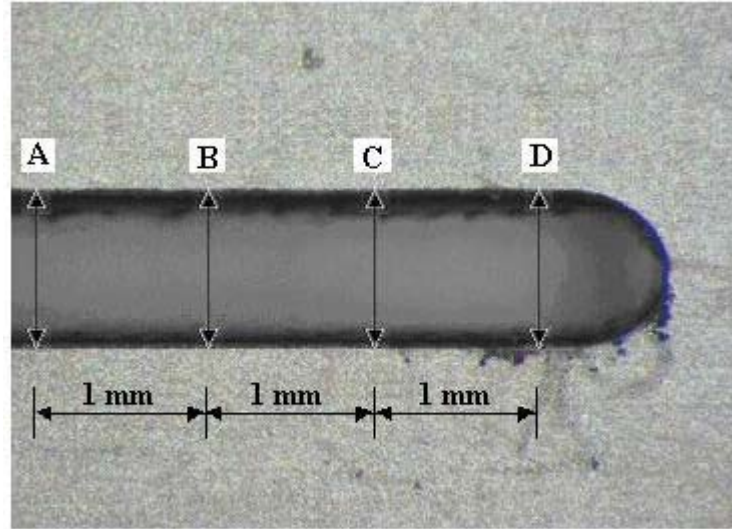
Figure 44. Kerf width measurement positions A, B, C and D

12.2 Perpendicularity measurement

After the kerf width measurements were done, the workpiece was cut through to reveal the cut cross-section showing the kerf width variation from top to bottom of the cut. The cut cross-section surface was ground and polished and digital photographs of the cut cross-section were made. The various shapes of the cut kerfs observed are shown in figure 45.
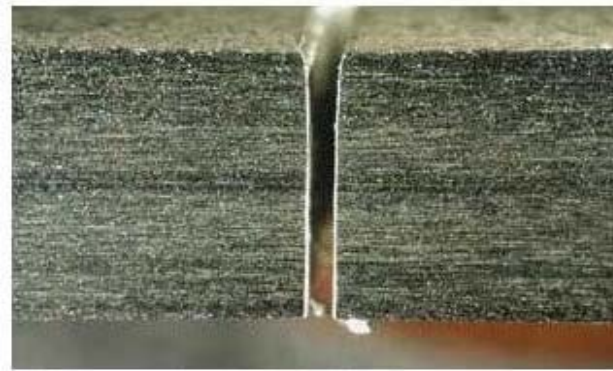
(a) A relatively uniform kerf width

(b) A smaller kerf width at the bottom

(c) A wider kerf width at the bottom

Figure 45. The variation of the cut kerf width from top to bottom of the cut

The greatest perpendicular distance between the actual surface and the intended surface of the cut edge was measured on both cut edges of each cut kerf using the AutoCAD 2002 program as illustrated in figure 46. The measured perpendicularity deviation of the cut edges was then used to classify the cut edges according to the EN ISO 9013:2002 standard for thermal cuts.
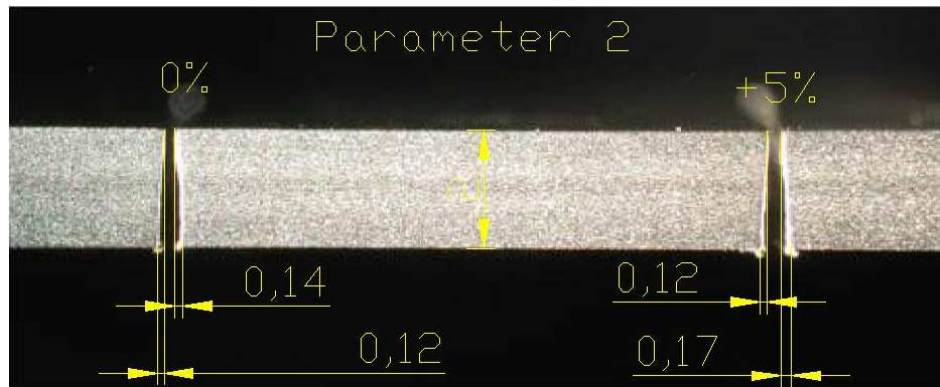
Figure 46. The cut cross-section showing the kerf width variation from top to bottom

12.3 Surface roughness measurement

After the kerf width and perpendicularity measurements, the cut surfaces were then separated so as to measure the surface roughness. The surface roughness was measured in terms of the integral of the absolute value of the roughness profile, R_a and the mean height of the profile, R_Z, using a Mitutoyo 201 stylus profile meter.

The surface roughness was measured randomly on different positions of the cut surfaces and the measuring points were located where the maximum measured values were expected on the cut thickness. The number and location of the measuring points depended on the shape and size of the workpiece. The sampling length for each measurement was 7.5 mm. For the 1.3mm, 1.85mm and 2.3mm sheet thickness, the roughness measurement was taken at the middle of the cut thickness and the roughness measurements for the 4.3mm, 4.4mm, 6.2mm and 6.4mm sheet thickness were taken at two positions along the cut thickness – one measurement position at the upper part and the other at the lower part of the cut thickness - as shown in figure 47. For the 6.2mm sheet thickness fiber laser cut surface, a third roughness measurement position was taken at the middle of the cut thickness, as three different regions of surface roughness were visible with the highest roughness being at the middle of the cut thickness.

Ra = 1,52 μm
Rz = 8,4 μm
Cutting direction: ←
Thickness: 1 mm
Cutting speed: 35 m/min
Nitrogen pressure: 8 bar

Ra = 3,22 μm
Rz = 23,3 μm
Cutting direction: ←
Thickness: 2 mm
Cutting speed: 17 m/min
Nitrogen pressure: 6 bar

Ra = 2,68 μm
Rz = 16,2 μm
Ra = 3,35 μm
Rz = 22,3 μm
Cutting direction: ←
Thickness: 4 mm
Cutting speed: 4,7 m/min
Nitrogen pressure: 25 bar

Ra = 3,75 μm
Rz = 24,9 μm
Ra = 10,22 μm
Rz = 58,7 μm
Cutting direction: ←
Thickness: 6 mm
Cutting speed: 2,3 m/min
Nitrogen pressure: 30 bar

Figure 47. Surface roughness of the disk laser cut surfaces showing both the R_a and R_z values (Laser power 4000 W)

13. EXPERIMENTAL RESULTS

The maximum cutting speeds and measured values of the kerf width, cut edge perpendicularity and surface roughness (R_a and R_z) are presented.

13.1 Maximum cutting speeds

The maximum cutting speeds at the 4 kW power level for the disk, fiber and CO_2 lasers are shown in figure 48. The cutting speeds were higher for the fiber and disk lasers at smaller

sheet thickness (thickness less 3mm) than for the CO_2 laser but the cutting speeds were lower when thicker sheets (thickness greater than 4mm) were cut. However, there was still a considerable percentage increase in cutting speeds of the fiber and disk lasers for the sheet thickness greater than 4mm compared to the cutting speeds of the CO_2 laser for the same sheet thickness. The enormous cutting speeds for the fiber and disk lasers can be attributed to their better beam quality.
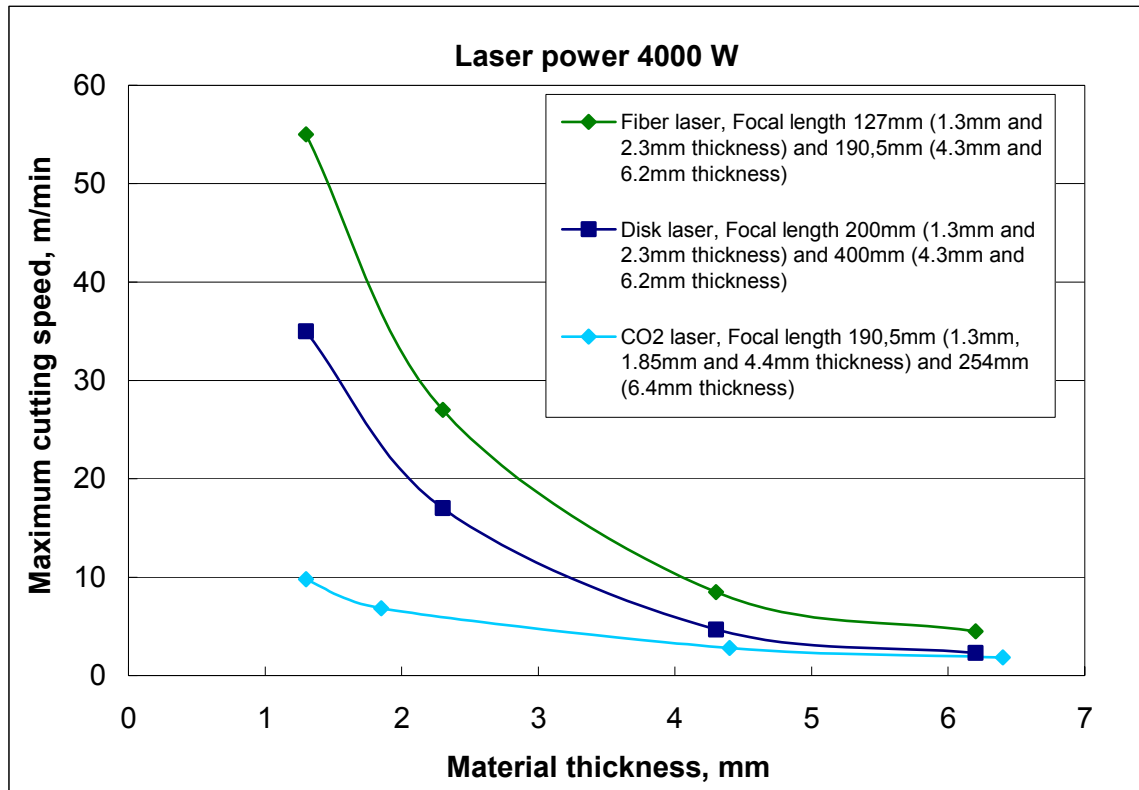
Figure 48. Maximum cutting speeds for the Disk, Fiber and CO_2 lasers

13.2 Kerf width

Generally, the kerf width varied over the length of the cut and it was not the same at the upper and lower surfaces. The cutting process is assumed to be more stable at the leading (end) position than at the trailing (start) position of the cut because it takes some time for the system to accelerate to the required cutting speed. Therefore, only the kerf widths at the leading (end) position of the cut are considered.

13.2.1 Disk laser

Continuous through cuts were obtained for most of the cutting speeds except for a few cases such as when the 2.3mm sheet thickness was cut at the cutting speed of 18,7m/min whereby there was resolidified melt that bound the bottom cut surfaces and also there was no penetration when the 6.2mm sheet thickness was cut at 2,4m/min cutting speed.

Effect of focus position on kerf width

Figure 49 illustrates the variation of kerf width with focus position for the 1.3mm and 2.3mm sheet thickness. The kerf width was smaller when the focus position was on the workpiece surface and above the surface. For the 2.3mm sheet thickness, the cut was incomplete at the focus position of +3mm inside the sheet due to lack of penetration and there was no cut at the focus position of +6mm inside the sheet.
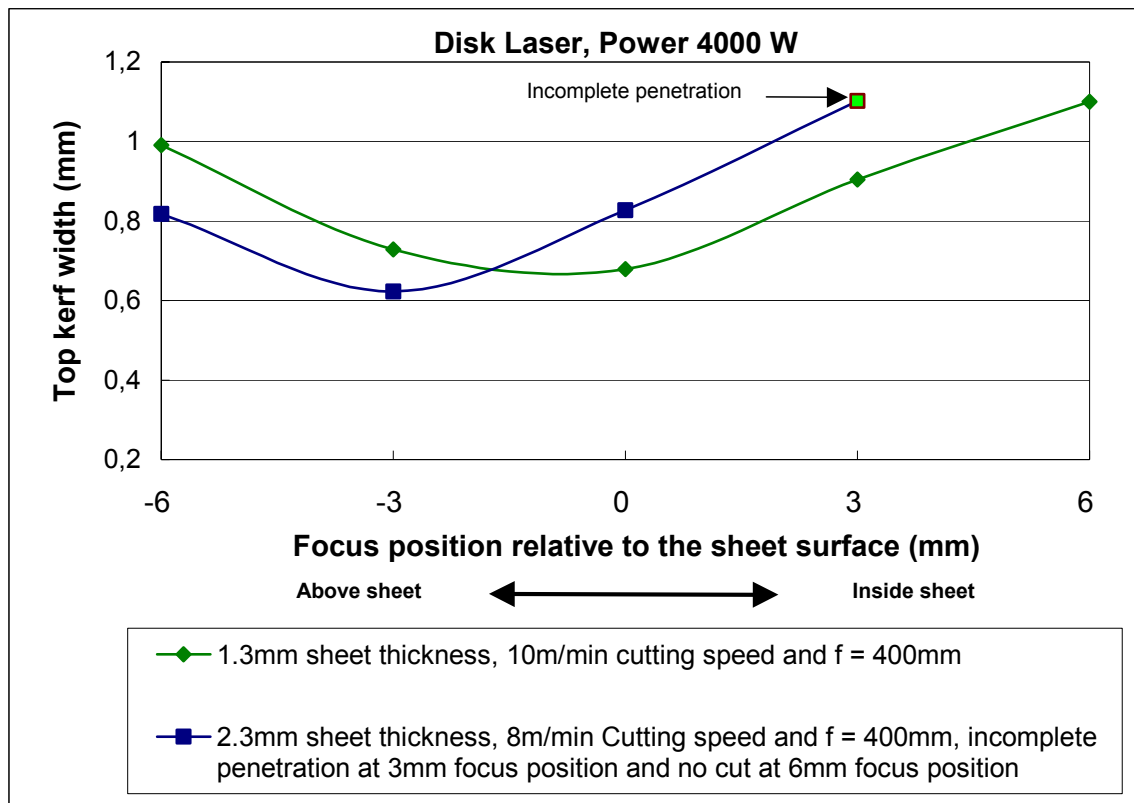
Figure 49. Kerf width variation with focus position for the 1.3mm and 2.3mm sheet thickness (Disk laser)

Effect of focused beam diameter and cutting speed on the kerf width obtained

Different focal lengths were used for focusing of the laser beam giving different focused beam diameters. A shorter focal length gives a smaller focused beam diameter and the kerf width is directly related to the focused beam diameter. A small focused beam diameter leads to a small kerf width. The variation of kerf width with focused beam diameter and cutting speed for 1.3mm and 2.3mm sheet thickness is shown in figure 50. The kerf width was smaller when a focal length of 200mm was used than when the focal lengths of 400mm and 600mm were used. This is because the 200mm focal length gives a smaller focused beam diameter than the 400mm and 600mm focal lengths. The top kerf width was generally larger than the bottom kerf width. However, there were a few cases, especially for the 2.3mm sheet thickness, where the bottom kerf width was larger than the top kerf width.
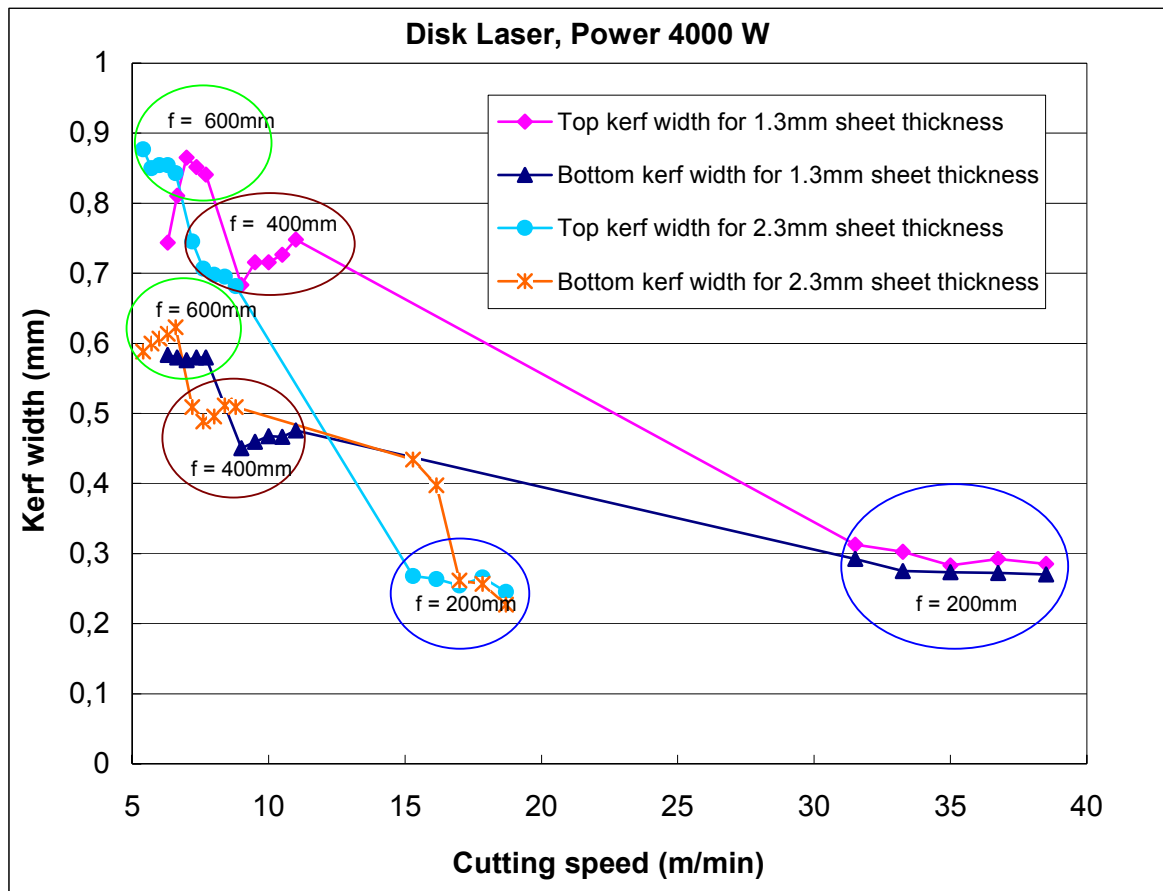
Figure 50. Effect of cutting speed on kerf width (1.3mm and 2.3mm sheet thickness)

Figure 51 shows the top and bottom kerf widths at maximum cutting speeds for the different sheet thickness considered. The kerf widths for the 1.3mm and 2.3mm sheet thickness were generally smaller than for the 4.3mm and 6.2mm sheet thickness. This is expected basing on the fact that the focal length was 200mm for 1.3mm and 2.3mm sheet thickness and a focal length of 400mm was used when the 4.3mm and 6.2mm sheet thickness was cut. It has already been shown in figure 50 that the kerf width is smaller when the focal length is shorter because the focal length determines the achievable focus spot size.

The difference between the top and bottom kerf width is large for the 4.3mm and 6.2mm sheet thickness but the difference is not significant for the 1.3mm and 2.3mm sheet thickness. Defocusing of the laser beam and accumulation of heat in the workpiece as the cut progresses could be the cause of the large difference between the top and bottom kerf width for the 4.3mm and 6.2mm sheet thickness.
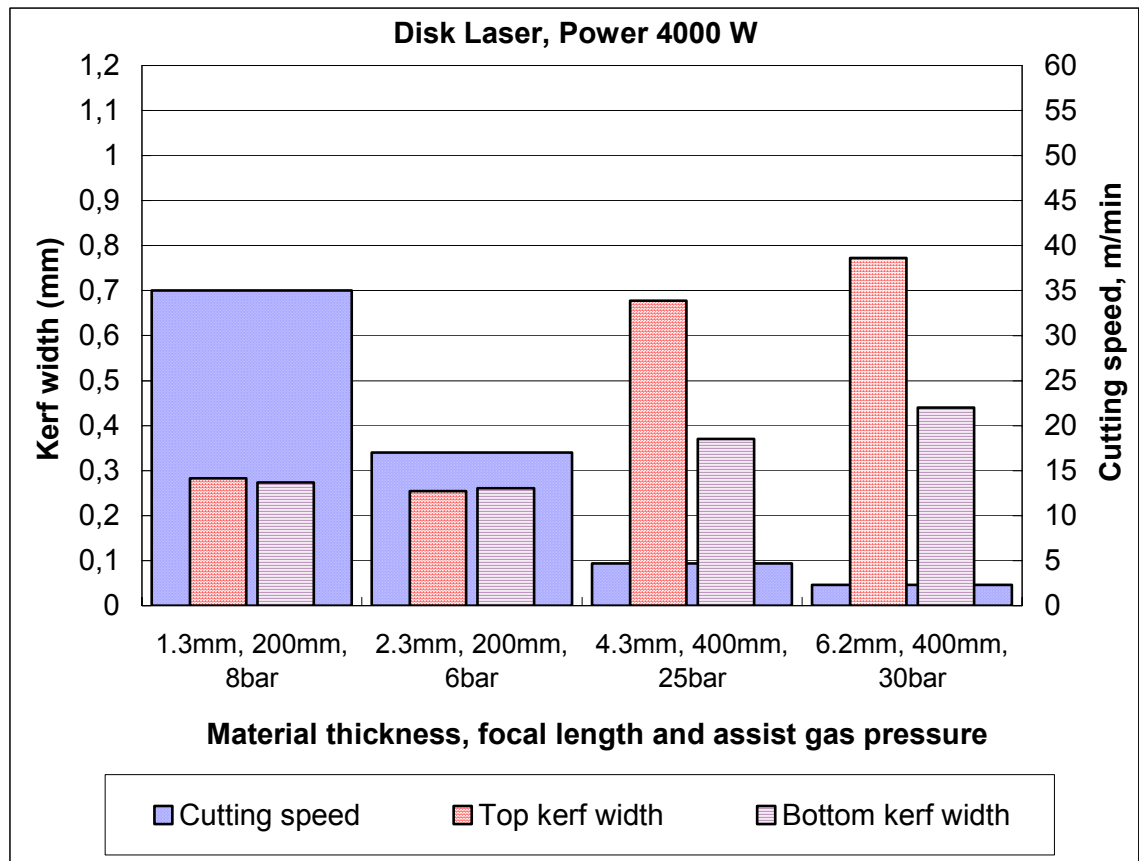
Figure 51. Disk laser kerf widths for the 1.3, 2.3, 4.3 and 6.2 mm sheet thickness

13.2.2 Fiber laser

Figure 52 shows that the difference between the top and bottom kerf widths is not significant in the 1.3mm and 2.3mm sheet thickness but it is great at the larger sheet thickness of 4.3mm and 6.2mm. This trend is similar to that of the disk laser cut kerfs shown in figure 51 and could also be caused by defocusing of the laser beam and accumulation of heat in the workpiece during the cutting process.
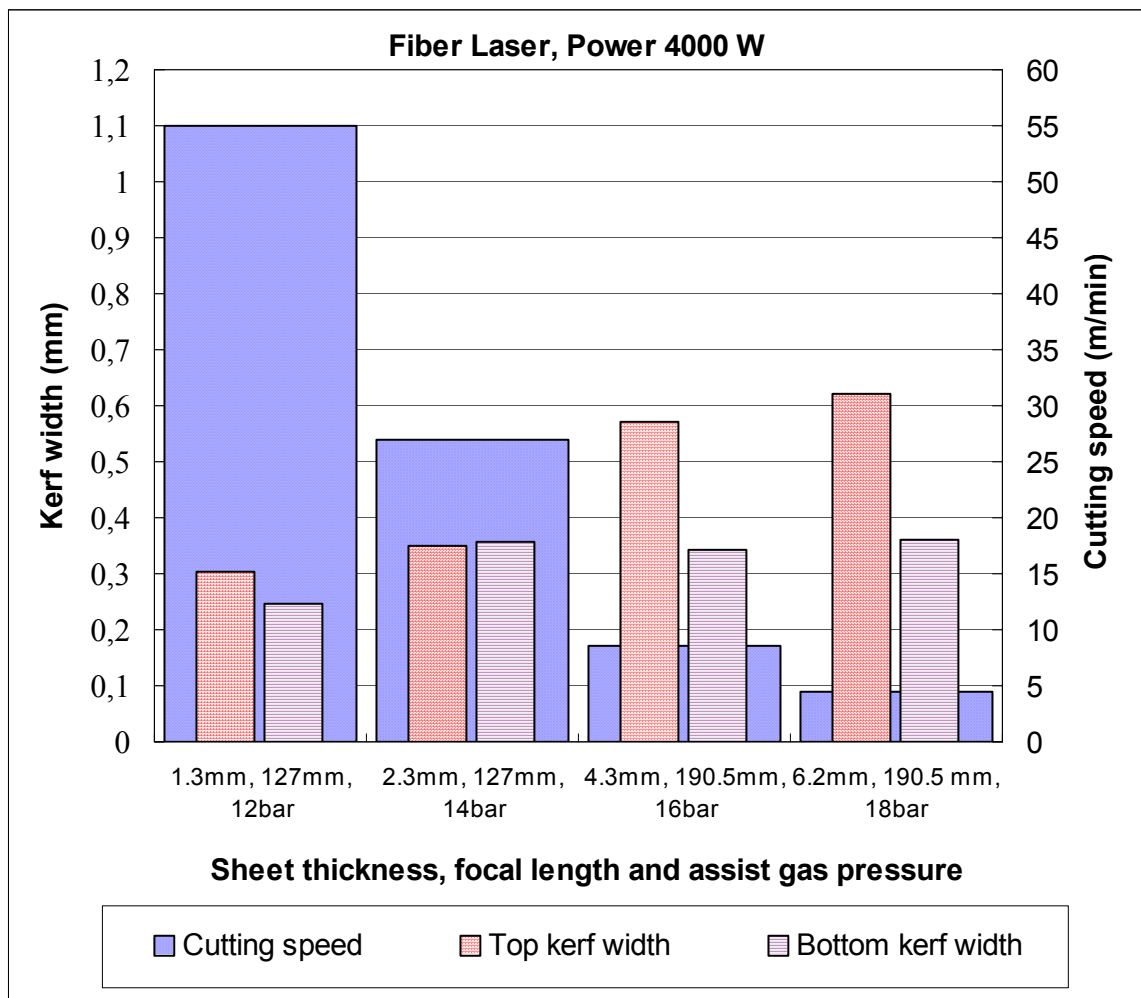
Figure 52. Fiber laser kerf widths for the 1.3, 2.3, 4.3 and 6.2 mm sheet thickness

13.2.3 CO$_2$ laser

In figure 53, the CO$_2$ laser cut kerfs also show a larger difference between the top and bottom kerf widths as the sheet thickness increases. This trend can be attributed to the widening of the laser beam after the focused spot and accumulation of heat in the workpiece during the cutting process.

CO2 Laser, Power 4000 W
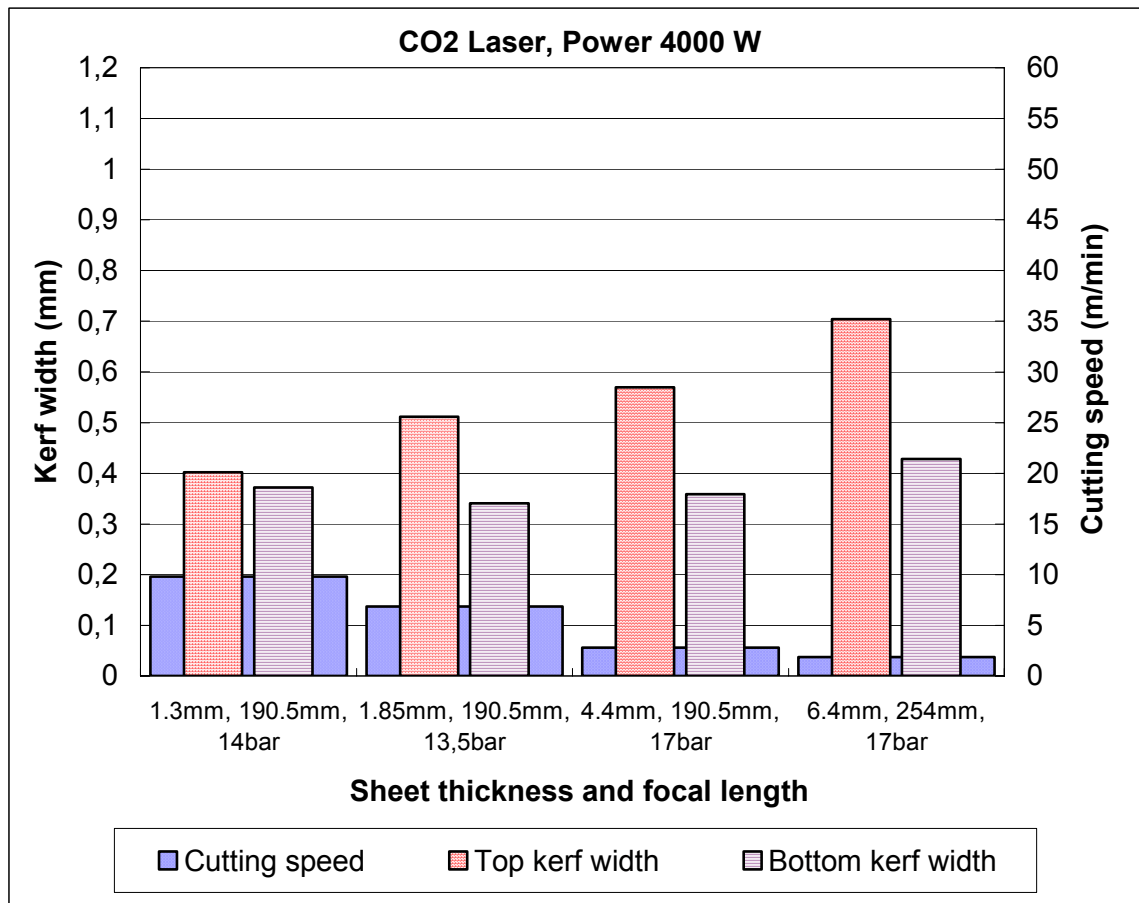
Figure 53. CO$_2$ laser kerf widths for the 1.3, 1.85, 4.4 and 6.4 mm sheet thickness

13.3 Perpendicularity deviation of cut edges

Perpendicularity deviation is the perpendicular distance between the actual cut edge obtained and the specified shape and location of the cut edge. It defines both straightness

and flatness deviations. The results for the perpendicularity deviation of the cut edges are shown in figures 54, 55 and 56. Perpendicularity measurements were taken on both edges of each cut kerf and each data point in these figures was the highest measured value for the perpendicularity deviation of the edges for each cut kerf.

13.3.1 Disk laser

All the disk laser cut edges had perpendicularity deviations of less than 0.18 mm. The perpendicularity deviation tended to decrease with increase in cutting speed except for the 2.3mm sheet thickness where there was an increase in perpendicularity deviation at cutting speeds above 15m/min.
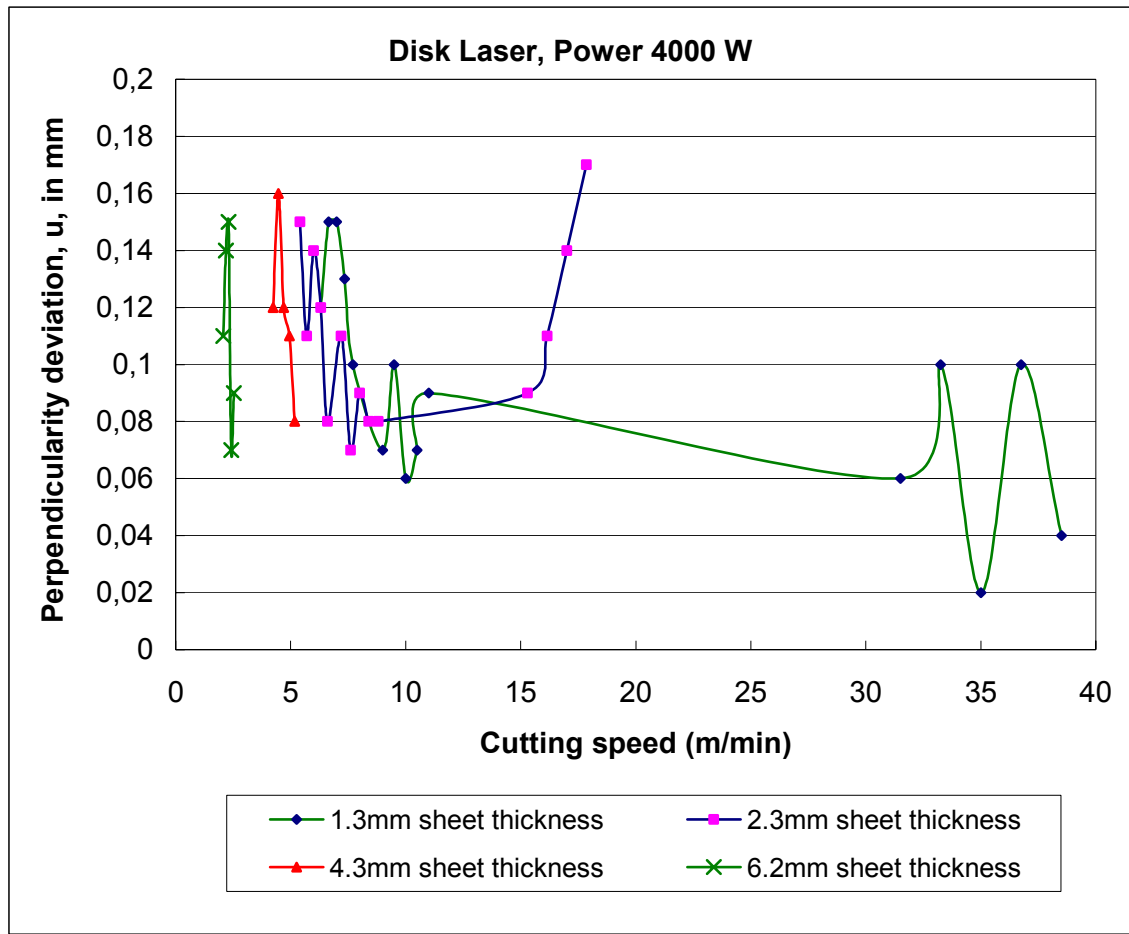
Figure 54. Perpendicularity deviation of the disk laser cut edges

13.3.2 Fiber laser

For the fiber laser cuts, the perpendicularity deviation was measured for each of the five cut edges per sheet thickness made at similar cutting conditions and at maximum cutting speed for each sheet thickness considered. The 1.3mm and 2.3mm sheet thickness cut edges had relatively small perpendicularity deviations (less than 0.08mm). The perpendicularity deviations of the 4.3mm and 6.2mm sheet thickness cut edges were higher than 0.08 mm but less than 0.18mm.
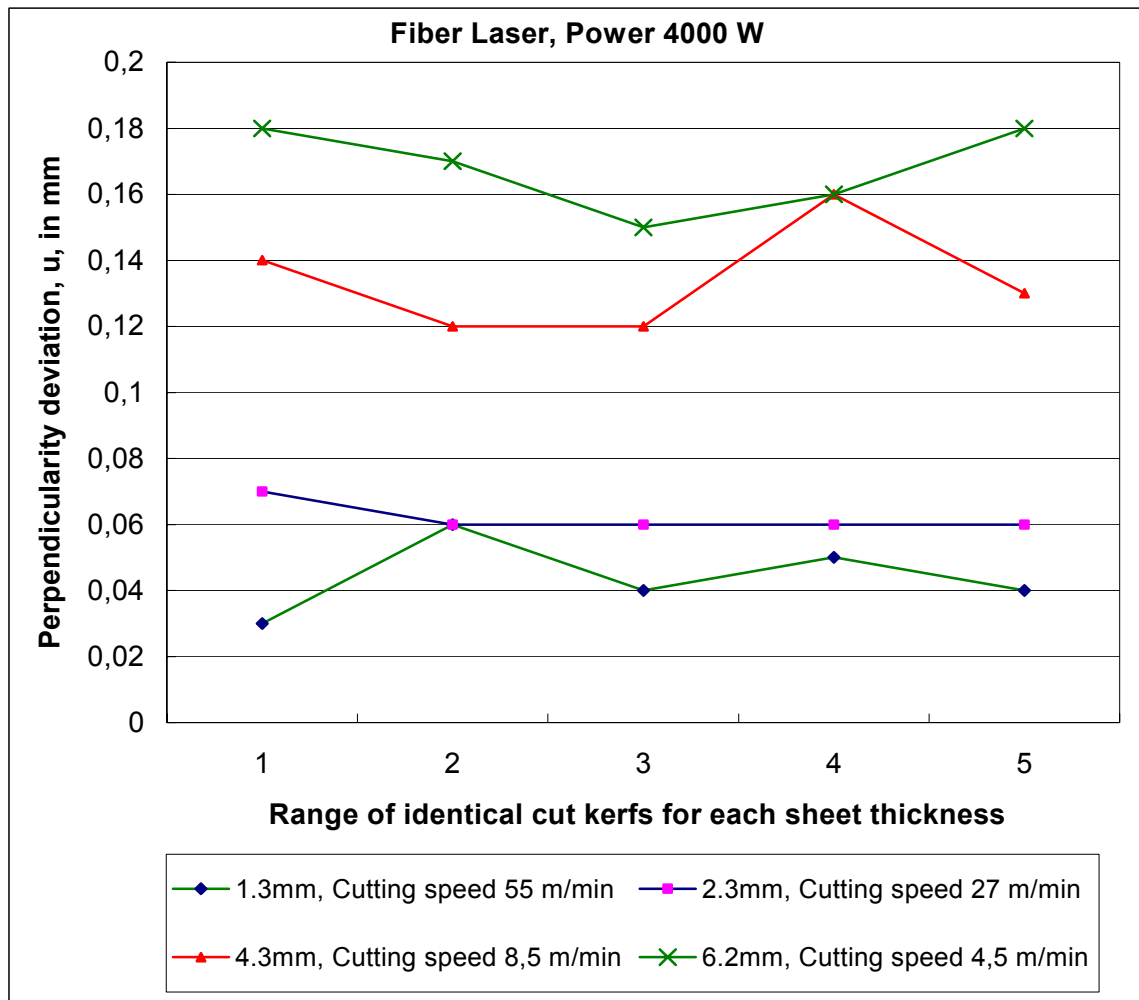
Figure 55. Perpendicularity deviation of the fiber laser cut edges; for each sheet thickness, five cut kerfs were made under similar cutting conditions

13.3.3 CO_2 laser

At a similar cutting speed and 1.3mm sheet thickness, the perpendicularity deviation of the CO_2 laser cut edge (0.02mm) was lower than that of the disk laser cut edge (0.06mm). Generally, the CO_2 laser cut edges had a low perpendicularity deviation for all the four sheet thickness (1.3mm, 1.85mm, 4.4mm and 6.4mm) considered, with the maximum perpendicularity deviation of the 6.4mm sheet thickness cut edges being less than 0.16mm.
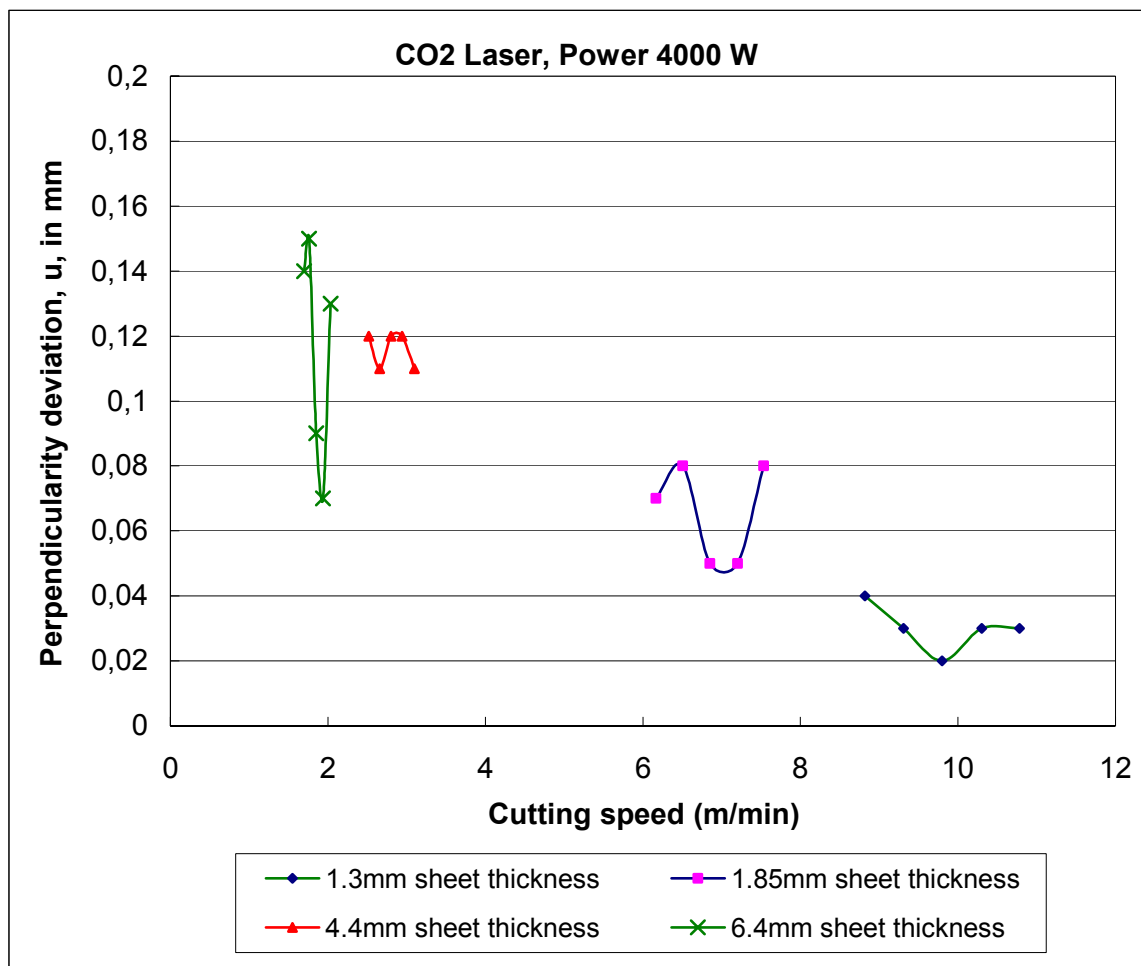
Figure 56. Perpendicularity deviation of the CO_2 laser cut edges

13.4 Surface roughness

The surface roughness (R_a) results are shown in figures 57, 58, and 59. The data points in these figures are the measured values for surface roughness in which the cut surfaces of sheet thickness less than 3mm have one roughness value for each cut surface while the cut surfaces of sheet thickness greater than 4mm have more than one roughness value.

The cut surfaces with sheet thickness less than 3mm showed uniform surface roughness throughout the cut thickness that is why only one roughness value was enough to describe the cut surface roughness. However, the surface roughness varied along the cut thickness of the cut surfaces with sheet thickness greater than 4mm therefore more than one roughness value was needed to describe the cut surface roughness.

13.4.1 Disk laser

Figure 57 shows the variation of the surface roughness (R_a) with cutting speed for the disk laser cuts and the different sheet thickness (1.3mm, 2.3mm, 4.3mm and 6.2mm). The 6.2mm sheet thickness showed a large variation between the surface roughness at the top of the cut thickness and that at the bottom of the cut thickness with the highest roughness being at the bottom of the cut thickness. The 4.3mm sheet thickness showed only a small difference between the roughness at the top and that at the bottom of the cut thickness.

The variation of surface roughness with cutting speed was not consistent probably because of the variation in other cutting parameters such as assist gas pressure for the different experiments. For instance at the various cutting speeds at which the 1.3mm sheet thickness was cut, the assist gas pressures were 8 bar, 15 bar and 20 bar and the assist gas pressures for the cutting experiments with 2.3mm sheet thickness were 6 bar and 20 bar for the various cutting speeds at which the 2.3mm sheet thickness was cut.   The variations in cutting speed as well as the variations in assist gas pressure may have had a combined effect on the surface roughness variation shown in figure 57.
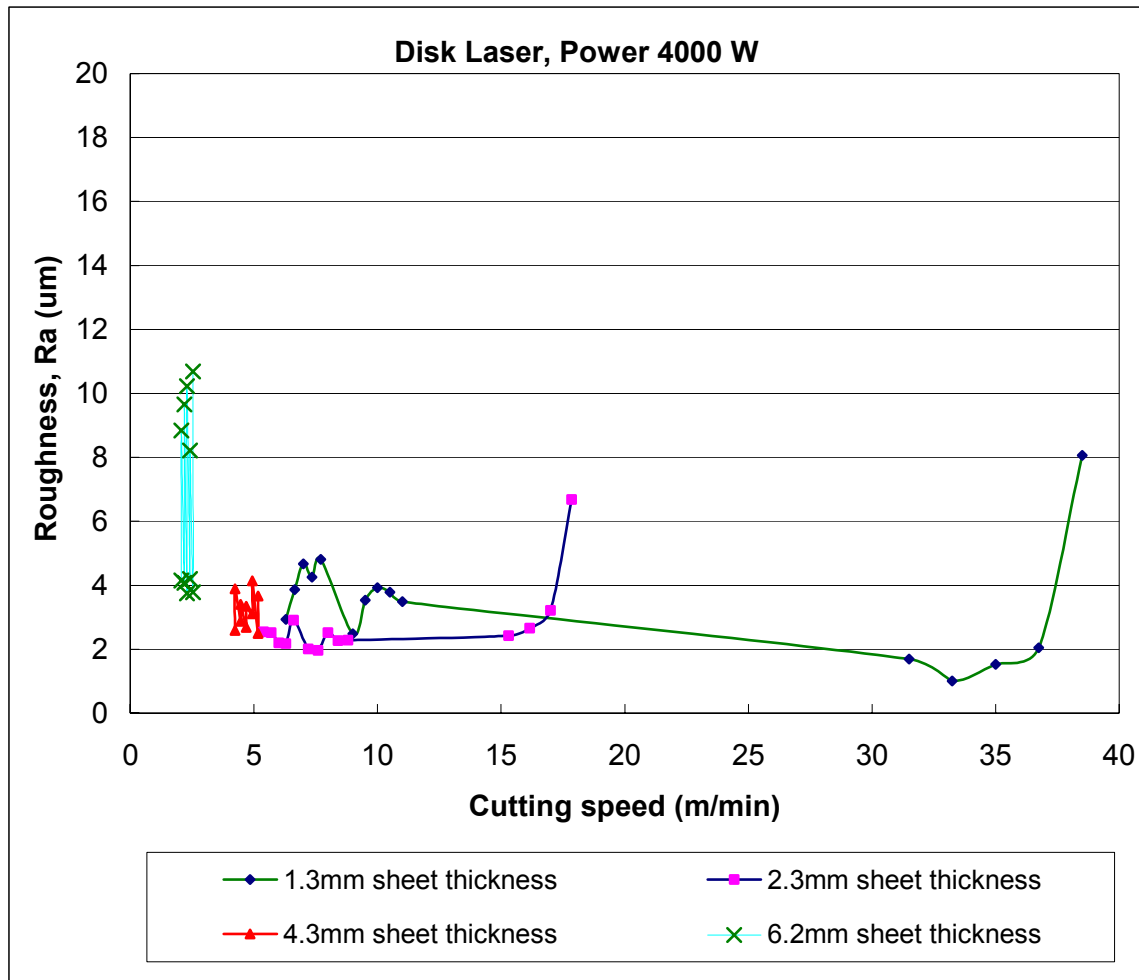
Figure 57. Surface roughness of the disk laser cut surfaces

13.4.2 Fiber laser

The surface roughness results for the fiber laser cuts are shown in figure 58. Generally, the 1.3mm and 2.3mm sheet thickness were cut at higher cutting speeds (above 10 m/min) and showed a lower surface roughness compared with the 4.3mm and 6.2mm sheet thickness that were cut at lower cutting speeds (less than 10 m/min). The 2.3mm sheet thickness showed an increase in surface roughness at cutting speeds beyond 20m/min. The data points for the 4.3mm and 6.2mm sheet thickness in figure 58 include roughness values at the various positions on the cut thickness. The 4.3mm sheet thickness showed higher

surface roughness at the bottom than at the top of the cut thickness while the 6.2mm sheet thickness showed highest surface roughness at the middle of the cut thickness with lower roughness at the top and bottom of the cut thickness. Both the cutting speeds and laser powers were varying in these fiber laser cutting experiments and the highest cutting speeds for each sheet thickness were achieved at the highest laser power of 4000W. The assist gas pressure, focal length and focus position were kept constant for each particular sheet thickness at the various cutting speeds and laser power. This could be the reason for the fairly consistent variation of the surface roughness with cutting speed as seen for the 1.3mm and 2.3mm sheet thickness in figure 58.
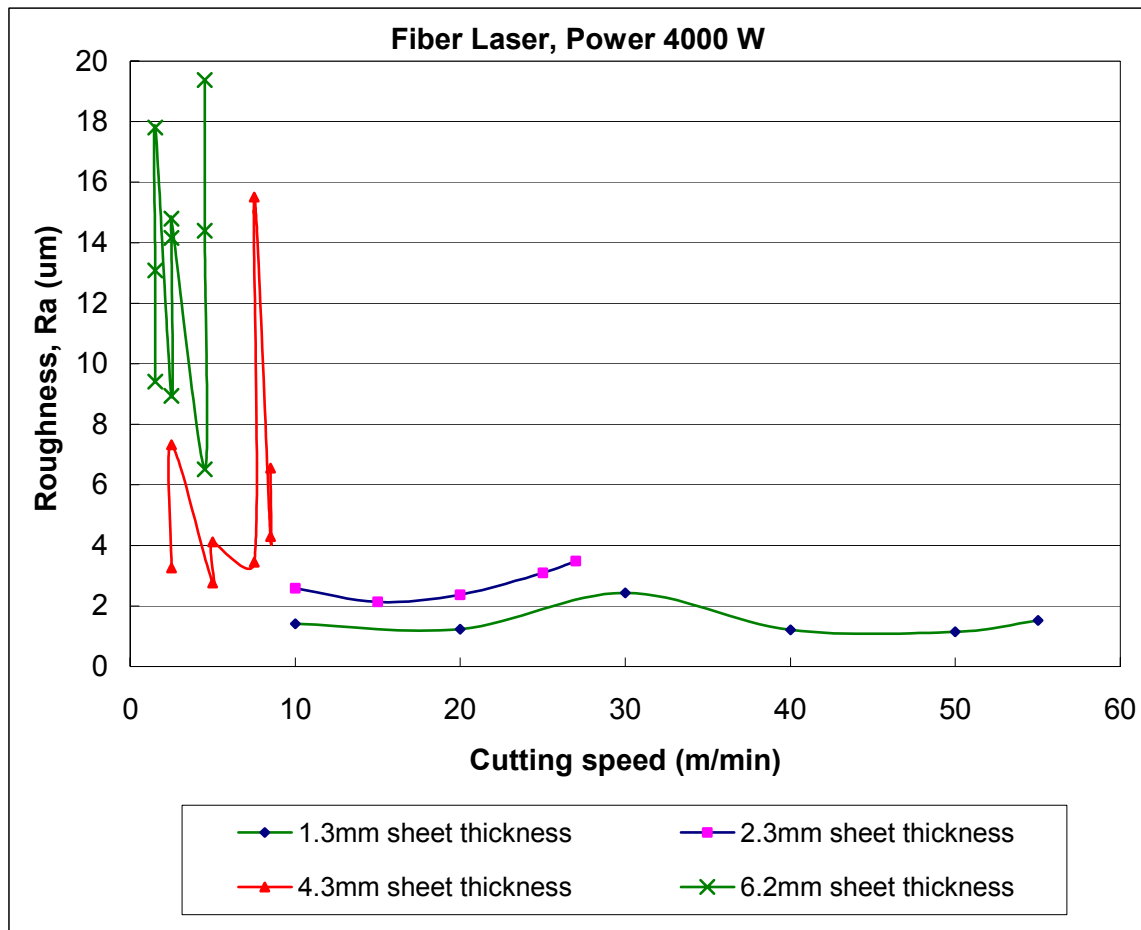
Figure 58. Surface roughness of the fiber laser cut surfaces

13.4.3 CO_2 laser

The CO_2 laser cut surfaces generally had low surface roughness for all the four sheet thickness considered as figure 59 shows. Even the 4.4mm and 6.4mm sheet thickness showed a relatively uniform surface roughness throughout the cut thickness as there was no significant difference between the roughness at the top and that at the bottom of the cut thickness. There was no significant change in surface roughness for the range of cutting speeds considered which cutting speeds were actually quite close as figure 59 shows.
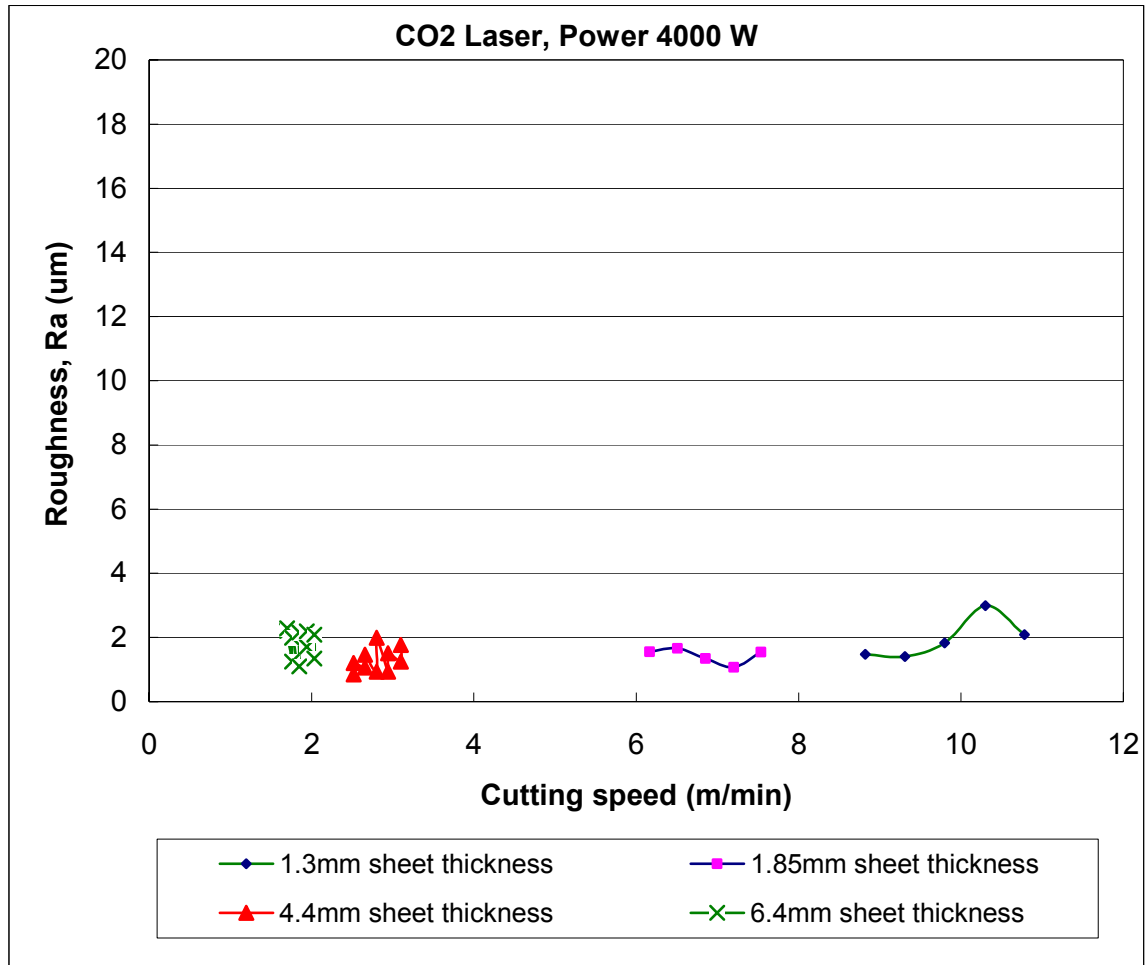
Figure 59. Surface roughness of the CO_2 laser cut surfaces

14. DISCUSSION

The cut quality obtained for the three different lasers was compared in terms of the kerf width, perpendicularity of the cut edges and surface roughness. Additionally, the cut kerfs were classified according to the EN ISO 9013 cutting standard which presents tolerances for surface roughness and cut edge perpendicularity. The perpendicularity of the cut edges and surface roughness are critical for some subsequent processing applications such as autogenous laser welding, which has stringent tolerances. The kerf width was not considered in this classification because the cutting standard used does not include tolerances for kerf width.

The description of the test material thickness in the discussion on maximum cutting speeds and kerf width is based on the nearest mm - 1mm, 2mm, 4mm and 6mm (see table 3) - for easy comparison across the three sets of experiments done with the disk, fiber and CO_2 lasers.

14.1 Maximum cutting speeds

The main focus in the cutting experiments performed in this master's thesis work was the maximum achievable cutting speeds with an appropriate cut quality for the disk, fiber and CO_2 lasers. The cutting experiments have shown that the disk and fiber lasers are capable of higher cutting speeds compared to the CO_2 laser especially at sheet thickness less than 4mm as shown in figure 48 and table 4.

The high cutting speeds achieved by the disk and fiber lasers can be directly attributed to their high beam qualities. Absorption is also higher in the case of the disk and fiber lasers because of their wavelength. The high beam quality and wavelength enable focusing of the laser beam to a smaller spot resulting into higher power densities and hence higher cutting speeds.

The high beam quality also enables use of longer focusing optics which increases the working distance thus reducing the risk of spatters damaging the focusing optics. A larger working distance is also advantageous when cutting is done in areas that are not easily accessible.

Table 4. Maximum cutting speeds for the disk, fiber and CO_2 lasers

Sheet thickness (mm)	Maximum cutting speed (m/min)			Percentage increase in cutting speeds compared to CO_2 laser	
	Disk laser BPP = 8mm.mrad $\lambda = 1.07\mu m$	Fiber laser BPP = 2.5mm.mrad $\lambda = 1.07\mu m$	CO_2 laser BPP = 6.14mm.mrad $\lambda = 10.6\mu m$	Disk laser	Fiber laser
1	35	55	9.8	257%	461%
2	17	27	6.85	148%	294%
4	4.7	8,5	2.8	68%	204%
6	2.3	4.5	1.85	24%	143%

Some CO_2 cutting experiments were done using compressed air as assist gas and considerably higher cutting speeds were realized compared to cutting with nitrogen (see appendix 3). However, it was visible that the cut edges were oxidized when compressed air was used even though the relative proportions of oxygen and nitrogen in compressed air is such that the proportion of oxygen is smaller than that of nitrogen. It maybe possible that the cutting speeds of the disk and fiber laser can also be much higher if either compressed air or oxygen is used as the assist gas in cases where productivity is of paramount importance compared to the cut edge quality.

14.2 Kerf width

The kerf width represents the amount of material melted during cutting and correlates to the focused spot size. A small kerf width can have advantages when small details are to be made such as when cutting sharp corners. The kerf width mainly depends upon the focused spot size. The size of the focus spot is determined by the laser beam quality and focusing optics. Changing the beam waist position relative to the workpiece surface modifies the power intensity at the workpiece surface thus affecting the size of the kerf as shown in figure 49. A shorter focal length also resulted in a smaller kerf width as shown in figure 50. This is expected because the focal length is also directly related to the focus spot size with a shorter focal length giving a smaller focus spot size and hence a smaller kerf width.

The comparison of kerf widths at maximum cutting speeds for the disk, fiber and CO_2 lasers at different material thickness (1mm, 2mm, 4mm and 6mm) are shown in figures 60, 61, 62 and 63. The disk and fiber laser cut kerfs showed a smaller kerf width than the CO_2 laser cut kerfs. The smaller kerf widths can be attributed to the smaller focus spot size that is associated with the better beam quality of the disk and fiber lasers as compared to the CO_2 laser beam quality.

The top kerf width was larger than the bottom kerf width for most of the cutting conditions indicating the tapered nature of laser cutting as caused by the loss of beam intensity due to widening of the focus spot size below the focus point and loss of gas pressure across the thickness of the cut especially for the larger sheet thickness (4mm and 6mm).

1mm and 2mm sheet thickness

Figures 60 and 61 (1mm and 2mm sheet thickness) show a smaller kerf width (approximately 0.3mm) for the disk and fiber lasers compared to the CO_2 laser kerf widths of around 0.4mm and 0.5mm for the 1mm and 2mm sheet thickness respectively. The smaller kerf width for the disk and fiber laser cut kerfs can be attributed to their better beam quality compared to the CO_2 laser beam quality. A high beam quality results in a smaller focus spot size and hence a smaller kerf width.
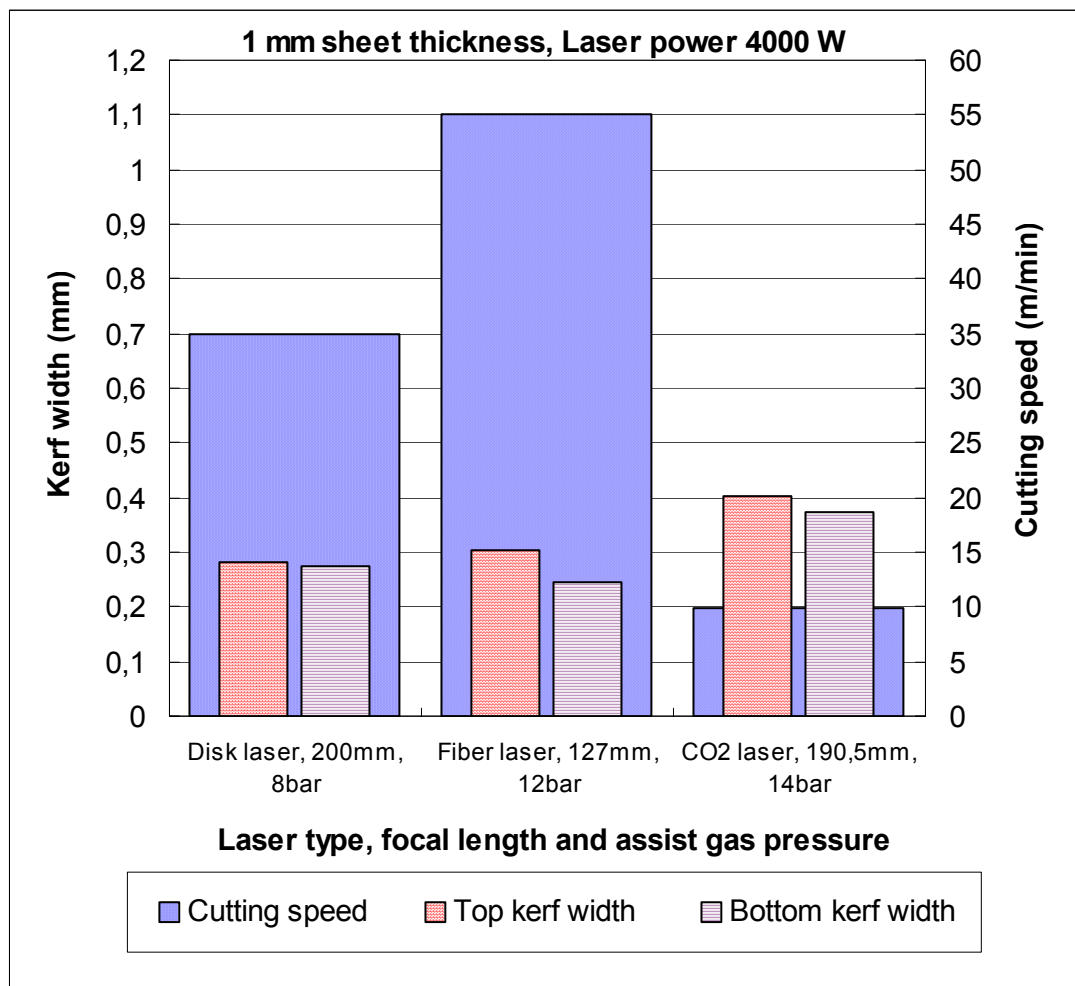
Figure 60. The top kerf width variation for the disk, CO_2 and fiber lasers at maximum cutting speed for 1mm sheet thickness (Disk: 35m/min, Fiber: 55m/min and CO_2 laser: 9.8m/min)
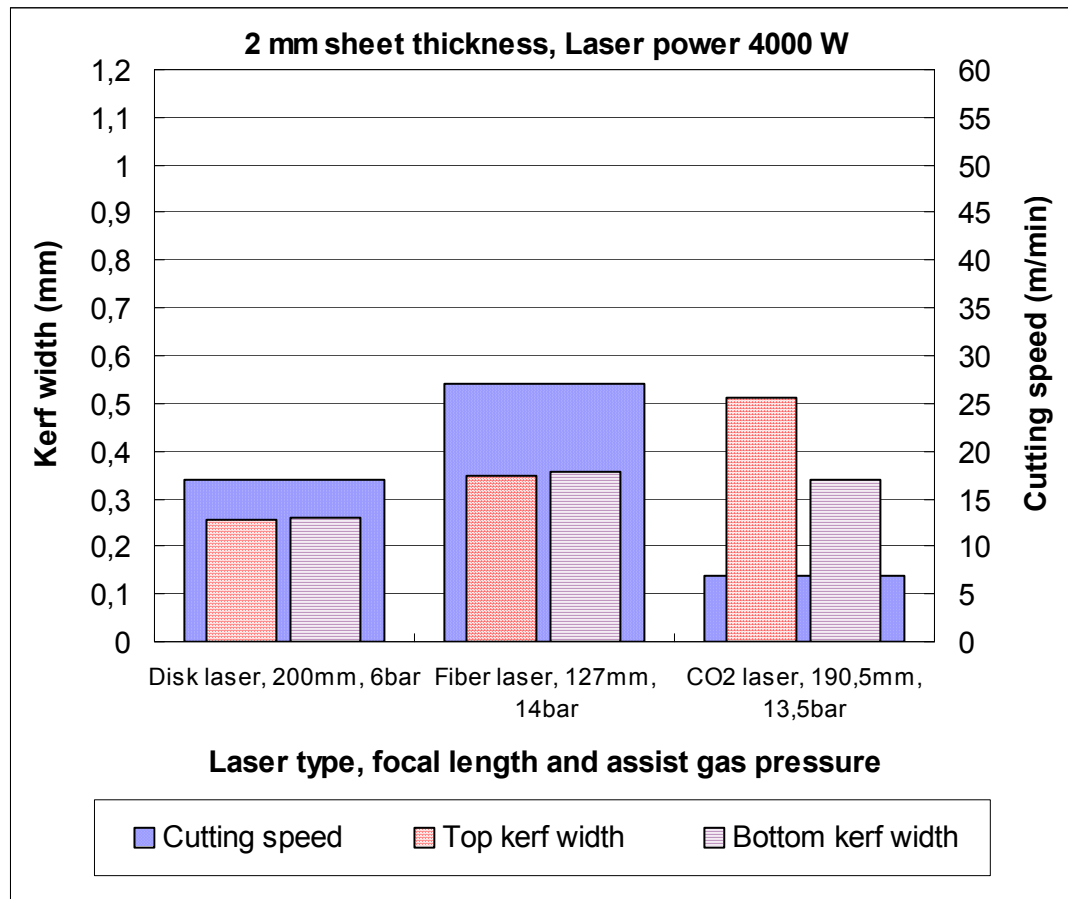
Figure 61. The top kerf width variation for the disk, CO_2 and fiber lasers at maximum cutting speed for 2mm sheet thickness (Disk: 17m/min, Fiber: 27m/min and CO_2 laser: 6.85m/min)

The smaller kerf width of the disk and fiber laser cut kerfs can also be attributed to the high cutting speeds of the disk and fiber lasers. The high cutting speeds cause a more localized melting of material along the cut kerf while ensuring that there is not enough time for heat conduction to the surrounding material. Heat conduction, which is favored by lower cutting speeds, causes melting of more material around the kerf and hence leads to a wider kerf.

4mm and 6mm sheet thickness

For the 4mm and 6mm sheet thickness (figures 62 and 63), there was not much difference in the kerf widths for the disk, fiber and CO_2 lasers. The difference between the top and bottom kerf widths was also generally larger at 4mm and 6mm sheet thickness than at 1mm

and 2mm sheet thickness. This could be because of the relatively lower cutting speeds at the 4mm and 6mm sheet thickness compared to the cutting speeds at 1mm and 2mm sheet thickness.

In the case of lower cutting speeds, the workpiece is heated up and melted within a relatively wide zone around the laser beam resulting in the formation of a wider kerf width at the top surface. Due to finite thermal conductivity, the top kerf width decreases with an increase in cutting speed until the top kerf width corresponds to the diameter of the focused laser beam. However, the focal length was not uniform in these cutting experiments with the different cutting lasers used and could have also had an effect on the kerf width variation observed in these experiments.
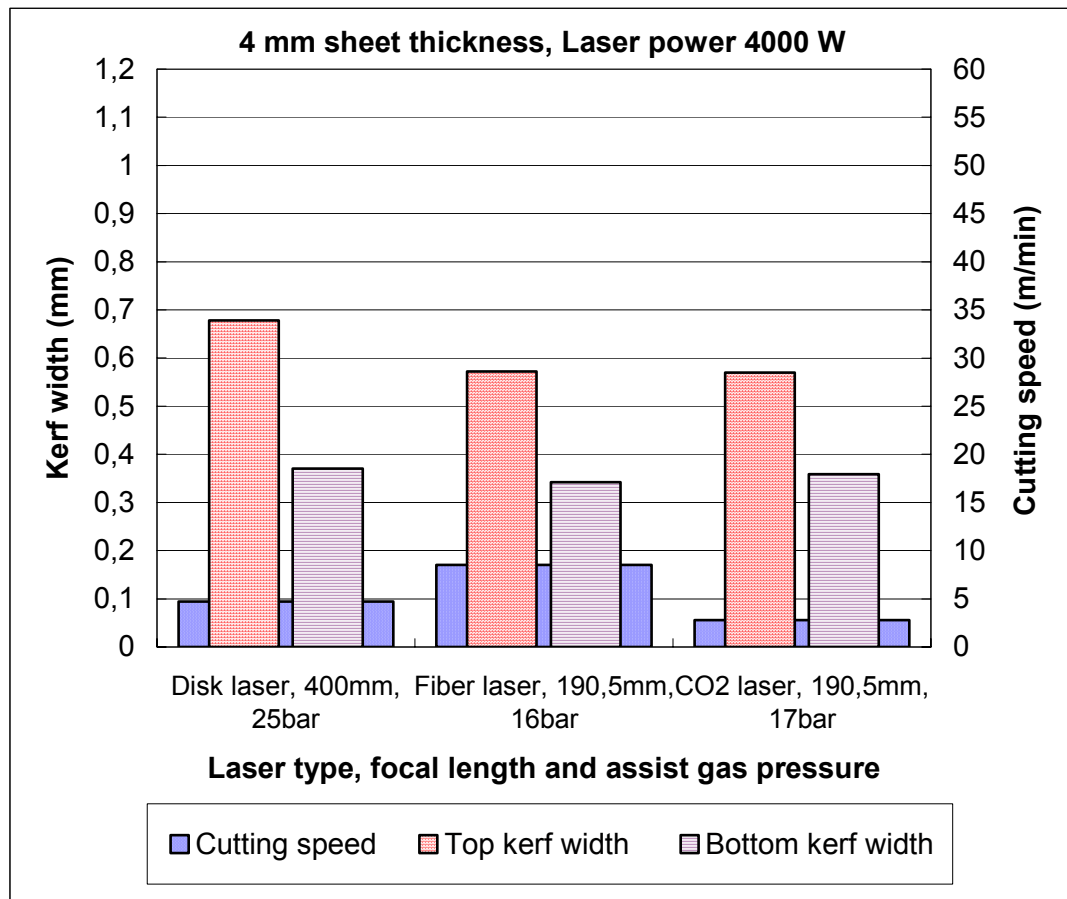
Figure 62. The top kerf width variation for the disk, CO_2 and fiber lasers at maximum cutting speed for 4mm sheet thickness (Disk laser: 4.7m/min, Fiber laser: 8.5m/min and CO_2 laser: 2.8m/min)
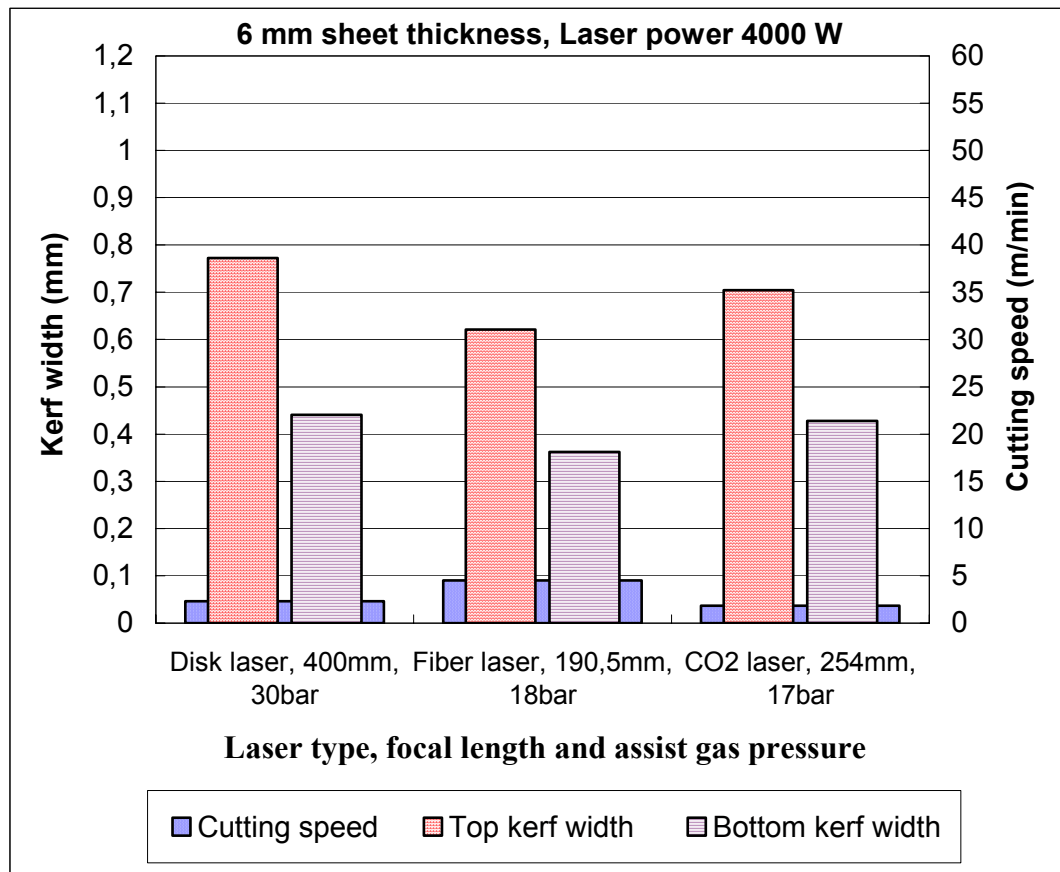
Figure 63. The top kerf width variation for the disk, CO_2 and fiber lasers at maximum cutting speed for 6mm sheet thickness (Disk laser: 2.3m/min, Fiber laser: 4.5m/min and CO_2 laser: 1.85m/min)

A larger amount of molten material is generated when cutting thicker sheets (4mm and 6mm) than when thinner sheets (1mm and 2mm) are cut. Therefore a higher gas pressure is necessary during cutting of thicker sheets in order to effectively blow out the melt from the cut kerf.

14.3 Perpendicularity deviation

Generally, the CO_2 laser cut surfaces showed the lowest perpendicularity deviation in these cutting experiments. Probably, the cutting speeds do not have a significant effect on the cut edge perpendicularity since the CO_2 laser cut kerfs were made at the lowest cutting speeds

compared to the disk and fiber laser experiments. However, in these particular cutting experiments the cutting speed was varied as well as the assist gas pressure, focal length and focus position. Therefore, the effects of the gas pressure, focal length and focus position on the perpendicularity of the cut edges could not be established. This could be investigated further by keeping all the other processing conditions constant while varying only the cutting speed.

The maximum measured values for perpendicularity deviation for each cut kerf were used for classification of the cut edges in the tolerance fields of the EN ISO 9013:2002 standard for thermal cuts. In the perpendicularity tolerance limits of this standard, range 1 corresponds to the best quality and range 5 the worst quality.

The perpendicularity classification of the disk laser cut edges shown in figure 64 revealed that for 1.3mm sheet thickness, the perpendicularity values were in ranges 1 and 2. The perpendicularity values for the 2.3mm, 4.3mm and 6.2mm sheet thickness were in range 2 and only one value for the 6.2mm thickness was in range 3.
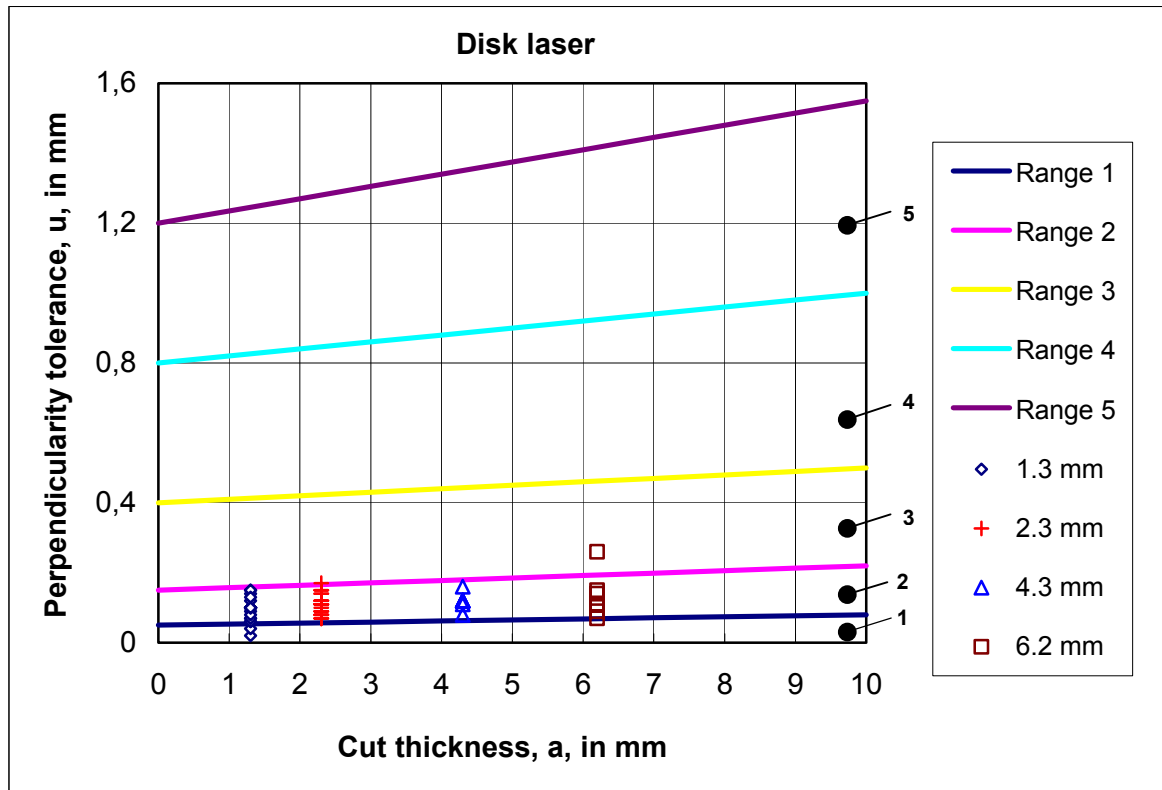
Figure 64. Perpendicularity tolerance classification of the disk laser cut edges

Figure 65 shows the perpendicularity classification of the fiber laser cuts in which the 1.3mm sheet thickness cuts were classified within ranges 1 and 2 while all the cuts for the 2.3mm, 4.3mm and 6.2mm sheet thickness were classified within range 2.
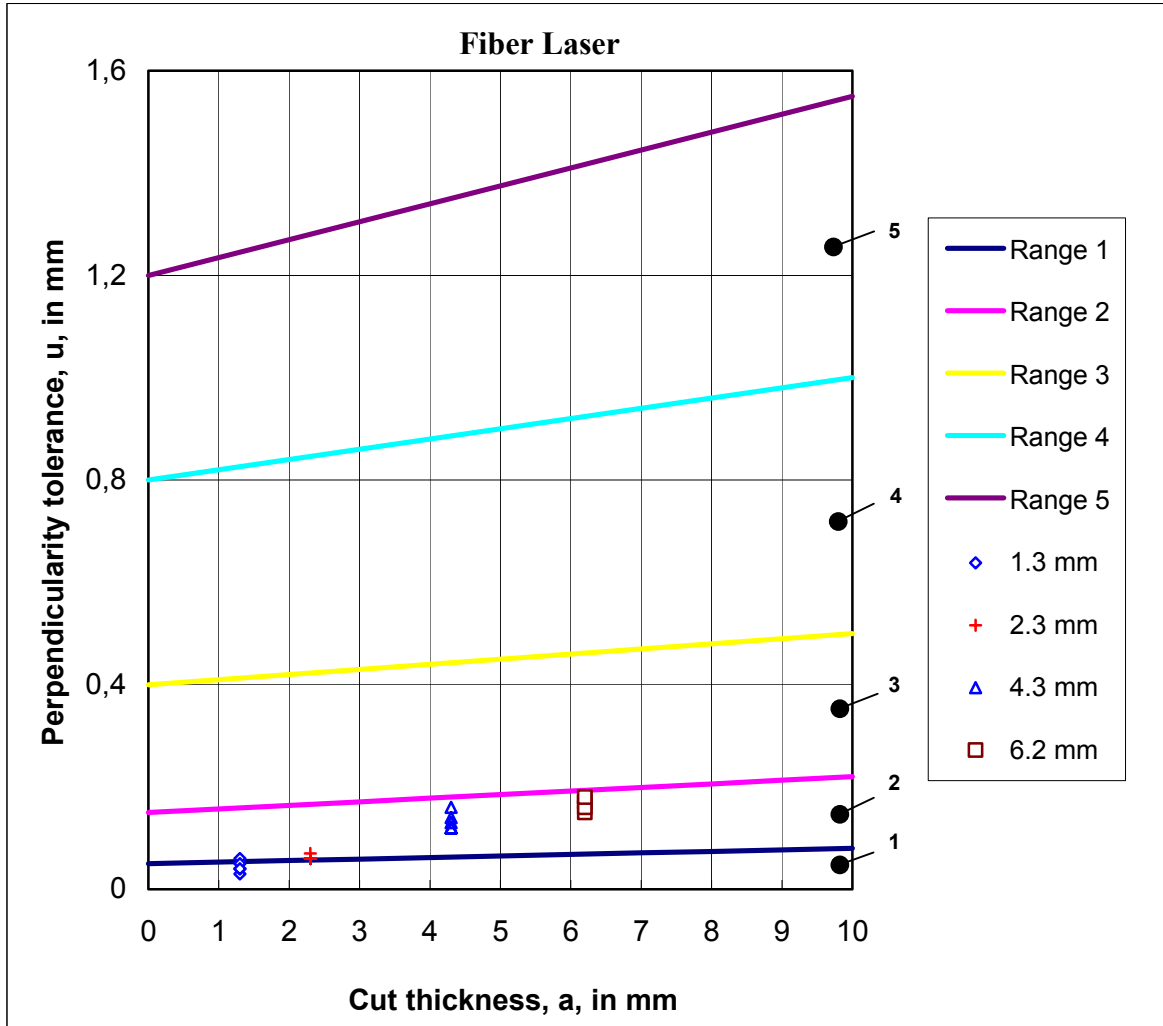
Figure 65. Perpendicularity tolerance classification of the fiber laser cut edges

The perpendicularity classification of the CO_2 laser cuts is shown in figure 66. All the perpendicularity values for the cuts of 1.3mm sheet thickness in range 1. The perpendicularity values for the 1.85mm, 4.4mm and 6.4mm sheet thickness cuts were in range 2.
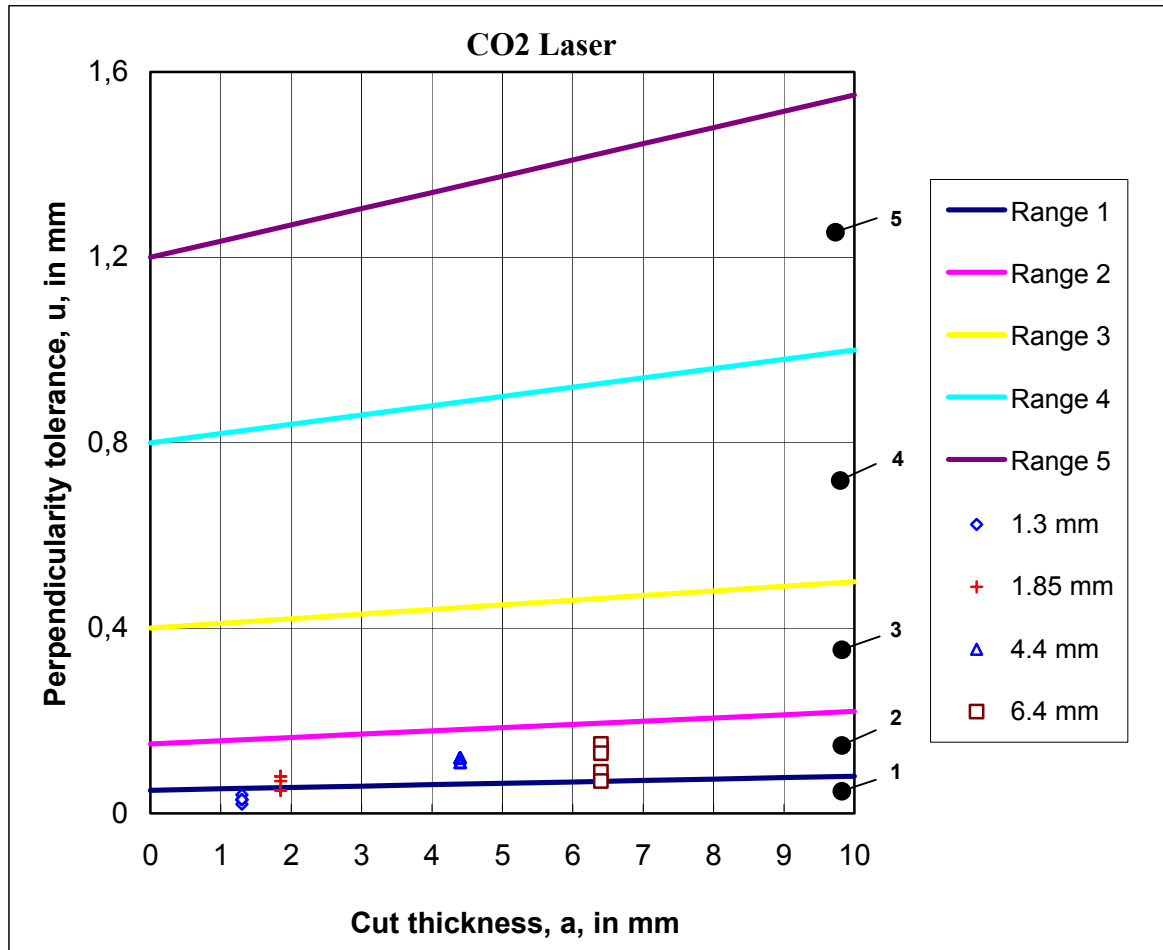
Figure 66. Perpendicularity tolerance classification of the CO_2 laser cut edges

The perpendicularity classification of the disk, fiber and CO_2 laser cuts shown in figures 64, 65 and 66 revealed that most of the cuts were within range 2. This perpendicularity deviation is not critical for the welding of thick sheets because filler material can easily be employed. However, it may be critical for the welding of thin sheets where use of filler material may cause uneven weld profile.

14.4 Surface roughness

The cut quality revealed a higher surface roughness for the cuts of 4.3mm and 6.2mm sheet thickness made with the disk and fiber lasers and the roughness varied along the cut thickness. The CO_2 laser cuts had a relatively low surface roughness even at 4.4mm and 6.4mm sheet thickness and the roughness was uniform through the cut thickness. Previous studies /2/ have shown that there is a critical cutting speed beyond which the surface roughness increases and this critical cutting speed is dependent on the power level.

There was increased surface roughness of the 6.2mm sheet thickness that was cut using the fiber laser at the maximum cutting speed of 4.5m/min and focal length of 7.5" (190.5mm). Probably, laser cutting of this sheet thickness with the cutting speed of 4.5m/min might be the boundary case for cutting with a focal length of 7.5" (190.5mm). Better results could probably be achieved by using a longer focal length, say 10" (254mm). This problem should be investigated further.

The cut surfaces were also classified in the tolerance fields of the EN ISO 9013 standard for thermal cuts according to the maximum measured values. Range 1 of the mean height of the profile, R_z5, tolerance limit corresponds to the best quality while range 4 corresponds to the worst quality.

The roughness classification of the disk laser cut surfaces is shown in figure 67. The cut surfaces for the 1.3mm sheet thickness had their roughness values within ranges 1 and 2. Similarly, the roughness values of the cut surfaces for the 2.3mm sheet thickness were also within ranges 1 and 2 except for one value that was in range 3. The cut surfaces for the 4.3mm sheet thickness had all their roughness values in range 2 and all the roughness values of the cut surfaces for the 6.2mm sheet thickness were in range 3.
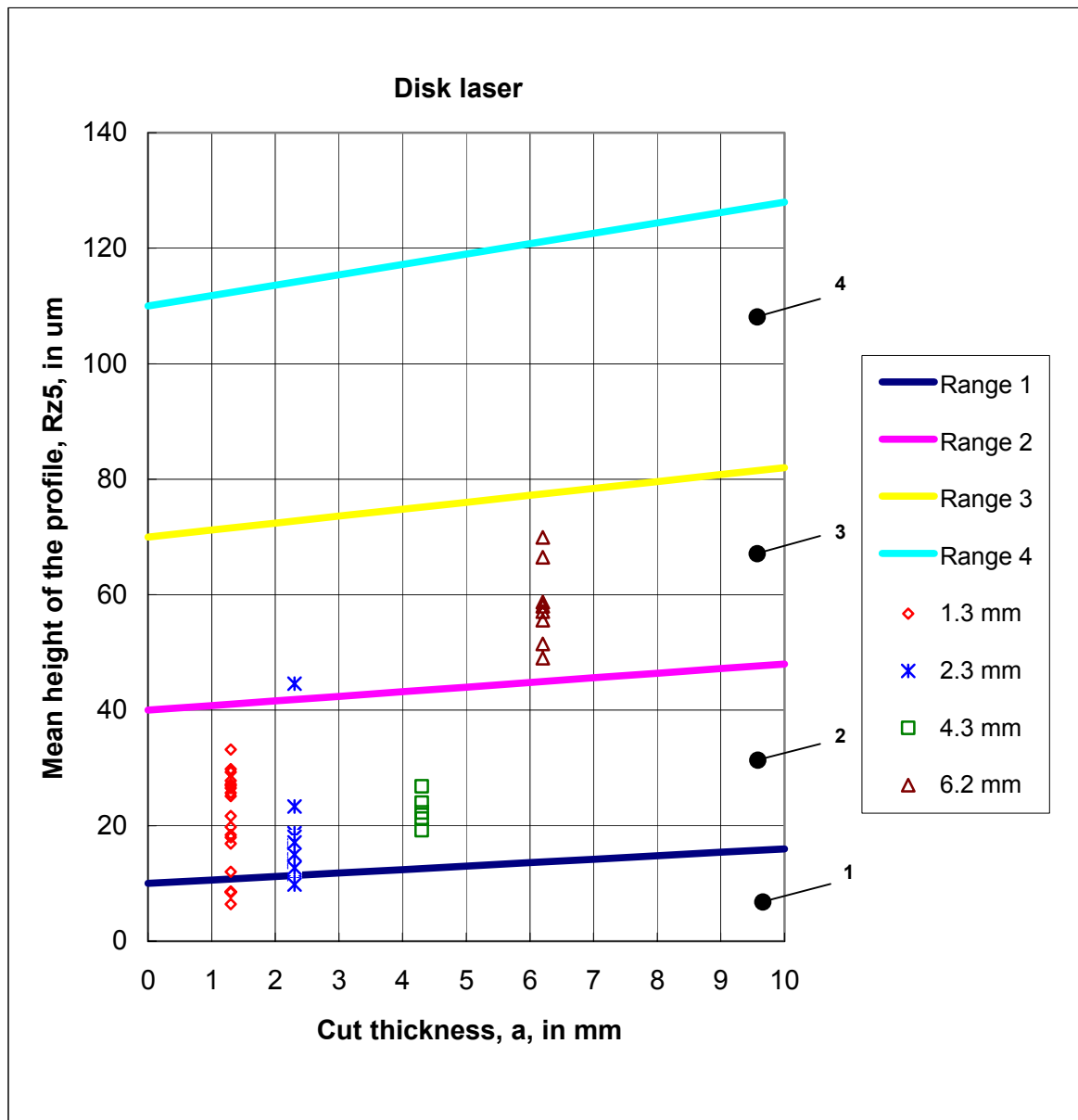
Figure 67. Roughness classification of the disk laser cut surfaces

Figure 68 shows the roughness classification of the fiber laser cut surfaces. The roughness values of the cut surfaces for the 1.3mm sheet thickness were in ranges 1 and 2 and all the roughness values of the cut surfaces for the 2.3mm sheet thickness were within range 2. The roughness values of the cut surfaces for the 4.3mm sheet thickness were in ranges 2, 3 and 4 while all the roughness values of the cut surfaces for the 6.2mm sheet thickness were in range 4.
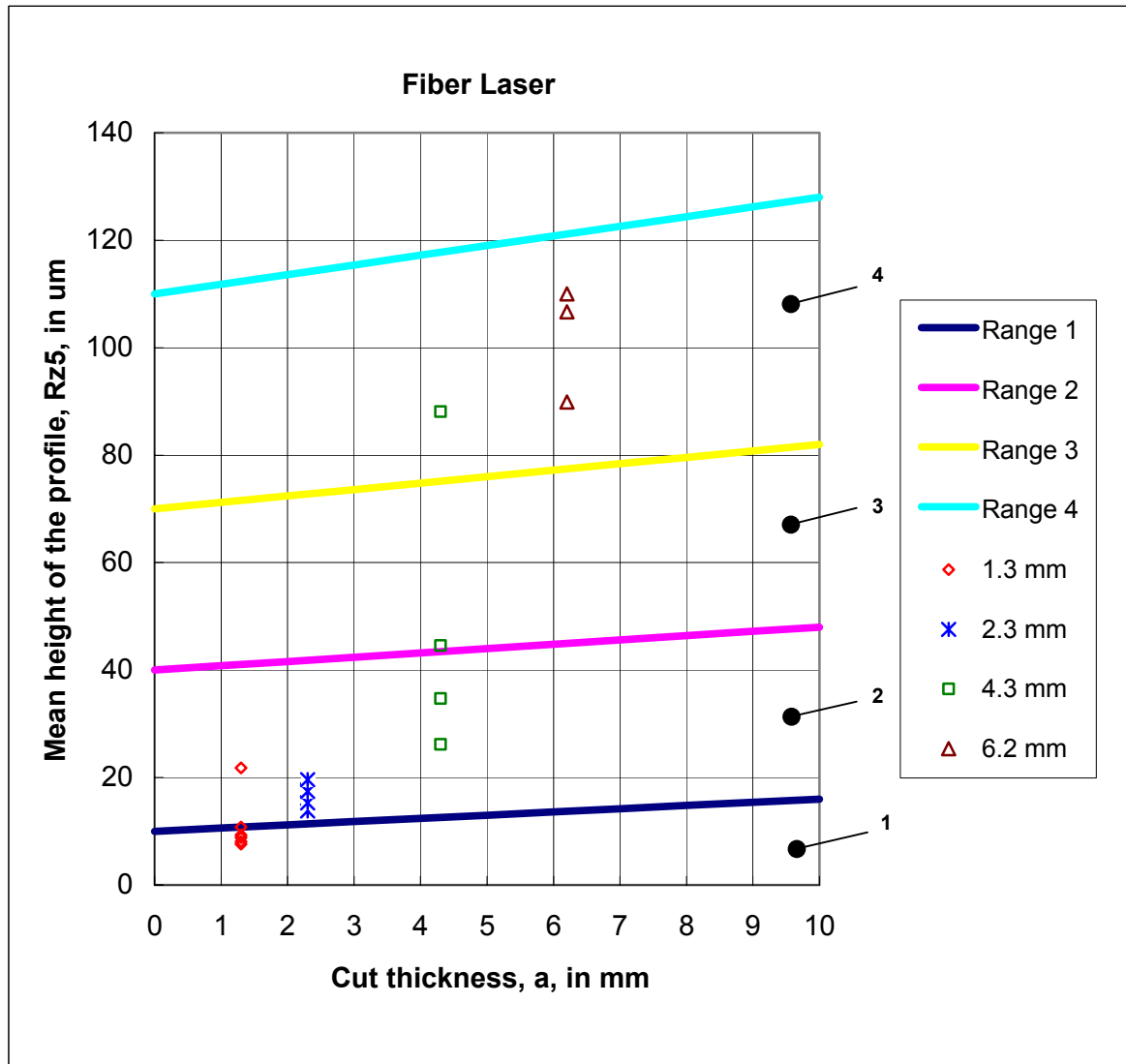
Figure 68. Roughness classification of the fiber laser cut surfaces

The roughness classification of the CO_2 laser cut surfaces is shown in figure 69. The roughness values of the cut surfaces for the 1.3mm sheet thickness were classified in ranges 1 and 2 while cut surfaces for the 1.85mm, 4.4mm and 6.4mm sheet thickness had all their roughness values in range 1.
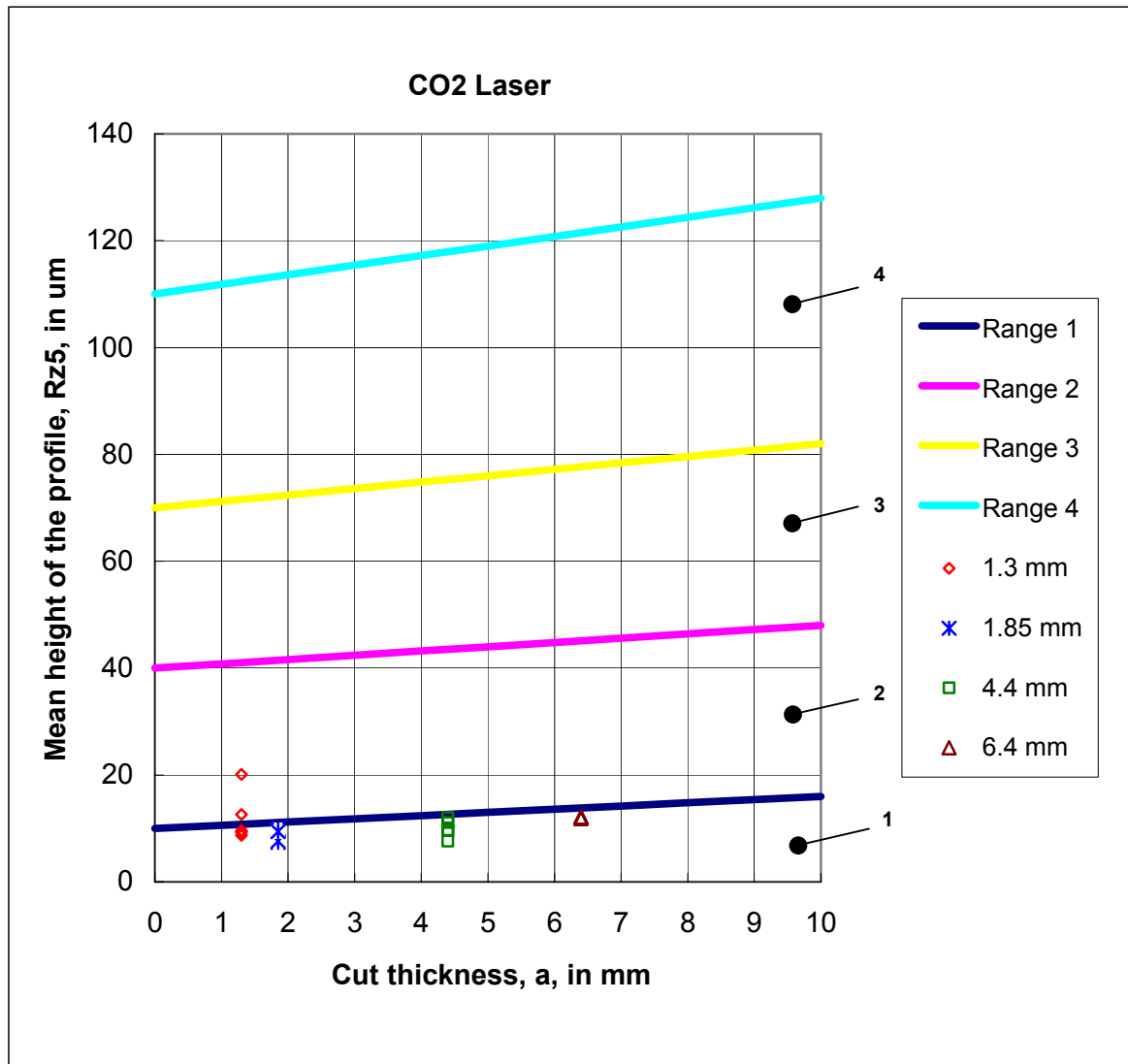
Figure 69. Roughness classification of the CO_2 laser cut surfaces

Generally, the CO_2 laser cut surfaces showed a lower surface roughness than the disk laser and fiber laser cut surfaces. The fiber laser cuts had the highest roughness at 6.2mm sheet thickness. Probably the disk and fiber laser cutting experiments for the 4.3mm and 6.2mm

sheet thickness did not have the appropriate combinations of focal length, focus position, cutting speeds and assist gas pressures for achievement of minimum surface roughness. For the case of fiber laser cutting of 6.2mm sheet thickness, it could be possible that the surface roughness can be reduced by the use of a longer focal length than the 7.5" (190.5mm) focal length that was used in this thesis.

As it has been shown in equations 2 and 3 in section 7.1.3 that both the focus spot size and depth of focus are directly proportional to the Beam Parameter Product (BPP), the high beam quality (BPP = 2.5mm.mrad) of the fiber laser gives a smaller spot size and shorter depth of focus which limit the effective cutting of thicker sheets. A shorter depth of focus limits the length along the cut thickness for effective cutting to take place and a smaller spot size results in a smaller kerf width that limits the effective removal of the large amount of molten material generated in thick section cutting. Therefore, cutting of thicker sheets requires a larger depth of focus for effective cutting throughout the whole sheet thickness and a wider kerf that would allow a larger part of the gas flow to penetrate the kerf and eject the molten material satisfactorily. The use of a longer focal length in this case would give a wider kerf and a larger depth of focus. The focus position can also be adjusted appropriately so as to achieve a wider kerf.

15. CONCLUSIONS AND RECOMMENDATIONS

The cutting speeds for the disk and fiber laser cutting experiments were enormous at sheet thickness less than 4mm as compared to the CO_2 laser cutting experiments. These high cutting speeds are a direct effect of the high power densities facilitated by the high beam quality. The cutting speeds for the disk and fiber lasers were lower at 6mm sheet thickness but there was still a considerable percentage increase compared to the CO_2 laser cutting speeds at this thickness (see table 4).

The disk and fiber cutting experiments in this study achieved the objective of maximum cutting speeds, which is a good parameter for higher productivity. However, optimization of the cut quality in relation to the maximum cutting speeds was not achieved for the 4.3mm and 6.2mm sheet thickness as seen by the high values of the surface roughness of the disk laser and fiber laser cut surfaces for the 4.3mm and 6.2mm sheet thickness. The classification of the cut surfaces revealed that the disk laser and fiber laser cutting experiments did not achieve the anticipated smooth cut surfaces (low surface roughness). The cut surface quality of the CO_2 laser cuts was even better than that of the disk laser and fiber laser cuts.

The cutting results showed that the disk laser and fiber laser have a potential for cutting applications and are capable of competing favorably with the CO_2 laser. It might be possible that the defects observed for thick sheets can be avoided by proper selection of process parameters especially focus position, cutting speed and gas pressure. The appropriate cutting parameters for the disk laser and fiber laser cutting of larger sheet thickness (thickness greater than 4mm) could not be established in this study as it was beyond the scope of this thesis.

Future studies on cutting of stainless steel with the disk laser and fiber laser could cover optimization of the cut quality by ensuring minimum surface roughness and minimum perpendicularity deviation. The focus could be on improving the surface quality for the thicker sheet.

REFERENCES

1. Gabzdyl J. T., "Effects of gases on laser cutting of stainless steels", In Laser Materials Processing: Proceedings of the International Congress on Applications of Lasers & Electro-Optics ICALEO '96 held in Detroit, Michigan, USA; 14-17 October 1996, pp. C39-C44

2. Rajaram N., Sheik-Ahmad J. and Cheraghi S. H., "CO_2 laser cut quality of 4130 steel", International Journal of Machine Tools & Manufacture Volume 43 (2003) pp. 351-358

3. Anon., "Stainless Steel Overview: Applications", http://www.ssina.com/overview/app_intro.html, referenced 10/01/2006

4. Anon., "Stainless Steel", http://www.nisshin-steel.co.jp/nisshin-steel/english/profile/stain.htm, referenced 10/01/2006

5. Anon., "Types of Stainless Steel: Austenitic" http://www.assda.asn.au/asp/index.asp?pgid=18041&cid=34330&id=56984, referenced 10/01/2006

6. Balbi M., Silva G., "Stainless steel plate cutting: thermal and mechanical cutting. Laser cutting - some observations", Avesta Stainless Bulletin, Oct.-Nov.-Dec. 1982, Volume 6, Number 4, pp. 3-11

7. Crafer R. C. and Oakley P. J., "Laser Processing in manufacturing", Chapman & Hall, ISBN 0-412-41520-8, pp. 1, 13-15

8. Golnabi H. and Mahdieh M. H., "Trend of laser research developments in global level", Optics & Laser Technology, Volume 38, Issue 2, March 2006, pp. 122-131

9. Dirk Petring, "Laser Cutting", LIA Handbook of Laser Materials Processing, Ist edition, 2001, Laser Institute of America, ISBN 0-912035-15-3, pp. 425-433

10. Thomas R. Kugler, "Nd:YAG Lasers", LIA Handbook of Laser Materials Processing, 1st edition, 2001, Laser Institute of America, ISBN 0-912035-15-3, pp. 37- 44

11. Rajendran Natarajan, Ph.D. Dissertation: "An experimental and theoretical study of heat transfer effects during a laser-cutting process", Iowa State University, 1990, U.M.I Dissertation Information Service, Order Number 9100495, pp. 1, 10-12, 69

12. Hügel H., "New solid-state lasers and their application potentials", Optics and Lasers in Engineering, Volume 34 (2000), pp. 213-229

13. Adolf Giesen, "Thin Disk Lasers - Power scalability and Beam quality", http://www.pro-physik.de/Phy/pdfs/NEWS_PDF_GER_6737.pdf and http://www.wiley-vch.de/berlin/journals/ltj/05-02/LTJ02_42_45.pdf, referenced 20/10/2005

14. Thomy C., Seefeld T. and Vollertsen F., "High-Power Fiber Lasers − Application Potentials for Welding of Steel and Aluminium Sheet Material", Advanced Materials research, Volumes 6-8, (2005) pp. 171-178, available online at http://www.scientific.net/

15. European Committee for Standardization, "Thermal cutting – Classification of thermal cuts, Geometrical product specification and quality tolerances", EN ISO 9013: 2002 (ISO 9013:2002)

16. Anon., "High-Powered Disk Laser" from http://www.trumpf-laser.com/208.img-cust/Disk_Laser.pdf; "The Disk Laser" from http://www.trumpf-laser.com/208.img-cust/Scheibenlaser_engl.pdf; "The HLD cw Lasers" from http://www.trumpf-

laser.com/208.img-cust/HLD_Laser_engl.pdf, and "Disk lasers – Technical data" from http://www.trumpf-laser.com/208.index.html, referenced 29/09/2005

17. Anon., "DS series (disc): principle", http://www.rofin.com/index-e.htm, referenced 24/09/2005

18. Zapata L. E., Beach R. A., Mitchell S. and Payne S. A., "Yb Thin Disk Laser results", http://www.llnl.gov/tid/lof/documents/pdf/246177.pdf, referenced 24/09/2005

19. John Vetrovec, Rashmi Shah, Tom Endo, Andrea Koumvakalis, Kevin Masters, William Wooster, Kenneth Widen, and Steven Lassovsky, "Progress in the development of solid-state disk laser", http://www.kigre.com/yb16.pdf, referenced 20/05/2005

20. Reinhart Poprawe and Wolfgang Schulz, "Development and application of new high-power laser beam sources", Fraunhofer Institut Lasertechnik ILT, Germany, http://www.ilt.fraunhofer.de/ilt/pdf/ger/50_003.pdf, referenced 24/09/2005

21. Anon., "The Thin Disk Laser Technology", http://www.fgsw.de/homepage/leistungen/produkte/scheibenlaser/ThinDiskTechnology _LOT_2005.pdf, referenced 29/09/2005

22. Anon., "Laser Focus World May, 1999" http://lfw.pennnet.com/Articles/Article_Display.cfm?Section=Archives&Subsection=D isplay&ARTICLE_ID=31572, referenced 20/09/2005

23. Christian Schmitz, "TRUMPF Disk Laser – Status and Prospect", Trumpf Technology Day - Disk Laser, Schramberg, 27th January 2004

24. Wolfram Rath, "Disc lasers and their applications", ROFIN-SINAR Laser GmbH, Open House Rofin Sinar 2004, 20th April 2004

25. John Powell, "CO$_2$ Laser Cutting", 1993, Springer Verlag, ISBN 3-540-19786-9, pp. 1,6,183-184

26. John F. Ready, "Absorption of Laser Irradiation: Variation During Irradiation", LIA Handbook of Laser Materials Processing, I[st] edition, 2001, Laser Institute of America, ISBN 0-912035-15-3, pp. 183-184

27. Paul Denney, "New Lasers in Automotive Applications", http://www.laserinstitute.org/publications/lia_today/archive/articles/newfiberlaser/index .php3, referenced 24/09/2005

28. John Canning, "Fibre lasers and related technologies", Optics and Lasers in Engineering, Volume 44, Issue 7, July 2006, pp. 647-676, available online at www.sciencedirect.com, referenced 22/08/2005

29. Bill Shiner, "Fiber Lasers for Material Processing", Laser institute of America, http://www.laserinstitute.org/publications/lia_today/archive/articles/fiberlaser/index.ph p3 /, referenced 25/01/2006

30. Anon., "Fibre Laser Technology at TWI Yorkshire", http://www.twi.co.uk/j32k/unprotected/band_1/twi_yorks_fibre.html, referenced 28/10/2005

31. Anon., **"YLR-HP Series: 1-50kW Ytterbium Fiber Lasers",** http://www.ipgphotonics.com/apps_mat_multi_YLR.htm/, referenced 30/04/2006

32. Anon., **"ELR Series: 1-100W Single Mode Erbium Fiber Lasers",** http://www.ipgphotonics.com/apps_mat_single_ELR.htm/, referenced 30/04/2006

33. David R. Whitehouse, "Guide to Laser Materials Processing", Laser Institute of America, 1993, ISBN 0-912035-11-0, pp. 46-50

34. Yilbas B. S., "The analysis of CO_2 laser cutting", Proceedings of the Institution of Mechanical Engineers, Part B: Journal of. Engineering Manufacture, Volume 211, Number 3 (1997), pp. 223-232

35. Anon., "CO_2 Lasers - Lasers for Industry", http://www.rofin-sinar.com/index-e.htm, referenced 20/11/2005

36. Anon., "Diode-pumped cw solid-state lasers", http://www.trumpf-laser.com/208.index.html, referenced 25/04/2006, referenced 2/05/2006

37. Anon., "The universal CO_2 - Laser for cutting and welding", http://www.trumpf-laser.com/208.img-cust/TLF_700_7000_E.pdf, referenced 2/05/2006

38. Anon., "Solid-State Lasers", http://www.rofin-sinar.com/index-e.htm, referenced 3/05/2006

39. Anon., "Introduction to Industrial Laser Materials Processing", Hamburg, 2003, Rofin Group, pp. 17-26

40. Anon, "Lasers and Laser systems, CO_2 lasers", http://www.coherent.com/Lasers , referenced 2/05/2006

41. Anon., Laser solutions, http://www.synrad.com/Products/overview.htm/, referenced 3/05/2006

42. Guillas C., Le Gall C., Theveney S. and Lefebvre P., "Comparative performances of CO_2 and YAG lasers in the cutting of stainless steel", Proceedings of SPIE: High-Power Solid State Lasers and Applications, August 1990, Volume 1277, pp. 244-255

43. Tech Tran Consultants Inc., "Lasers in Materials Processing, A summary and forecast", 1989, ISBN # 0-918989-07-08, pp. 43-39

44. Anon., "YLR-HP Series: 1-20kWatt Ytterbium Fiber Lasers", http://www.ipgphotonics.com/html/90_1-20kw_mm_@1070nm.cfm, referenced 27/02/2006

45. John C. Ion, "Laser Processing of Engineering materials", ISBN 0 7506 6079 1, pp. 347-365

46. Anon., "CNC Laser Cutting", http://www.emachineshop.com/machines-kerf/laser-cutting.htm, referenced 22/09/2005

47. Yilbas B. S., Davies R. and Yilbas Z., "Study into penetration speed during CO_2 laser cutting of stainless steel", Optics and Lasers in Engineering, Volume 17, Issue 2, 1992, pp. 69-82

48. Anon., "Absorption, Heating and Phase Changes", http://info.tuwien.ac.at/iflt/safety/misc/ba_3_1.htm, referenced 29/09/2005

49. Anon., "Facts about: Laser cutting techniques", AGA Group Ltd, pp. 4-12

50. Anon., "Benefits of Direct Diode Lasers for Welding", http://www.nuvonyx.com/overview/index.html, referenced 22/09/2005

51. Robert Lambert, Rodolfo Cortes Martinez, Alan Greenaway, Julian Jones and Duncan Hand, "Monitoring of high power laser beams and their application to laser machining", http://www.aop.hw.ac.uk/Projects/mat17.htm, referenced 12/02/2006

52. Olsen Flemming O., "Polarization Effects in Laser Cutting: Basics", LIA Handbook of Laser Materials Processing, Ist edition, 2001, Laser Institute of America, ISBN 0-912035-15-3, pp. 433 – 436

53. Modest Michael F., "Reflectivity and Absorptivity of Opaque surfaces", LIA Handbook of Laser Materials Processing, Ist edition, 2001, Laser Institute of America, ISBN 0-912035-15-3, pp.180

54. Kanaoka M. and Kitani M., "Report on Current CO_2 Laser Applications in Japan", SPIE Volume 952 (Proceedings of the Conference on Laser Technologies in Industry, Oporto 1988) (188) pp. 600-608

55. Olsen, F.O., "Cutting with polarized laser beams", DVS-berichte 63 (1980), Deutsche Verband für Schweisstechnik, ISBN 3-87155-364-6, pp. 197-200

56. Ivarson Anders, PhD Thesis: "On the physics and chemical thermodynamics of laser cutting," Luleå University of Technology, Sweden. 1993: 114D, ISSN 0348-8373, pp. 7, 35-37, 73-74,105-124

57. Fieret J., Terry M. J. and Ward B. A., "Overview of flow dynamics in gas assisted laser cutting", Presented in the fourth International Symposium on optical and Optoelectronic Applied Science and Engineering, Topical Meeting on High Power Lasers: Sources, Laser-Material interactions, High Excitations, and Fast Dynamics in Laser Processing and Industrial Applications, 30 March – 3 April 1987, The Hague, The Netherlands, (Culham laboratories) report CLM-P 818

58. Chen Kai, Yao Lawrence Y. and Modi Vijay, "Gas jet – Workpiece interactions in laser machining", Journal of Manufacturing Science and Engineering, August 2000, Volume 122, pp. 429 – 438

59. Ketting, H.-O. & Olsen, F.O., "High pressure off-axis laser cutting of stainless steel and aluminium", Proceedings of International Conference on Laser Advanced Materials Processing (Science and Applications), LAMP' 92, 7-12 June 1992, Nagaoka, Japan, ISSN 0918-2993, pp. 607-612

60. Anon., "Assisting gas for cutting", http://www.airliquide.com/en/medias/pdf/business/industry/welding/laser_cutting.pdf, referenced 24/09/2005

61. Pfeiffer E., "Laser beam cutting in the IWS Dresden", Fraunhofer IWS Dresden

62. Faerber M., "Applications of Laser Technology in Materials Processing, Components and Process Assistance, Gases for increased productivity of laser processing", Optical and Quantum Electronics, Springer Netherlands, ISSN: 0306-8919 (Paper) 1572-817X (Online), Volume 27, Number 12, December 1995, pp. 1449 – 1455

63. Steen William M., "Laser Material Processing", Third Edition, 2003, ISBN 1-85233-698-6, pp. 137

64. Migliore Leonard, "Laser Cutting of Metals", LIA Handbook of Laser Materials Processing, I[st] edition, 2001, Laser Institute of America, ISBN 0-912035-15-3, pp. 438

65. Yilbas B. S., "Effect of process parameters on the kerf width during the laser cutting process", Proceedings of the Institution of Mechanical Engineers, Part B: Journal of Engineering Manufacture, Volume 215, Number 10, 2001, ISSN: 0954-4054, pp. 1357 – 1365

66. Yilbas B. S., "Laser cutting quality assessment and thermal efficiency analysis", Journal of Materials Processing Technology, Volumes 155-156, 30 November 2004, pp. 2106-2115

67. Olsen, F.O., "Fundamental mechanisms of cutting front formation in laser cutting", Proceedings of International Conference on Laser materials Processing: Industrial and Microelectronics Applications, Europto Series, SPIE vol. 2207, ISBN 0-8194-1508-1, 1994, pp. 235-247

68. Steen William M., "Laser Material Processing", Springer-Verlag, 1991, ISBN 3-540-19670-6, pp. 82

69. Miyamoto I. and Maruo H., "The Mechanism of Laser Cutting", Welding in the World, 1991, I-882-89 IIW-1024-89, Volume 29, No. 9/10, pp. 283-294

70. Schuöcker D., "Dynamic phenomena in laser cutting and cut quality", Applied Physics B: Lasers and Optics, Volume 40, Number 1, May 1986, Springer Berlin/Heidelberg, ISSN 0946-2171 (paper) 1432-0649 (online), pp. 9-14

71. Ghany Abdel K. and Newishy M., "Cutting 1.2mm thick austenitic stainless steel sheet using pulsed and CW Nd:YAG laser", Journal of Materials Processing Technology 168 (2005), pp. 438-447

72. Powell John, "CO_2 Laser Cutting of Metals", LIA Handbook of Laser Materials Processing, I[st] edition, 2001, Laser Institute of America, ISBN 0-912035-15-3, pp. 439-446

73. Sheng P.S. and Joshi V.S., "Analysis of heat-affected zone formation for laser cutting of stainless steel", Journal of Materials Processing Technology, Volume 53, Number 3, September 1995, pp. 879-892

APPENDICES

Appendix 1. Disk laser cutting parameters

Appendix 2. Fiber laser cutting parameters

Appendix 3. CO_2 laser cutting parameters

APPENDIX 1. DISK LASER CUTTING PARAMETERS

Nr.	Geometry	Thickness [mm]	Cutting speed [m/min]	Laser power [W]	Focal length [mm]	Focus point position [mm]	Working distance [mm]	Assist gas	Gas pressure [bar]	Nozzle diameter [mm]	Remark
Material: Stainless steel AISI 304 (sheet thickness: 1.3mm, 4.3mm and 6.2mm) and AISI 316 (sheet thickness: 2.3mm)												
1	Line 100 mm	1.3	31,5	4000	200	0	0,3	N_2	8	1,2	Good
2	Line 100 mm	1.3	33,25	4000	200	0	0,3	N_2	8	1,2	Good
3	Line 100 mm	1.3	35	4000	200	0	0,3	N_2	8	1,2	Very good
4	Line 100 mm	1.3	36,75	4000	200	0	0,3	N_2	8	1,2	Good
5	Line 100 mm	1.3	38,5	4000	200	0	0,3	N_2	8	1,2	Good
6	Line 100 mm	1.3	9	4000	400	-1	0,5	N_2	20	1,7	Good
7	Line 100 mm	1.3	9,5	4000	400	-1	0,5	N_2	20	1,7	Good
8	Line 100 mm	1.3	10	4000	400	-1	0,5	N_2	20	1,7	Good
9	Line 100 mm	1.3	10,5	4000	400	-1	0,5	N_2	20	1,7	Good, small burr
10	Line 100 mm	1.3	11	4000	400	-1	0,5	N_2	20	1,7	Good, small burr
11	Line 100 mm	1.3	10	4000	400	6	0,5	N_2	20	1,7	Cut, burrs
12	Line 100 mm	1.3	10	4000	400	3	0,5	N_2	20	1,7	Cut, burrs
13	Line 100 mm	1.3	10	4000	400	0	0,5	N_2	20	1,7	Good, nearly no burr
14	Line 100 mm	1.3	10	4000	400	-3	0,5	N_2	20	1,7	Cut, burrs
15	Line 100 mm	1.3	10	4000	400	-6	0,5	N_2	20	1,7	Not good, much burrs

16	Line 100 mm	1.3	6,3	4000	600	-3	0,3	N_2	15	2,3	Good, nearly no burr
17	Line 100 mm	1.3	6,65	4000	600	-3	0,3	N_2	15	2,3	Good, nearly no burr
18	Line 100 mm	1.3	7	4000	600	-3	0,3	N_2	15	2,3	Good, nearly no burr
19	Line 100 mm	1.3	7,35	4000	600	-3	0,3	N_2	15	2,3	Good, nearly no burr
20	Line 100 mm	1.3	7,7	4000	600	-3	0,3	N_2	15	2,3	Good, nearly no burr
21	Line 100 mm	2.3	15,3	4000	200	0	0,3	N_2	6	1,2	Good, small burr
22	Line 100 mm	2.3	16,15	4000	200	0	0,3	N_2	6	1,2	Good, small burr
23	Line 100 mm	2.3	17	4000	200	0	0,3	N_2	6	1,2	Good, nearly no burr
24	Line 100 mm	2.3	17,85	4000	200	0	0,3	N_2	6	1,2	Good, small burr
25	Line 100 mm	2.3	18,7	4000	200	0	0,3	N_2	6	1,2	Burrs and resolidified melt
26	Line 100 mm	2.3	7,2	4000	400	-2	0,3	N_2	20	2,3	Good, nearly no burr
27	Line 100 mm	2.3	7,6	4000	400	-2	0,3	N_2	20	2,3	Good, nearly no burr
28	Line 100 mm	2.3	8	4000	400	-2	0,3	N_2	20	2,3	Good, nearly no burr
29	Line 100 mm	2.3	8,4	4000	400	-2	0,3	N_2	20	2,3	Good, nearly no burr
30	Line 100 mm	2.3	8,8	4000	400	-2	0,3	N_2	20	2,3	Good, nearly no burr
31	Line 100 mm	2.3	8	4000	400	6	0,3	N_2	20	2,3	No cut
32	Line 100 mm	2.3	8	4000	400	3	0,3	N_2	20	2,3	No penetration
33	Line 100 mm	2.3	8	4000	400	0	0,3	N_2	20	2,3	Good, small burr
34	Line 100 mm	2.3	8	4000	400	-3	0,3	N_2	20	2,3	Good, small burr
35	Line 100 mm	2.3	8	4000	400	-6	0,3	N_2	20	2,3	Good, small burr
36	Line 100 mm	2.3	5,4	4000	600	-3	0,5	N_2	20	2,3	Good, small burr
37	Line 100 mm	2.3	5,7	4000	600	-3	0,5	N_2	20	2,3	Good, small burr

38	Line 100 mm	2.3	6	4000	600	-3	0,5	N$_2$	20	2,3	Good, small burr
39	Line 100 mm	2.3	6,3	4000	600	-3	0,5	N$_2$	20	2,3	Good, small burr
40	Line 100 mm	2.3	6,6	4000	600	-3	0,5	N$_2$	20	2,3	Good, small burr
41	Line 100 mm	4.3	4,23	4000	400	-0,5	0,3	N$_2$	25	2,3	Cut, burrs
42	Line 100 mm	4.3	4,465	4000	400	-0,5	0,3	N$_2$	25	2,3	Cut, burrs
43	Line 100 mm	4.3	4,7	4000	400	-0,5	0,3	N$_2$	25	2,3	Good, small burrs
44	Line 100 mm	4.3	4,935	4000	400	-0,5	0,3	N$_2$	25	2,3	Cut, burrs
45	Line 100 mm	4.3	5,17	4000	400	-0,5	0,3	N$_2$	25	2,3	Cut, burrs
46	Line 100 mm	6.2	2,07	4000	600	-3	0,5	N$_2$	30	2,3	Cut, burrs
47	Line 100 mm	6.2	2,185	4000	600	-3	0,5	N$_2$	30	2,3	Cut, burrs
48	Line 100 mm	6.2	2,3	4000	600	-3	0,5	N$_2$	30	2,3	Cut, burrs
49	Line 100 mm	6.2	2,415	4000	600	-3	0,5	N$_2$	30	2,3	No penetration
50	Line 100 mm	6.2	2,07	4000	600	-0,5	0,3	N$_2$	30	2,3	Cut, burrs
51	Line 100 mm	6.2	2,185	4000	600	-0,5	0,3	N$_2$	30	2,3	Cut, burrs
52	Line 100 mm	6.2	2,3	4000	600	-0,5	0,3	N$_2$	30	2,3	Cut, small burrs
53	Line 100 mm	6.2	2,415	4000	600	-0,5	0,3	N$_2$	30	2,3	Cut, burrs
54	Line 100 mm	6.2	2,53	4000	600	-0,5	0,3	N$_2$	30	2,3	Cut, burrs

APPENDIX 2. FIBER LASER CUTTING PARAMETERS

Nr.	Geometry	Thickness [mm]	Cutting speed [m/min]	Laser power [W]	Focal length [mm]	Focus point position [mm]	Working distance [mm]	Assist Gas	Gas pressure [bar]	Nozzle diameter [mm]	Remark
					Material: Stainless steel AISI 304 (sheet thickness: 1.3 mm)						
1	Line 150 mm	1.3	10	1500	127	0	0,5	N$_2$	12	2	Good
2	Line 150 mm	1.3	10	1000	127	0	0,5	N$_2$	12	2	Burr
3	Line 150 mm	1.3	10	1100	127	0	0,5	N$_2$	12	2	Very good
4	Line 150 mm	1.3	10	1100	127	0	0,5	N$_2$	10	2	Burr
5	Line 150 mm	1.3	10	1100	127	0	0,5	N$_2$	14	2	Burr
6	Line 150 mm	1.3	10	1100	127	-0,5	0,5	N$_2$	12	2	Burr
7	Line 150 mm	1.3	10	1100	127	-0,3	0,5	N$_2$	12	2	Burr
8	Line 150 mm	1.3	10	1100	127	0,3	0,5	N$_2$	12	2	Very good
9	Line 150 mm	1.3	10	1100	127	0,2	7	N$_2$	12	2	Very good
10	Line 150 mm	1.3	10	1100	127	0,2	0,7	N$_2$	12	1,5	Burr
11	Line 150 mm	1.3	10	1100	127	0	0,5	N$_2$	12	2	Good
12	Line 150 mm	1.3	20	1500	127	0	0,5	N$_2$	12	2	Very good
13	Line 150 mm	1.3	20	1425	127	0	0,5	N$_2$	12	2	Very good
14	Line 150 mm	1.3	20	1350	127	0	0,5	N$_2$	12	2	No cut
15	Line 150 mm	1.3	20	1575	127	0	0,5	N$_2$	12	2	Very good

16	Line 150 mm	1.3	20	1650	127	0	0,5	N$_2$	12	2	Very good
17	Line 150 mm	1.3	30	2000	127	0	0,5	N$_2$	12	2	Very good
18	Line 150 mm	1.3	30	1925	127	0	0,5	N$_2$	12	2	No cut
19	Line 150 mm	1.3	30	2075	127	0	0,5	N$_2$	12	2	Very good
20	Line 150 mm	1.3	30	2150	127	0	0,5	N$_2$	12	2	Very good
21	Line 150 mm	1.3	40	3000	127	0	0,5	N$_2$	12	2	Very good
22	Line 150 mm	1.3	40	2925	127	0	0,5	N$_2$	12	2	Very good
23	Line 150 mm	1.3	40	2850	127	0	0,5	N$_2$	12	2	Very good
24	Line 150 mm	1.3	40	2775	127	0	0,5	N$_2$	12	2	Burr
25	Line 150 mm	1.3	40	3075	127	0	0,5	N$_2$	12	2	Very good
26	Line 150 mm	1.3	50	3500	127	0	0,5	N$_2$	12	2	Very good
27	Line 150 mm	1.3	50	3425	127	0	0,5	N$_2$	12	2	No complete cut
28	Line 150 mm	1.3	50	3575	127	0	0,5	N$_2$	12	2	Very good
29	Line 150 mm	1.3	60	4000	127	0	0,5	N$_2$	12	2	No cut
30	Line 150 mm	1.3	55	4000	127	0	0,5	N$_2$	12	2	Very good
Material: Stainless steel AISI 316 (sheet thickness: 2.3 mm)											
31	Line 150 mm	2.3	10	2000	127	0	0,5	N$_2$	12	2	Burr
32	Line 150 mm	2.3	10	1800	127	0	0,5	N$_2$	12	2	Burr
33	Line 150 mm	2.3	10	1600	127	0	0,5	N$_2$	12	2	Burr
34	Line 150 mm	2.3	10	1500	127	0	0,5	N$_2$	10	2	Burr
35	Line 150 mm	2.3	10	1400	127	0	0,5	N$_2$	14	2	Burr
36	Line 150 mm	2.3	10	1400	127	-0,5	0,5	N$_2$	12	2	No cut

37	Line 150 mm	2.3	10	1500	127	-0,5	0,5	N$_2$	12	2	No cut
38	Line 150 mm	2.3	10	1800	127	-0,5	0,5	N$_2$	12	2	Burr
39	Line 150 mm	2.3	10	1800	127	-1	0,5	N$_2$	12	2	Good, nearly no burr
40	Line 150 mm	2.3	10	1800	127	-1,5	0,5	N$_2$	12	2	Good, nearly no burr
41	Line 150 mm	2.3	10	1800	127	-1,5	0,5	N$_2$	14	2	Very good
42	Line 150 mm	2.3	10	1725	127	-1,5	0,5	N$_2$	14	2	Burr
43	Line 150 mm	2.3	10	1650	127	-1,5	0,5	N$_2$	14	2	No cut
44	Line 150 mm	2.3	10	1875	127	-1,5	0,5	N$_2$	14	2	Very good
45	Line 150 mm	2.3	10	1950	127	-1,5	0,5	N$_2$	14	2	Very good
46	Line 150 mm	2.3	10	1875	127	-1,5	0,5	N$_2$	10	2	Burr
47	Line 150 mm	2.3	10	1875	127	-1,3	0,7	N$_2$	14	2	Burr
48	Line 150 mm	2.3	10	1875	127	-1,5	0,5	N$_2$	14	1,5	Burr
49	Line 150 mm	2.3	15	3000	127	-1,5	0,5	N$_2$	14	2	Burr
50	Line 150 mm	2.3	15	2925	127	-1,5	0,5	N$_2$	14	2	Burr
51	Line 150 mm	2.3	15	2850	127	-1,5	0,5	N$_2$	14	2	Good, nearly no burr
52	Line 150 mm	2.3	15	2800	127	-1,5	0,5	N$_2$	14	2	Burr
53	Line 150 mm	2.3	15	2700	127	-1,5	0,5	N$_2$	14	2	Burr
54	Line 150 mm	2.3	15	2600	127	-1,5	0,5	N$_2$	14	2	Burr
55	Line 150 mm	2.3	15	2500	127	-1,5	0,5	N$_2$	14	2	Burr
56	Line 150 mm	2.3	15	2500	127	-1	0,5	N$_2$	14	2	Burr
57	Line 150 mm	2.3	15	2850	127	-1	0,5	N$_2$	14	2	Burr
58	Line 150 mm	2.3	15	2850	127	-2	0,5	N$_2$	14	2	Burr

59	Line 150 mm	2.3	15	2850	127	-1,5	0,5	N$_2$	14	2	Good, nearly no burr
60	Line 150 mm	2.3	20	3500	127	-1,5	0,5	N$_2$	14	2	Burr
61	Line 150 mm	2.3	20	3300	127	-1,5	0,5	N$_2$	14	2	Good, nearly no burr
62	Line 150 mm	2.3	20	3300	127	-1	0,5	N$_2$	14	2	Burr
63	Line 150 mm	2.3	20	3300	127	-0,5	0,5	N$_2$	14	2	Burr
64	Line 150 mm	2.3	20	3300	127	-1,2	0,8	N$_2$	14	2	Burr
65	Line 150 mm	2.3	20	3225	127	-1,5	0,5	N$_2$	14	2	Burr
66	Line 150 mm	2.3	20	3375	127	-1,5	0,5	N$_2$	14	2	Small melt belts
67	Line 150 mm	2.3	25	3800	127	-1,5	0,5	N$_2$	12	2	Burr
68	Line 150 mm	2.3	25	3800	127	-1,5	0,5	N$_2$	14	2	Good, nearly no burr
69	Line 150 mm	2.3	25	3700	127	-1,5	0,5	N$_2$	14	2	Good, nearly no burr
70	Line 150 mm	2.3	25	3600	127	-1,5	0,5	N$_2$	14	2	No cut
71	Line 150 mm	2.3	25	3700	127	-1,5	0,5	N$_2$	12	2	Burr
72	Line 150 mm	2.3	25	3700	127	-2	0,5	N$_2$	14	2	No cut
73	Line 150 mm	2.3	25	3700	127	-1	0,5	N$_2$	14	2	Good, nearly no burr
74	Line 150 mm	2.3	25	3700	127	-0,5	0,5	N$_2$	14	2	Good, nearly no burr
75	Line 150 mm	2.3	25	3700	127	-1,2	0,8	N$_2$	14	2	Good, nearly no burr
76	Line 150 mm	2.3	30	4000	127	-1,5	0,5	N$_2$	14	2	No cut
77	Line 150 mm	2.3	27	4000	127	-1,5	0,5	N$_2$	14	2	Good, nearly no burr
Material: Stainless steel AISI 304 (sheet thickness: 4.3 mm)											
78	Line 150 mm	4.3	2,5	2000	127	-1,5	0,5	N$_2$	14	2	Burr
79	Line 150 mm	4.3	2,5	2000	127	-2,5	0,5	N$_2$	14	2	Burr

80	Line 150 mm	4.3	2,5	2000	127	-3,5	0,5	N_2	14	2	Burr
81	Line 150 mm	4.3	2,5	2000	127	-4,5	0,5	N_2	14	2	Burr
82	Line 150 mm	4.3	2,5	2000	127	-5,5	0,5	N_2	14	2	Burr
83	Line 150 mm	4.3	3	2000	127	-5,5	0,5	N_2	14	2	Burr
84	Line 150 mm	4.3	2,5	2000	190.5	0	0,5	N_2	14	2	Burr
85	Line 150 mm	4.3	2,5	2000	190.5	-2	0,5	N_2	14	2	Burr
86	Line 150 mm	4.3	2,5	2000	190.5	-3	0,5	N_2	14	2	Burr
87	Line 150 mm	4.3	2,5	2000	190.5	-4	0,5	N_2	14	2	Burr
88	Line 150 mm	4.3	2,5	2000	190.5	-5	0,5	N_2	14	2	Small burr
89	Line 150 mm	4.3	2,5	2000	190.5	-6	0,5	N_2	14	2	Good, nearly no burr
90	Line 150 mm	4.3	2,5	2150	190.5	-6	0,5	N_2	14	2	Good, nearly no burr
91	Line 150 mm	4.3	2,5	2000	190.5	-6	0,5	N_2	16	2	Very good
92	Line 150 mm	4.3	5	3000	190.5	-6	0,5	N_2	16	2	Very good
93	Line 150 mm	4.3	5	2850	190.5	-6	0,5	N_2	16	2	Very good
94	Line 150 mm	4.3	5	2700	190.5	-6	0,5	N_2	16	2	No cut
95	Line 150 mm	4.3	5	2800	190.5	-6	0,5	N_2	16	2	Burr
96	Line 150 mm	4.3	5	3075	190.5	-6	0,5	N_2	16	2	Good, nearly no burr
97	Line 150 mm	4.3	7,5	3800	190.5	-6	0,5	N_2	14	2	Good, nearly no burr
98	Line 150 mm	4.3	8,5	4000	190.5	-6	0,5	N_2	16	2	Good, nearly no burr
99	Line 150 mm	4.3	8,5	4000	190.5	-6	0,5	N_2	14	2	Burr
100	Line 150 mm	4.3	9,5	4000	190.5	-6	0,5	N_2	16	2	No cut
101	Line 150 mm	4.3	8,5	4000	190.5	-6	0,5	N_2	16	2	Good, nearly no burr

										Material: Stainless steel AISI 304 (sheet thickness: 6.2 mm)
102	Line 150 mm	6.2	2,5	3000	190.5	0	0,5	N$_2$	14	2	Burr
103	Line 150 mm	6.2	2,5	3000	190.5	-3	0,5	N$_2$	14	2	Burr
104	Line 150 mm	6.2	2,5	3000	190.5	-6	0,5	N$_2$	14	2	Burr
105	Line 150 mm	6.2	2,5	3000	190.5	-8	0,5	N$_2$	14	2	Small burr
106	Line 150 mm	6.2	2,5	3000	190.5	-8	0,5	N$_2$	16	2	Burr
107	Line 150 mm	6.2	2,5	3000	190.5	-8	0,5	N$_2$	20	2	Burr
108	Line 150 mm	6.2	2,5	2750	190.5	-8	0,5	N$_2$	16	2	Burr
109	Line 150 mm	6.2	2,5	2500	190.5	-8	0,5	N$_2$	18	2	No cut
110	Line 150 mm	6.2	2,5	2600	190.5	-8	0,5	N$_2$	18	2	No cut
111	Line 150 mm	6.2	2,5	2650	190.5	-8	0,5	N$_2$	18	2	Burr
112	Line 150 mm	6.2	2,5	2650	190.5	-7,9	0,6	N$_2$	18	2	Burr
113	Line 150 mm	6.2	2,5	2650	190.5	-7,8	0,7	N$_2$	18	2	Burr
114	Line 150 mm	6.2	2,5	2650	190.5	-7,7	0,8	N$_2$	18	2	Burr
115	Line 150 mm	6.2	2,5	2650	190.5	-7,6	0,9	N$_2$	18	2	Burr
116	Line 150 mm	6.2	2,5	2650	190.5	-7,5	1	N$_2$	18	2	Burr
117	Line 150 mm	6.2	2,5	2800	190.5	-8	0,5	N$_2$	18	2	Burr
118	Line 150 mm	6.2	2,5	2800	190.5	-9	0,5	N$_2$	18	2	Burr
119	Line 150 mm	6.2	2,5	2800	190.5	-7	0,5	N$_2$	18	2	Burr
120	Line 150 mm	6.2	2,5	2800	190.5	-8	0,5	N$_2$	18	2,5	Small burr
121	Line 150 mm	6.2	1,5	2750	190.5	-8	0,5	N$_2$	18	2,5	Good, nearly no burr
122	Line 150 mm	6.2	1	2750	190.5	-8	0,5	N$_2$	18	2,5	Burr

123	Line 150 mm	6.2	1,5	2200	190.5	-8	0,5	N$_2$	18	2,5	Good, nearly no burr
124	Line 150 mm	6.2	3,5	3500	190.5	-6	0,5	N$_2$	18	2,5	Cut
125	Line 150 mm	6.2	4	4000	190.5	-6	0,5	N$_2$	18	2,5	Cut
126	Line 150 mm	6.2	4,5	4000	190.5	-6	0,5	N$_2$	18	2,5	Cut, small burr
127	Line 150 mm	6.2	5	4000	190.5	-6	0,5	N$_2$	18	2,5	No cut

APPENDIX 3. CO$_2$ LASER CUTTING PARAMETERS

Nr.	Geometry	Thickness [mm]	Cutting speed [m/min]	Laser power [W]	Focal length [mm]	Focus point position [mm]	Working distance [mm]	Assist gas	Gas pressure [bar]	Nozzle diameter [mm]	Remark
Material: Stainless steel AISI 304 (sheet thickness: 1.3mm, 1.85mm, 4.4 and 6.4mm)												
1	Line 100 mm	1.3	8,8	4000	190.5	2,5	0,8	N$_2$	14	1,4	Very good
2	Line 100 mm	1.3	9,3	4000	190.5	2,5	0,8	N$_2$	14	1,4	Very good
3	Line 100 mm	1.3	9,8	4000	190.5	2,5	0,8	N$_2$	14	1,4	Very good
4	Line 100 mm	1.3	10,3	4000	190.5	2,5	0,8	N$_2$	14	1,4	Good
5	Line 100 mm	1.3	10,8	4000	190.5	2,5	0,8	N$_2$	14	1,4	Good
6	Line 100 mm	1.3	15,3	4000	190.5	0	0,8	Air	3	1,4	Oxidized cut surfaces
7	Line 100 mm	1.3	16,2	4000	190.5	0	0,8	Air	3	1,4	Oxidized cut surfaces
8	Line 100 mm	1.3	17	4000	190.5	0	0,8	Air	3	1,4	Oxidized cut surfaces
9	Line 100 mm	1.3	17,8	4000	190.5	0	0,8	Air	3	1,4	Oxidized cut surfaces
10	Line 100 mm	1.3	18,7	4000	190.5	0	0,8	Air	3	1,4	Oxidized cut surfaces
11	Line 100 mm	1.85	6,2	4000	190.5	0	0,7	N$_2$	13,5	1,4	Good
12	Line 100 mm	1.85	6,5	4000	190.5	0	0,7	N$_2$	13,5	1,4	Good
13	Line 100 mm	1.85	6,85	4000	190.5	0	0,7	N$_2$	13,5	1,4	Good
14	Line 100 mm	1.85	7,2	4000	190.5	0	0,7	N$_2$	13,5	1,4	Small burrs

15	Line 100 mm	1.85	7,5	4000	190.5	0	0,7	N$_2$	13,5	1,4	Small burrs
16	Line 100 mm	1.85	7,8	4000	190.5	1	0,7	Air	3	1,4	Oxidized cut surfaces
17	Line 100 mm	1.85	8,3	4000	190.5	1	0,7	Air	3	1,4	Oxidized cut surfaces
18	Line 100 mm	1.85	8,7	4000	190.5	1	0,7	Air	3	1,4	Oxidized cut surfaces
19	Line 100 mm	1.85	9,1	4000	190.5	1	0,7	Air	3	1,4	Oxidized cut surfaces
20	Line 100 mm	1.85	9,6	4000	190.5	1	0,7	Air	3	1,4	Oxidized cut surfaces
21	Line 100 mm	4.4	2,5	4000	190.5	-2,5	0,7	N$_2$	17	1,7	Good
22	Line 100 mm	4.4	2,7	4000	190.5	-2,5	0,7	N$_2$	17	1,7	Good
23	Line 100 mm	4.4	2,8	4000	190.5	-2,5	0,7	N$_2$	17	1,7	Very good
24	Line 100 mm	4.4	2,9	4000	190.5	-2,5	0,7	N$_2$	17	1,7	Good
25	Line 100 mm	4.4	3,1	4000	190.5	-2,5	0,7	N$_2$	17	1,7	Good
26	Line 100 mm	4.4	4,1	6000	190.5	-2,5	0,7	N$_2$	17	1,7	Very good
27	Line 100 mm	4.4	4,3	6000	190.5	-2,5	0,7	N$_2$	17	1,7	Very good
28	Line 100 mm	4.4	4,5	6000	190.5	-2,5	0,7	N$_2$	17	1,7	Very good
29	Line 100 mm	4.4	4,7	6000	190.5	-2,5	0,7	N$_2$	17	1,7	Very good
30	Line 100 mm	4.4	4,95	6000	190.5	-2,5	0,7	N$_2$	17	1,7	Good, small burrs
31	Line 100 mm	6.4	1,7	4000	254	-3,5	0,7	N$_2$	17	1,7	Good
32	Line 100 mm	6.4	1,85	4000	254	-3,5	0,7	N$_2$	17	1,7	Very good
33	Line 100 mm	6.4	1,9	4000	254	-3,5	0,7	N$_2$	18	1,7	Incomplete penetration